

2m 11. 2567. 9

Université de Montréal

Investigation neuro-vasculaire de la rétine en conditions d'hyperoxie et
d'hypercapnie systémique chez l'humain

par

Caroline Faucher

École d'optométrie

Mémoire présenté à la Faculté des études supérieures
en vue de l'obtention du grade de
Maître ès sciences (M.Sc.)
en optique physiologique

octobre 1997

© Caroline Faucher, 1997



WW

5

US8

1998

U.001

Université de Montréal

Investigation neuro-vasculaire de la rétine en conditions d'hypoxie et d'hypoxie systémique chez l'humain

par

Caroline Faucher

École d'optométrie

Mémoire présenté à la Faculté des études supérieures
en vue de l'obtention du grade de
Maître ès sciences (M.Sc.)
en optique physiologique

octobre 1997

Caroline Faucher, 1997



Université de Montréal
Faculté des études supérieures

Ce mémoire intitulé :

Investigation neuro-vasculaire de la rétine en conditions d'hyperoxie et
d'hypercapnie systémique chez l'humain

présenté par :

Caroline Faucher

a été évalué par un jury composé des personnes suivantes :

Hélène Kergoat

John V. Lovasik

Christian Casanova

Mémoire accepté le : 07.12.1997

SOMMAIRE

L'oxygène (O_2) entraîne une constriction des vaisseaux sanguins rétiniens et une réduction du flot sanguin rétinien, tandis que le dioxyde de carbone (CO_2) provoque une vasodilatation et une augmentation du flot sanguin rétinien. Les résultats publiés à ce jour chez l'humain concernant l'action de ces deux gaz sur la circulation choroïdienne sont toutefois controversés. De plus, on ne connaît pas l'impact qu'ont ces gaz et les modifications hémodynamiques qui leur sont associées sur la fonction rétinienne. Le but de ce projet était de déterminer de façon objective l'influence de l'hyperoxie et de l'hypercapnie systémiques sur la régulation vasculaire de la choroïde et l'activité neuro-rétinienne.

La pression intra-oculaire (PIO) et le flot sanguin oculaire pulsatile (FSOP), indice global du flot sanguin choroïdien, ont été évalués avec un tonographe automatisé pour chacune des conditions suivantes : 1) à l'air ambiant, 2) pendant la respiration d' O_2 pur ou de carbogène (5% CO_2 / 95% O_2), et 3) à l'air ambiant, 10 minutes après l'arrêt de l'administration d' O_2 ou de carbogène.

La fonction neuro-rétinienne a été évaluée par l'enregistrement de potentiels oscillatoires (POs) et d'électrorétinogrammes (ERGs) par éclairs en adaptation à l'obscurité 1) à l'air ambiant, 2) pendant la respiration d' O_2 pur ou de carbogène, 3) immédiatement après l'arrêt de la respiration des gaz, et 4) à l'air ambiant, 10 minutes plus tard.

De 16 à 22 adultes volontaires sains ont participé à chacune des études.

Le FSOP n'a pas été affecté par la respiration d' O_2 pur, mais a augmenté pendant la respiration de carbogène. La PIO a diminué pendant et après la période de respiration d' O_2 ou de carbogène. Cette

réduction a été attribuée à la fois à l'hyperoxie et à la prise de mesures successives de PIO.

Certains POs ont été sélectivement affectés pendant et/ou après la respiration d'O₂ ou de carbogène. L'ERG n'a pas varié durant la respiration de l'un ou l'autre des gaz, mais a été altéré dix minutes après l'arrêt de l'administration d'O₂ pur ou de carbogène. Les composantes du complexe des POs et de l'ERG ont été affectées différemment, selon les gaz utilisés.

La stabilité du FSOP pendant la respiration d'O₂ pur nous suggère que l'ensemble du réseau choroïdien est peu sensible à l'hyperoxie systémique. Les résultats obtenus lors de l'inspiration de carbogène indiquent par contre que la choroïde réagit au CO₂ de façon similaire aux vaisseaux sanguins rétiniens et cérébraux.

La plus grande sensibilité de certains POs aux modifications des concentrations sanguines d'O₂ et de CO₂ appuie la notion selon laquelle les POs individuels seraient générés à des niveaux différents de la rétine.

L'altération de certains potentiels rétiniens après l'administration d'O₂ ou de carbogène était inattendue et n'avait jamais été rapportée jusqu'à maintenant. Nous avons suggéré que l'arrêt subit de l'administration d'O₂ pouvait avoir créé une « pseudo-hypoxie » rétinienne, et que des modifications de pH tissulaire, et possiblement de la concentration de catécholamines plasmatiques, pouvaient entrer en jeu dans l'atteinte de la réponse rétinienne suite à une période d'hypercapnie systémique.

Mots clés : électrorétinographie, potentiels oscillatoires, flot sanguin oculaire pulsatile, hyperoxie, hypercapnie.

TABLE DES MATIÈRES

Identification du jury	II
Sommaire	III
Table des matières	VI
Liste des tableaux	X
Liste des figures	XI
Liste des abréviations	XIII
Remerciements	XIV
Introduction	1
Anatomie rétinienne	2
Anatomie et physiologie vasculaire de la rétine	4
Influence de l'oxygène et du dioxyde de carbone sur le système vasculaire	5
Impact sur la circulation rétinienne	5
Impact sur la circulation choroïdienne	5
Définition et usage clinique du carbogène	6
Le flot sanguin oculaire pulsatile	6
L'électrorétinogramme par éclair	7
Effets de la modulation d'oxygène et de dioxyde de carbone sur l'activité électrique de la rétine	9
Références	12
 Chapitre 1 : The effect of oxygen and carbogen on choroidal hemodynamics	 16
Abstract	17
Introduction	19
Materials and methods	21
Subjects	21

Pulsatile ocular blood flow and intraocular pressure	22
Experiment 1: oxygen breathing	24
Experiment 2: carbogen breathing	24
End-tidal CO ₂ and respiratory rate monitoring	25
Arterial blood pressure, oxygen saturation and heart rate monitoring	25
Data analyses	25
Results	26
Effect of oxygen breathing	26
Effect of carbogen breathing	26
Discussion	31
Physiological variables	31
Intraocular pressure	32
Pulsatile ocular blood flow	33
Acknowledgements	35
References	36
Chapitre 2 : The after-effect of systemic hyperoxia on scotopic ERG in man	40
Abstract	41
Introduction	43
Materials and methods	45
Subjects	45
Recording the retinal potentials	45
Oxygen breathing	46
Statistical analyses	48
Results	48
Discussion	56
During hyperoxia	56
Oscillatory potentials	56
ERG b-wave	57
ERG a-wave	58
After hyperoxia	58

Acknowledgements	62
References	63
Chapitre 3 : Effect of carbogen breathing on the scotopic ERG and oscillatory potentials in man	68
Abstract	69
Introduction	71
Materials and methods	72
Subjects	72
Recording the retinal potentials	72
Carbogen breathing	73
Physiological variables	74
Statistical analyses	75
Results	75
Physiological variables	75
Electrophysiological findings	77
Discussion	81
Physiological variables	81
Electrophysiological findings	82
1) During carbogen breathing	82
The ERG a and b-waves	82
Oscillatory potentials	83
2) After carbogen breathing	84
The ERG a-wave	84
The ERG b-wave	84
Oscillatory potentials	85
Conclusions	86
Acknowledgements	87
References	88
Conclusions	93
Flot sanguin oculaire pulsatile et rétine externe	94
Rétine interne	95

Bibliographie	97
---------------------	----

Annexe I : Influence de l'oxygène sur la tonométrie à applanation sans contact prolongé avec la cornée	XV
--	----

Introduction	XVI
Matériel et méthodes	XVI
Sujets	XVI
Pression intra-oculaire	XVI
Respiration d'oxygène	XVII
Résultats	XVII
Discussion	XVIII
Références	XX

Annexe II : Stabilité de l'électrorétinogramme et des potentiels oscillatoires dans le temps	XXI
--	-----

Introduction	XXII
Matériel et méthodes	XXII
Expérience 1	XXIII
Expérience 2	XXIII
Résultats	XXIV
Conclusions	XXV

LISTE DES TABLEAUX

Hemoglobin oxygen saturation level and heart rate	48
Amplitude des potentiels oscillatoires et des ondes a et b (expérience 2)	XXXIV

LISTE DES FIGURES

Introduction

Anatomie de la rétine	3
L'électrorétinogramme par éclair	8
Les potentiels oscillatoires	10

Chapitre 1

Intraocular pressure recording	23
End-tidal CO ₂ as a function of time for one subject during carbogen modulation	28
Intraocular pressure during oxygen and carbogen breathing	29
Pulsatile ocular blood flow during oxygen and carbogen breathing	30

Chapitre 2

Timing of experimental protocole	47
Oscillatory potential amplitudes during oxygen modulation	50
Variation of OP3 amplitude during oxygen breathing	51
A and b-wave amplitudes during oxygen modulation	52
A and b wave amplitudes and implicit times after systemic hyperoxia	53
Oscillatory potential implicit times during oxygen modulation	54
A and b-wave implicit times during oxygen modulation	55

Chapitre 3

End-tidal CO ₂ as a function of time during carbogen modulation.....	76
The impact of carbogen breathing on the scotopic ERG b-wave and OP5	78
Amplitude of the a and b waves during carbogen modulation	79

Amplitude of the oscillatory potentials during carbogen modulation	80
--	----

Annexe I

Influence de l'oxygène sur la pression intra-oculaire	XIX
---	-----

Annexe II

Amplitude des potentiels oscillatoires en fonction du temps ..	XXVI
Amplitude des ondes a et b en fonction du temps	XXVII
Temps de latence des potentiels oscillatoires en fonction du temps	XXVIII
Temps de latence des ondes a et b en fonction du temps	XXIX
Amplitude des potentiels oscillatoires avant, pendant et après le port d'un masque modifié.....	XXX
Amplitude des ondes a et b avant, pendant et après le port d'un masque modifié.....	XXXI
Temps de latence des potentiels oscillatoires avant, pendant et après le port d'un masque modifié.....	XXXII
Temps de latence des ondes a et b avant, pendant et après le port d'un masque modifié.....	XXXIII

ABRÉVIATIONS

ACR : artère centrale de la rétine

BP : blood pressure

bpm : beats per minute

CO₂ : dioxyde de carbone

ÉPR : épithélium pigmenté rétinien

ERG : électrorétinogramme

EtCO₂ : end-tidal CO₂

FSOP : flot sanguin oculaire pulsatile

HR : heart rate

IOP : intraocular pressure

O₂ : oxygène

OPs : oscillatory potentials

PIO : pression intra-oculaire

POBF : pulsatile ocular blood flow

POs : potentiels oscillatoires

SaO₂ : degré de saturation en oxygène de l'hémoglobine

REMERCIEMENTS

Je tiens tout d'abord à remercier le docteur Hélène Kergoat, directrice de recherche, pour m'avoir encadrée au cours de ce projet.

Je remercie également le docteur John V. Lovasik pour ses conseils judicieux et pour avoir mis à notre disposition certains équipements, et le docteur Daniel Forthomme pour le prêt d'un appareil.

Je tiens de plus à remercier les docteurs Christian Casanova, Hélène Kergoat et John V. Lovasik, membres du jury ayant évalué ce mémoire.

J'aimerais aussi remercier les sujets qui se sont portés volontaires pour cette étude, ainsi que les autres personnes qui ont contribué, de près ou de loin, au bon déroulement du projet.

Je remercie finalement les organismes suivants pour leur contribution financière :

- Le Fonds de la recherche en santé du Québec (FRSQ), qui m'a accordé une bourse de formation de deuxième cycle;
- Le Fonds de fiducie des optométristes canadiens pour l'éducation (FFOCE) pour ses subventions de recherche;
- Le Comité de recherche de l'American Academy of Optometry (AAO), qui m'a attribué une bourse de voyage (Irvin M. and Beatrice Borish Student Travel Fellowship) me permettant de participer à la rencontre annuelle de l'AAO, tenue en décembre 1996.

Je tiens enfin à exprimer ma gratitude tout particulièrement à mes parents et amis, qui ont su m'appuyer tout au long de mes études.

INTRODUCTION

ANATOMIE RÉTINIENNE

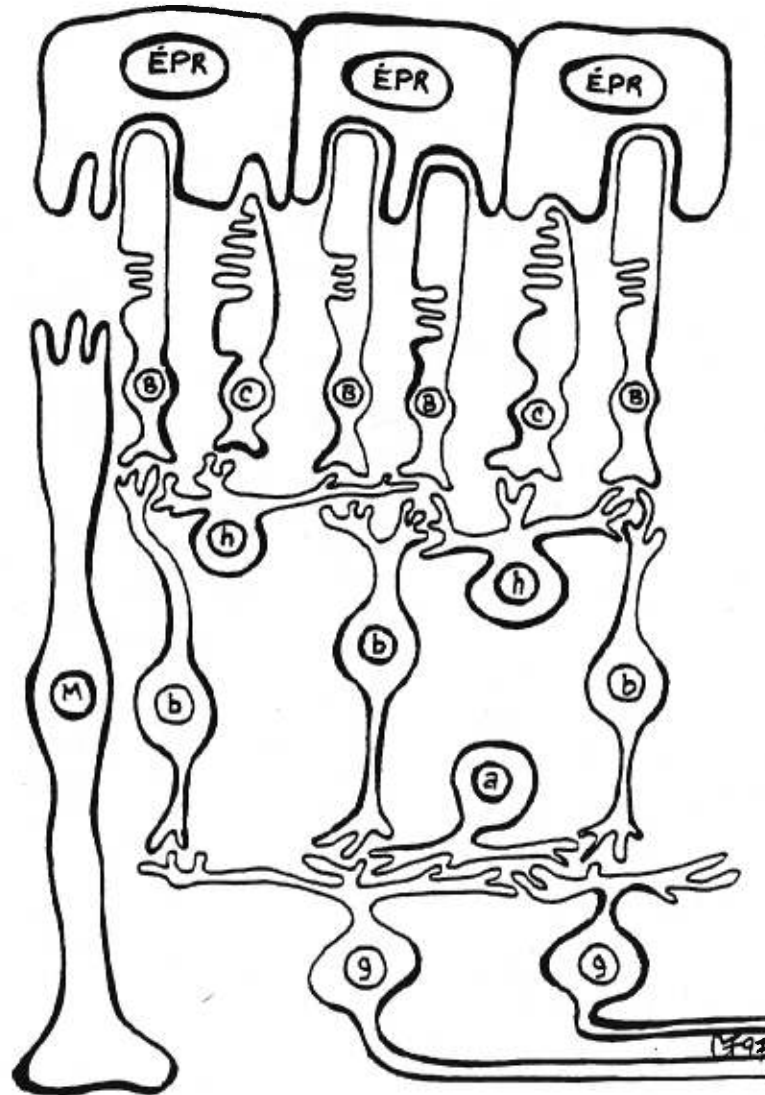
Lorsque la lumière parvient à la rétine, l'énergie lumineuse est transformée en énergie chimique au niveau des photorécepteurs, puis en énergie électrique. L'influx nerveux résultant se dirige vers l'aire 17 du cortex cérébral. La participation d'autres aires cérébrales est alors requise afin que la perception visuelle soit possible.

Dans la rétine, on peut distinguer trois ordres de neurones en série. Les neurones de premier ordre sont les photorécepteurs. Les bâtonnets, au nombre de 130 millions, constituent près de 95% des photorécepteurs. Ils sont très sensibles et sont spécialisés pour la vision à l'obscurité. La rétine contient aussi environ 7 millions de cônes, de sensibilité moindre et spécialisés pour la vision à la lumière (1). Les cellules bipolaires sont les neurones de deuxième ordre. Elles font synapse avec les photorécepteurs et les cellules ganglionnaires, neurones de troisième ordre. Les axones des cellules ganglionnaires forment la couche des fibres nerveuses de la rétine, puis s'unissent pour former le nerf optique.

On retrouve aussi deux autres types de neurones disposés parallèlement au plan de la rétine : les cellules horizontales, formant des synapses avec les photorécepteurs et les cellules bipolaires, et les cellules amacrines situées en rétine plus interne et faisant synapse avec les cellules bipolaires et ganglionnaires.

Enfin, les cellules de Müller sont des cellules gliales disposées perpendiculairement au plan de la rétine qui s'étendent de la portion interne des photorécepteurs jusqu'à la membrane limitante interne apposée au vitré. La figure 1 illustre les relations existant entre les diverses cellules nerveuses de la rétine.

Anatomie de la rétine



vers le nerf optique --->

Figure 1. Schéma illustrant les relations entre les neurones de la rétine. ÉPR : épithélium pigmenté rétinien; B : bâtonnet; C : cône; h : cellule horizontale; M : cellule de Müller; b : cellule bipolaire; a : cellule amacrine; g : cellule ganglionnaire.

ANATOMIE ET PHYSIOLOGIE VASCULAIRE DE LA RÉTINE

L'apport de sang à la rétine est assuré d'une part par le réseau vasculaire rétinien, qui nourrit les couches internes de la rétine, et d'autre part par le réseau vasculaire ciliaire choroïdien, qui en nourrit les couches externes par diffusion, soit de l'épithélium pigmenté rétinien (ÉPR) jusqu'à la couche nucléaire externe, où se situent les corps cellulaires des photorécepteurs. La fovéa, ainsi que l'extrême périphérie rétinienne, dépourvues de vaisseaux rétiniens, sont uniquement irriguées par la choroïde.

L'artère centrale de la rétine (ACR) est une branche de l'artère ophtalmique qui pénètre l'oeil par le nerf optique. À son entrée dans l'oeil, l'ACR se divise en branches artérielles, puis en artérioles et capillaires rétiniens répartis dans les quatre quadrants de la rétine. Les capillaires rétiniens sont constitués de cellules endothéliales relativement épaisses et non fenestrées, unies entre elles par des jonctions serrées. Ils constituent une des deux barrières hémato-rétiniennes. Les vaisseaux rétiniens sont dépourvus d'innervation en provenance du système nerveux autonome (2). Ils ont par contre une grande capacité d'autorégulation vasculaire, c'est-à-dire qu'ils sont sous l'influence de mécanismes myogéniques et métaboliques de régulation locale, qui contrôlent la circulation rétinienne selon les besoins métaboliques de la rétine (3).

La choroïde est un réseau de vaisseaux sanguins de gros calibre, qui reçoit le sang des artères ciliaires postérieures, branches de l'artère ophtalmique. Les vaisseaux choroïdiens forment la choriocapillaire, un dense réseau d'une seule couche de capillaires minces et fenestrés ayant une relation anatomique étroite avec l'ÉPR (2). Ce dernier, grâce aux jonctions serrées entre les cellules qui le constituent, forme une

seconde barrière hémato-rétinienne, essentielle à la préservation de l'intégrité rétinienne, étant donné la grande perméabilité des capillaires choroïdiens. La choroïde, contrairement à la circulation rétinienne, est en grande partie sous le contrôle du système nerveux sympathique. Sa capacité d'autorégulation vasculaire est pratiquement absente (2-4) ou limitée (5-7). Le flot sanguin de la choroïde est très élevé comparativement à la rétine et à d'autres lits vasculaires (8). Contrairement aux vaisseaux rétiniens, la différence de contenu en oxygène (O_2) entre le sang artériel et le sang veineux est très faible, indiquant que le flot sanguin y est plus élevé que ce qui est requis par les besoins métaboliques locaux (2).

INFLUENCE DE L'OXYGÈNE ET DU DIOXYDE DE CARBONE SUR LE SYSTÈME VASCULAIRE

Impact sur la circulation rétinienne

Une concentration élevée d' O_2 dans le sang diminue le calibre des vaisseaux sanguins rétiniens (9-13), ainsi que la vitesse du flot sanguin rétinien (10, 11, 13, 14). Le dioxyde de carbone (CO_2) a généralement une action contraire, c'est-à-dire qu'il a un effet vasodilatateur et permet une augmentation de la vitesse et du flot sanguins rétiniens (8, 14-16).

Impact sur la circulation sur la circulation choroïdienne

La choroïde semble réagir de façon similaire aux vaisseaux rétiniens en conditions d'hyperoxie et d'hypercapnie, à tout le moins chez l'animal. Plusieurs études animales ont en effet rapporté une réduction du flot sanguin choroïdien avec l' O_2 (17-19), et une augmentation en présence de CO_2 (8, 17-19). Chez l'homme, toutefois, peu d'études existent sur le sujet et les résultats obtenus sont controversés.

DÉFINITION ET USAGE CLINIQUE DU CARBOGÈNE

Le carbogène est un mélange de gaz contenant 4-7% de CO₂ dans 93-96% d'O₂. Cette combinaison de gaz est administrée lors d'occlusions de l'artère centrale de la rétine dans l'espoir d'améliorer l'oxygénation de la rétine, tout en minimisant la diminution du flot sanguin rétinien grâce à son contenu en CO₂ (9, 11, 14). Il peut aussi être utilisé pour stimuler la ventilation alvéolaire afin de favoriser l'élimination de l'oxyde de carbone lors d'intoxication (20). Enfin, le carbogène est parfois prescrit pour augmenter l'oxygénation de certaines tumeurs, ce qui améliore la réponse aux traitements de radiations, ainsi qu'à d'autres traitements thérapeutiques (21, 22).

Il existe encore une controverse concernant l'action du carbogène sur les circulations rétinienne et choroïdienne chez les animaux, et pratiquement aucune donnée n'est disponible chez l'homme.

LE FLOT SANGUIN OCULAIRE PULSATILE (FSOP)

Cette technique permet d'évaluer le flot sanguin choroïdien pulsatile en se basant sur la variation de la pression intra-oculaire (PIO) en fonction du pouls cardiaque. Le flot sanguin total arrivant à l'oeil via l'artère ophtalmique et se distribuant ensuite dans les réseaux vasculaires rétinien et ciliaire comporte une portion non pulsatile, c'est-à-dire une entrée constante de sang dans l'oeil, et une portion pulsatile, suivant le rythme cardiaque. La contribution des portions pulsatile et non pulsatile au flot sanguin oculaire total est encore indéterminée (23, 24). L'élasticité du réseau vasculaire et la rigidité relative de la sclère

permettent à chaque entrée de sang dans l'oeil de faire augmenter le volume oculaire et la PIO (23, 25, 26). Le FSOP peut être calculé à partir de mesures de fluctuations rythmiques de la PIO grâce à la relation existant entre ces deux paramètres. L'appareil utilisé pour évaluer le FSOP est un tonomètre pneumatique qui mesure la PIO à intervalles allant de 55 microsecondes (25) à 30 millisecondes (23). Des équations mathématiques permettent ensuite la transformation des mesures de pression (mmHg) en mesures de volume (μl) par unité de temps (min), soit le FSOP ($\mu\text{l}/\text{min}$), qui reflète principalement le flot sanguin choroïdien.

L'ÉLECTRORÉTINOGRAMME PAR ÉCLAIR (ERG)

L'enregistrement de l'ERG est une méthode objective pour évaluer l'intégrité rétinienne. Le signal électrique généré par différentes cellules rétiniennes lors de la présentation d'éclairs de lumière peut être détecté de façon non-invasive au niveau de la cornée par une électrode placée sur celle-ci. Le signal peut ensuite être filtré et amplifié par un système d'enregistrement des potentiels évoqués.

En adaptation à l'obscurité, des éclairs blancs de faible intensité présentés à une fréquence inférieure à 10 Hz stimulent les photorécepteurs de l'ensemble de la rétine, principalement les bâtonnets.

La courbe obtenue est formée des ondes a, b (figure 2) et c. La composante la plus précoce, l'onde a, est négative par rapport à la cornée et provient des photorécepteurs. L'onde b est positive, et est générée en rétine interne par les cellules de Müller. Les cellules amacrines et bipolaires sont possiblement aussi impliquées dans la génération de l'onde b (27). L'onde c, plus tardive, est moins souvent considérée chez l'homme. Elle est formée de l'addition d'un potentiel

L'électrorétinogramme par éclair

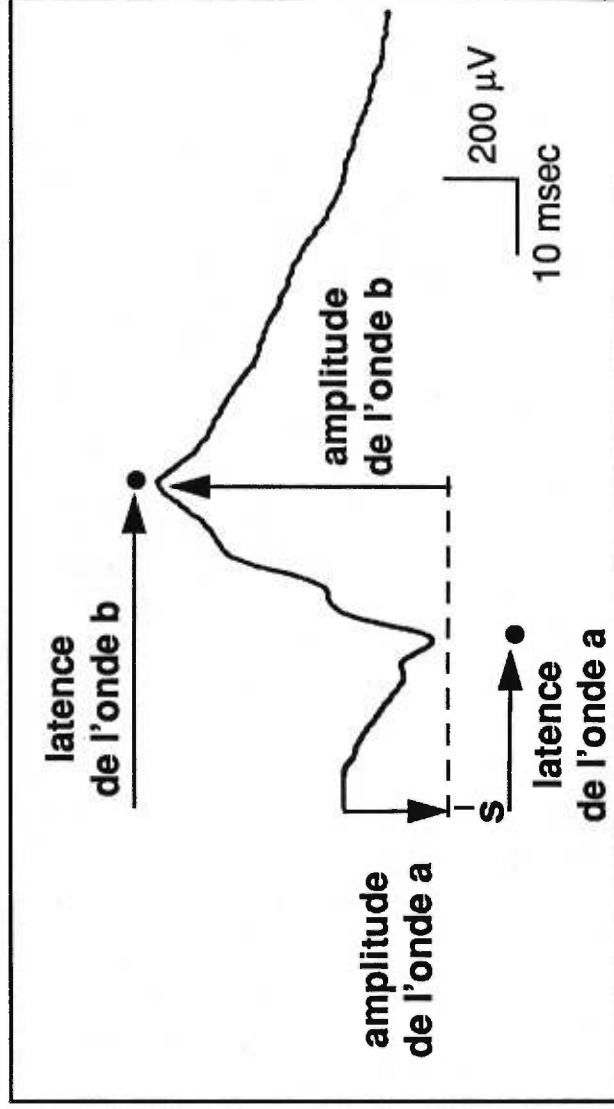


Figure 2. Exemple d'électrorétinogramme par éclair chez l'homme. L'amplitude de l'onde a se mesure de la ligne de base jusqu'au sommet négatif de l'onde a; celle de l'onde b de mesure à partir du sommet de l'onde a jusqu'au sommet positif de l'onde b. Le temps de latence des ondes a et b est le temps écoulé entre le moment où le stimulus est généré (s), et leurs sommets respectifs.

positif provenant des membranes apicales des cellules de l'ÉPR, et par un potentiel négatif, appelé « slow p-III » généré à la portion distale des cellules de Müller. L'onde c résultante est positive par rapport à la cornée, et dépend des mouvements d'ions potassium dans l'espace extracellulaire entre les photorécepteurs et l'ÉPR (27).

Sur la portion ascendante de l'onde b, on retrouve de petites oscillations, appelées potentiels oscillatoires (POs), dont le nombre varie habituellement de 4 à 6, selon les conditions d'adaptation et les couleurs de stimuli utilisés (28). Leur signal peut être isolé de l'onde b en utilisant des filtres de fréquences appropriées. La figure 3 illustre un exemple de POs isolés de la portion ascendante de l'onde b chez l'humain lors de l'enregistrement d'ERG par éclairs de lumière blanche, en condition d'adaptation à l'obscurité. Ces ondelettes sont générées dans les couches internes de la rétine mais se distinguent de l'onde b. On croit également de plus en plus à la nature individuelle de chacun des POs les uns par rapport aux autres. Les POs sont très sensibles à l'ischémie et à l'hypoxie rétiniennes. Ils sont notamment affectés lors d'une rétinopathie diabétique (29-35), même lorsque celle-ci est minime (33, 34).

EFFETS DE LA MODULATION D'OXYGÈNE ET DE DIOXYDE DE CARBONE SUR L'ACTIVITÉ ÉLECTRIQUE DE LA RÉTINE.

Puisqu'une modification des concentrations en O_2 et CO_2 de l'air inspiré influence la circulation rétinienne et choroïdienne, il est essentiel de déterminer si la fonction rétinienne en est aussi affectée. Les études animales démontrent que l'hyperoxie systémique n'affecte pas l'onde b de l'ERG, mais diminue l'amplitude de l'onde c, probablement à cause de perturbations au niveau de la circulation choroïdienne (36).

Les potentiels oscillatoires

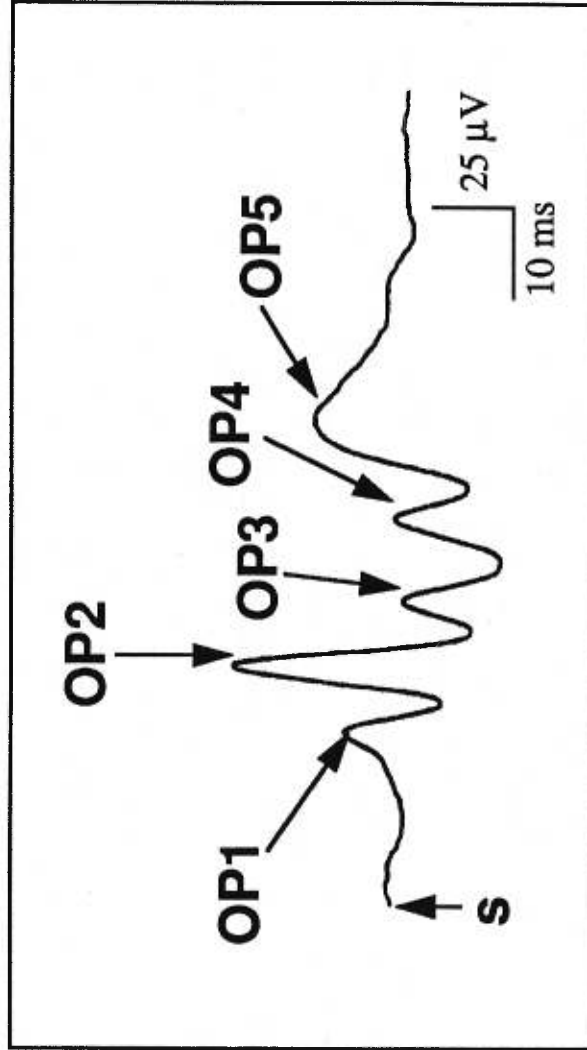


Figure 3. Exemple de potentiels oscillatoires chez l'homme, isolés de l'onde b de l'ERG scotopique à l'aide d'un filtre de fréquences (75-250 Hz). S indique le moment où le stimulus est généré.

L'hypercapnie systémique chez les animaux réduit l'amplitude de l'onde b (36-40) et celle du pic de dépolarisation à la lumière (« light peak ») (37, 38); et augmente l'amplitude de l'onde c (36-38, 40).

Chez l'humain, l'hypoxie systémique réduit l'amplitude de l'onde b (41) et le pic à la lumière (« light rise ») de l'électro-oculogramme (42). Aucune donnée n'est cependant disponible en conditions d'hyperoxie et d'hypercapnie.

La connaissance de l'influence de l'O₂ et du CO₂ sur le flot sanguin de la choroïde chez l'humain est essentielle afin de mieux définir ses mécanismes de régulation vasculaire, et ainsi mieux comprendre certains phénomènes conduisant à plusieurs pathologies oculaires telles la rétinopathie diabétique et le glaucome. De plus, ces deux gaz sont couramment utilisés cliniquement, sans qu'aucune donnée ne soit toutefois disponible concernant leur action sur la fonction visuelle chez l'humain. Il est donc primordial d'en étudier l'impact sur la fonction neuro-rétinienne.

Le but de ce projet était d'évaluer l'hémodynamique choroïdienne et la fonction neuro-rétinienne avant, pendant et après une courte période d'hyperoxie systémique, accompagnée ou non d'hypercapnie. Le chapitre 1 du présent document est consacré à l'influence de l'oxygène et du carbogène sur le FSOP, tandis que les chapitres 2 et 3 traitent respectivement de l'impact de l'oxygène et du carbogène sur les POs et l'ERG enregistrés en condition scotopique chez le jeune adulte.

RÉFÉRENCES

1. Carr RE, Siegel IM. The electrodiagnostic testing of the visual system: a clinical guide. Philadelphia: F.A. Davis Company, 1990.
2. Bill A, Nilsson SFE. Control of ocular blood flow. *J Cardiovascular Pharm* 1985; 7(suppl. 3):s96-s102.
3. Bill A, Sperber GO. Control of retinal and choroidal blood flow. *Eye* 1990; 4:319-25.
4. Bill A. Blood circulation and fluid dynamics in the eye. *Physiological Reviews* 1975; 55:383-417.
5. Kiel JW, Shepherd P. Autoregulation of choroidal blood flow in the rabbit. *Invest Ophthalmol Vis Sci* 1992; 33:2399-2410.
6. Kiel JW. Choroidal myogenic autoregulation and intraocular pressure. *Exp Eye Res* 1994; 58:529-44.
7. Kiel JW, van Heuven WAJ. Ocular perfusion pressure and choroidal blood flow in the rabbit. *Invest Ophthalmol Vis Sci* 1995;36:579-85.
8. Alm A, Bill A. The oxygen supply to the retina, II. Effects of high intraocular pressure and of increased arterial carbon dioxide tension on uveal and retinal blood flow in cats. *Acta Physiol Scand* 1972; 84:306-19.
9. Deutsch TA, Read JS, Ernest JT, Goldstick TK. Effects of oxygen and carbon dioxide on retinal vasculature in humans. *Arch Ophthalmol* 1983; 101:1278-80.
10. Fallon TJ, Maxwell DL, Kohner EM. Retinal vascular autoregulation in conditions of hyperoxia and hypoxia using the blue field entoptic phenomenon. *Ophthalmology* 1985; 92:701-5.
11. Pakola SJ, Grunwald JE. Effects of oxygen and carbon dioxide on human retinal circulation. *Invest Ophthalmol Vis Sci* 1993; 34:2866-70.
12. Bachmann K, Vilser W, Riemer TH, Strobel J, Lang GE. The effect of oxygen-inhalation on retinal vessels. *Invest Ophthalmol Vis Sci* 1997; 38:s779.

13. Kagokawa H, Sakomoto T, Takakusaki K, Ogasawara H, Yoshida A. The effect of pure oxygen breathing on retinal blood flow in the cat using a new laser Doppler velocimetry system. *Invest Ophthalmol Vis Sci* 1997; 38:s781.
14. Sponsel WE, DePaul KL, Zetlan SR. Retinal hemodynamic effects of carbon dioxide, hyperoxia, and mild hypoxia. *Invest Ophthalmol Vis Sci* 1992; 33:1864-9.
15. Harino S, Grunwald JE, Petrig BJ, Riva CE. Rebreathing into a bag increases human retinal macular blood velocity. *Br J Ophthalmol* 1995; 79:380-3.
16. Harris A, Arend O, Wolf S, Cantor LB, Martin BJ. CO₂ dependence of retinal arterial and capillary blood velocity. *Acta Ophthalmol Scand* 1995; 73:421-4.
17. Trokel S. Effect of respiratory gases upon choroidal hemodynamics. *Arch Ophthalmol* 1965; 73:838-42.
18. Friedman E, Chandra SR. Choroidal blood flow III. Effects of oxygen and carbon dioxide. *Arch Ophthalmol* 1972; 87:70-1.
19. Flower RW, Fryczkowski AW, McLeod DS. Variability in choriocapillaris blood flow distribution. *Invest Ophthalmol Vis Sci* 1995; 36:1247-58.
20. Nunn JF. *Nunn's applied respiratory physiology*, 4th ed. Oxford: Butterworth-Heinemann, 1993.
21. Laurence VM, Ward R, Dennis IF, Bleeher NM. Carbogen breathing with nicotinamide improves the oxygen status of tumours in patients. *Br J Cancer* 1995; 72:198-205.
22. Cerniglia GJ, Wilson DF, Pawlowski M, Vinogradov S, Biaglow J. Intravascular oxygen distribution in subcutaneous 9L tumors and radiation sensitivity. *J Appl Physiol* 1997; 82:1939-1945.
23. Langham ME, Farrell RA, O'Brien V, Silver DM, Schilder P. Blood flow in the human eye. *Acta Ophthalmol (Supp)* 1989; 191:9-13.
24. Krakau CET. A model for pulsatile and steady ocular blood flow. *Graefe's Arch Clin Exp Ophthalmol* 1995; 233:112-8.

25. Schilder P. Ocular blood flow changes with increased vascular resistance external and internal to the eye. *Acta Ophthalmol (Supp)* 1989; 191:19-23.
26. Kothe AC. Human ocular haemodynamics I. Choroidal blood flow. *Can J Optom* 1993; 55:160-5.
27. Berson EL. Electrical phenomena in the retina. In: Hart WM, ed. *Adler's physiology of the eye, clinical application*. St.Louis: Mosby Year Book, 1992:641-707.
28. Lovasik JV, Kergoat H. Influence of transiently altered retinal vascular perfusion pressure on rod/cone contribution to scotopic oscillatory potentials. *Ophthal Physiol Opt* 1991; 11:370-80.
29. Simonsen SE. The value of the oscillatory potential in selecting juvenile diabetics at risk of developing proliferative retinopathy. *Acta Ophthalmol* 1980; 58:865-78.
30. Bresnick GH, Korth K, Groo A, Palta M. Electroretinographic oscillatory potentials predict progression of diabetic retinopathy Preliminary report. *Arch Ophthalmol* 1984; 102:1307-11.
31. Bresnick GH, Palta M. Predicting progression to severe proliferative diabetic retinopathy. *Arch Ophthalmol* 1987; 105:810-4.
32. Holopigian K, Seiple W, Lorenzo M, Carr R. A comparison of photopic and scotopic electroretinographic changes in early diabetic retinopathy. *Invest Ophthalmol Vis Sci* 1992; 33:2773-80.
33. Li X, Sun X, Hu Y, Huang J, Zhang H. Electroretinographic oscillatory potentials in diabetic retinopathy. An analysis in the domains of time and frequency. *Doc Ophthalmol* 1992; 81:173-9.
34. Lovasik JV, Kergoat H. Electroretinographic results and ocular vascular perfusion in type I diabetes. *Invest Ophthalmol Vis Sci* 1993; 34:1731-43.
36. Niemeyer F, Nagahara K, Demant E. Effects of change in arterial PO_2 and PCO_2 on the electroretinogram in the cat. *Invest Ophthalmol Vis Sci* 1982; 23:678-83.
37. Linsenmeier RA, Mines AH, Steinberg RH. Effects of hypoxia on the light peak and electroretinogram of the cat. *Invest Ophthalmol Vis Sci* 1983; 24:37-46.

38. Niemeyer G, Steinberg RH. Differential effects of $p\text{CO}_2$ and pH on the ERG and light peak of the perfused cat eye. *Vis Res* 1984; 24:275-80.
39. Dawson WW, Parmer R, Hope GM. Division of the pattern-evoked retinal response by respiratory acidosis. *Vis Res* 1988; 28:363-9.
40. Hiroi K, Yamamoto F, Honda Y. Analysis of electroretinogram during systemic hypercapnia with intraretinal K^+ -microelectrodes in cats. *Invest Ophthalmol Vis Sci* 1994; 35:3957-61.
41. Brown JL, Hill JH, Burke RE. The effect of hypoxia on the human electroretinogram. *Am J Ophthalmol* 1957; 44:57-67.
42. Linsenmeier RA, Smith VC, Pokorny J. The light rise of the electrooculogram during hypoxia. *Clin Vis Sci* 1987; 2:111-6.

CHAPITRE 1

THE EFFECT OF OXYGEN AND CARBOGEN ON CHOROIDAL HEMODYNAMICS

ABSTRACT

Introduction. Oxygen (O_2) reduces the retinal vessel caliber and blood flow, whereas carbon dioxide (CO_2) usually has opposite effects. The influence of O_2 and CO_2 on the choroidal circulation in man is however not fully understood. This study was conducted to determine the effect of systemic hyperoxia and hypercapnia on the global choroidal hemodynamics, as evaluated by pulsatile ocular blood flow (POBF) tonography.

Methods. *Experiment 1:* 16 healthy volunteers participated in this experiment. After a resting period of 10 to 15 minutes, the POBF and IOP were measured twice with a UK OBF tonograph for each of the following conditions: 1) in normal room air breathing, 2) after 5 minutes of pure oxygen breathing through a face mask, and 3) in normal room air, 10 minutes after the oxygen mask removal. The heart rate (HR), hemoglobin oxygen saturation level (SaO_2), and arterial blood pressure were monitored throughout testing.

Experiment 2: 22 healthy subjects volunteered for this study. After a 10 to 15 minute resting period, 2 consecutive POBF and IOP measurements were taken for 3 conditions: 1) during normal room air breathing, 2) at the end of a 10 minute period of breathing carbogen, a gas mixture containing 5% CO_2 in oxygen, and 3) in room air 10 minutes later. The following variables were monitored throughout the experiment: HR, SaO_2 , arterial blood pressure (BP), end-tidal CO_2 ($EtCO_2$) and respiratory rate (RR).

Results. The HR was reduced ($p < 0.004$) and the SaO_2 was increased ($p = 0.0001$) during both oxygen and carbogen breathing, whereas arterial BP remained stable throughout both experiments. The $EtCO_2$ was increased during carbogen breathing ($p = 0.0001$), whereas the RR was reduced ($p = 0.0175$). The IOP was decreased during both experiments

($p=0.0001$). The POBF was not altered by pure O₂ breathing ($p=0.5081$), but was increased on average by 7.7% during carbogen breathing ($p=0.0222$).

Conclusions. Our POBF results indicate that the choroid reacts like the retinal and brain vessels to an increased blood CO₂ concentration, but not to systemic hyperoxia.

Key words: pulsatile ocular blood flow, hyperoxia, hypercapnia, vascular regulation

INTRODUCTION

The ocular circulation is divided into two vascular systems: the central retinal artery circulation, which nourishes the inner layers of the retina, and the uveal vessels distributed within the iris, ciliary body and choroid. The choroid irrigates the retinal pigment epithelium and outer layers of the retina.

The control of the circulation is complex, and depends on the metabolic needs of the tissue, myogenic factors, circulating substances and innervation from the autonomic nerves (1). The retinal vessels do not receive any autonomic innervation. However, sympathetic nerves may somehow influence the retinal circulation since the ophthalmic artery and the extraocular part of the central retinal artery have a rich sympathetic innervation (2). Local O_2 and CO_2 tension (PO_2 and PCO_2), tissue pH and myogenic factors all contribute to adjust the retinal blood flow according to the metabolic needs of the retina (1).

The response of the retinal circulation to variations in the inspired O_2 and CO_2 concentrations has been widely studied in the past decades in animals and humans. Hyperoxia is known to constrict retinal vessels (3-6) and reduce retinal blood flow (4-7), while hypoxia (4) and hypercapnia (7-10) dilate retinal vessels and increase blood flow. Carbogen, a gas mixture usually containing 4 to 7% CO_2 and 93 to 96% O_2 , is used in the treatment of central retinal artery occlusion with the hope that CO_2 will prevent the oxygen-induced vasoconstriction, in order to maintain or even increase retinal blood flow, while providing the retina with increased oxygenation (3, 5, 7). Recent findings indicate that carbogen breathing does in fact oxygenate the retina better than oxygen alone, as was anticipated (11, 12). Retinal hemodynamic results obtained

with carbogen are however still controversial. In some studies, carbogen did not reduce the vasoconstrictive effect of pure oxygen breathing (3, 5, 13), whereas other results indicate that carbogen decreased retinal blood flow to a lesser extent than 100% O₂ (5) and increased perimacular leucocyte velocity (7) and retinal blood velocity (13).

The control of the choroidal circulation is quite different than the retinal vascular regulation. The choroidal blood flow is very high compared to other vascular beds in the body (8), and is even greater than what is required for local metabolic needs. This high flow rate likely plays a role in stabilizing the temperature of the eye according to the environment, such as is the case during intense light stimulation (1, 14). It has been accepted over the years that variations in the choroidal circulation are mostly due to autonomic innervation, rather than myogenic factors or metabolism within the outer retina (1, 2, 14). However, recent investigations in rabbits demonstrate that myogenic factors regulate the choroid to minimize arterial pressure changes in choroidal blood volume and its consequent fluctuations in IOP (15-17). Perturbations in the choroidal hemodynamics may also be induced by variations in blood O₂ and CO₂ concentrations.

Studies investigating the effect of inspired O₂ and CO₂ concentrations on the choroidal circulation are limited, especially in humans. Systemic hyperoxia decreases choroidal blood flow in albino rabbits (18) and cats (19) whereas hypercapnia increases choroidal blood flow and volume (8, 18, 19). Carbogen breathing also increases choroidal blood volume and flow, and reduces the choroidal peripheral resistance in albino rabbits (18). In the monkey, hyperoxia slightly decreases blood circulation within the choriocapillaris at the level of the posterior pole only, whereas CO₂ breathing increases blood flow

throughout the choriocapillaris (20). These modifications are likely due to altered vessel compliance within the choroidal arteries during blood gas perturbation (21).

In humans, laser Doppler flowmetry measurements indicate that hyperoxia does not affect the foveolar choroidal blood flow (22), whereas hypercapnia does increase choroidal flow at the fovea. Other studies measuring the fundus pulsations at the macula by laser interferometry showed that hyperoxia slightly reduces choroidal blood flow (23, 24), whereas CO₂ combined with either air (23) or oxygen (24) increases the fundus pulsations at the macula.

The purpose of this study was to evaluate the more global response of the choroidal vasculature to 100% O₂ and carbogen breathing in humans through noninvasive recordings of the pulsatile ocular blood flow (POBF).

MATERIALS AND METHODS

Subjects

Sixteen healthy subjects (7 males, 9 females) volunteered for the study with pure O₂, and 22 subjects (9 males, 13 females) participated in the experiment with carbogen. The subjects were between 18 and 35 years of age, and had no ocular or systemic disease. All subjects had 20/20 or better monocular visual acuity. Written informed consent was obtained from each subject after the nature of the procedures had been explained. The experimental protocol was previously approved by the human ethic committee of our institution.

Pulsatile ocular blood flow and intraocular pressure

The POBF was measured with a hand held ocular blood flow pneumatic tonometer (OBF labs UK Ltd.). This instrument allows repeated tonometry recordings at a rate of 200/sec, and measures the dynamic changes in IOP over time. Typical IOP pulse waves as a function of time are presented in Figure 1. The computerized tonometer system analyses the various characteristics of each pulse and compares them to one another on line as they are recorded. The pulses are compared for morphology, amplitude, systolic and diastolic time and base level of IOP. The five most representative pulses are selected and processed to mathematically derive the POBF values from the IOP readings. This method provides a high fidelity measure of the IOP and its time variation (25).

Prior to the measurements, the subject was asked to sit down on a comfortable chair and rest for ten to fifteen minutes in order to stabilize the various pressures within the body. The cornea of the right eye was anesthetised with one or two drops of proparacaine HCl 0.5%. Care was taken to ensure that the head was resting straight up against the chair, without any bending of the neck forwards or backwards, to avoid any perturbation of the blood flow in the vessels of the neck. The head was kept in the same position throughout testing. The subject was asked to fixate either the red LED housed within the tonometer probe, or a fixation target on the wall. Two POBF measurements were taken for each of 3 conditions: 1) while breathing normal room air (baseline), 2) at the end of a 5 minute period of pure O₂ breathing (oxygen experiment) or at the end of a 10 minute period of carbogen breathing (carbogen experiment), and 3) while breathing room air, 10 minutes after removing the mask.

Intraocular pressure recording

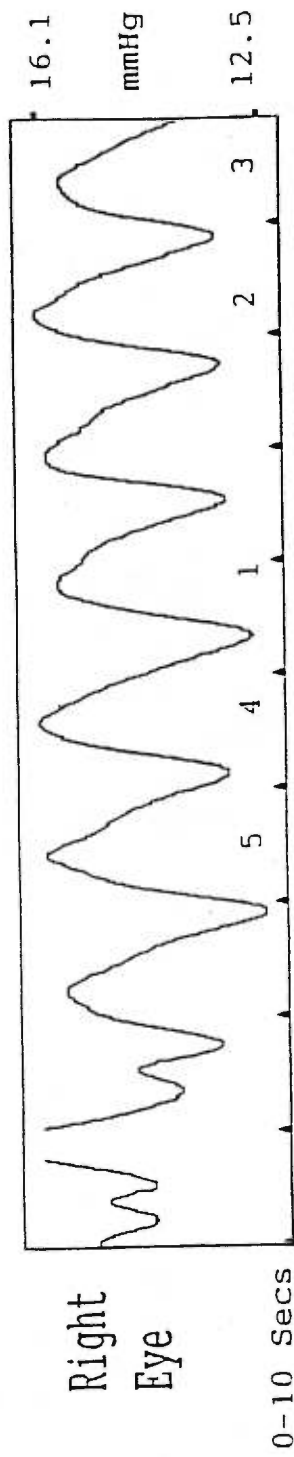


Figure 1. Graphical representation of the IOP waveform as a function of time for one subject. Numbers 1 to 5 indicate the pulses selected for analysis by the computerized tonometer system.

One or two drops of artificial tears were administered on the surface of the eye prior to the second measurement within each test condition. This precaution was found to optimize the quality of the results by improving the contact between the probe and the cornea and to better preserve the integrity of the corneal epithelium. All manipulations were performed by the same experimenter.

Experiment 1: oxygen breathing

Pure O₂ from a cylinder tank was administered through a disposable high concentration oxygen mask with a one-way valve and a 1 L reservoir bag (Inspiron, Intertech Resources Inc.). The mask was adjusted as tight and comfortable as possible, and the subject was asked to breathe normally within the mask. The flow rate of oxygen was adjusted to 5L/minute, level that was found to be adequate for all subjects. The O₂ breathing period considered in most studies investigating ocular circulation during O₂ modulation (5,22,23) varies between 3 and 10 minutes. Our pilot studies have shown that the SaO₂ already reaches its higher level within the first minute of O₂ breathing. A 5 minute period of O₂ breathing is then adequate to induce stable systemic hyperoxia.

Experiment 2: carbogen breathing

The carbogen used contained a mixture of 5% CO₂ and 95% O₂. High concentration disposable oxygen masks with a one-way valve and a 1L reservoir bag (Inspiron, Intertech Resources Inc.) were modified slightly for the carbogen study to increase their airtightness even further. The flow rate of carbogen was started at 8.5 L/minute and adjusted for each subject according to the speed at which the reservoir bag was deflated and inflated during the respiratory cycle. Our pilot studies have shown that a ten minute period of carbogen breathing was adequate to stabilize the EtCO₂ and induce stable systemic hypercapnia.

End-tidal CO₂ and respiratory rate monitoring

The end-tidal CO₂ (EtCO₂) and respiratory rate (RR) were monitored during the carbogen experiment. A disposable nasal cannula (no 1606, Salter Labs, Arvin, California) was connected to a capnograph (EtCO₂/SaO₂ monitor, model 7100, CO₂SMO, Novamatrix, Medical Systems Inc.) that monitored and recorded the EtCO₂ and RR every 8 seconds. The tips of the cannula tubes inserted in the nostrils were cut whenever required to fit the subject's nose and avoid blocking of the tubes on the nose sides. The subject was asked to breathe as normally as possible by the nose only, to enable a portion of the expired gas to be evacuated by the cannula, and then collected and analysed by the capnograph. The exceeding expired gas was evacuated through the one-way valve on the side of the face mask.

Arterial blood pressure, oxygen saturation and heart rate monitoring

The arterial blood pressure was monitored with a 90601 SpaceLabs monitor (SpaceLabs, Inc., Redmond, WA). Two consecutive measurements of systolic, diastolic and mean arterial blood pressure were taken 2 to 3 minutes before the POBF measurement within each phase of the experiment. The heart rate (HR) and arterial hemoglobin oxygen saturation level (SaO₂) were continuously monitored by finger pulse oximetry.

Data analyses

The mean of the two consecutive measurements of the POBF, IOP and BP data were calculated for each subject, and repeated measure ANOVAs were performed across the mean values taken before, during and after the gas inhalation. For the carbogen experiment, the data

acquired within the last 5 minutes of each condition were averaged and taken as representative values for EtCO₂, RR, SaO₂ and HR. This corresponded to the phase within each test condition where the EtCO₂ levels were most stable, as depicted for one subject in Figure 2. The mean values were calculated, and repeated measure ANOVAs were performed to compare the results between test conditions. For all variables, the level of significance was set to $p=0.05$.

RESULTS

Effect of oxygen breathing

The mean SaO₂ was 98.0% at baseline, increased to 99.1% during pure O₂ breathing and returned to baseline values 10 minutes after the mask was removed ($p=0.0001$). The mean heart rate decreased from 76.0 beats per minute (bpm) at baseline to 73.1 bpm during O₂ breathing (-3.8%), and recovered to baseline within 10 minutes of room air breathing ($p=0.0032$). All subjects had normal baseline systolic, diastolic and mean arterial blood pressures which remained stable throughout the experiment. The IOP decreased from 16 to 14.5 mmHg during O₂ breathing and was lowered again to 13.4 mmHg after 10 minutes in room air ($p=0.0001$; Figure 3). The mean POBF was 821 $\mu\text{L}/\text{min}$ at baseline, and did not vary across test conditions ($p=0.5081$; Figure 4).

Effect of carbogen breathing

Carbogen breathing was well tolerated by all subjects. The mean SaO₂ increased from 97.3% to 98.5% with carbogen breathing, and recovered to baseline values within 10 minutes of normal room air breathing ($p=0.0001$). The EtCO₂ increased by a mean of 10.1% during

carbogen breathing, and immediately decreased when the mask was removed, to be back to its baseline level after 10 minutes in room air ($p=0.0001$).

The RR was reduced from 15.7 to 14.2 breaths/minute (-9.6%) with carbogen, and recovered to 15.5 breaths/minute after 10 minutes in room air ($p=0.0175$).

The mean HR was reduced from 75.4 to 72.8 bpm (-3.5%) during carbogen inhalation, and returned to its baseline value 10 minutes after the mask was removed ($p=0.0005$).

All subjects had normal baseline systolic, diastolic and mean arterial blood pressures that remained stable throughout the experiment ($p>0.05$).

The mean IOP was reduced from 15.2 mmHg in room air to 14.0 mmHg during carbogen inhalation, and remained low 10 minutes after the end of carbogen breathing ($p=0.0001$; Figure 3). The mean POBF at baseline was 822 $\mu\text{L}/\text{min}$. The POBF increased on average by 7.7% with carbogen breathing. ($p=0.0222$; Figure 4). The amount of change in POBF with carbogen breathing varied from -12.2% to +37.2% across subjects. The POBF at the end of the experiment was not different from the POBF recorded for the baseline and carbogen breathing conditions.

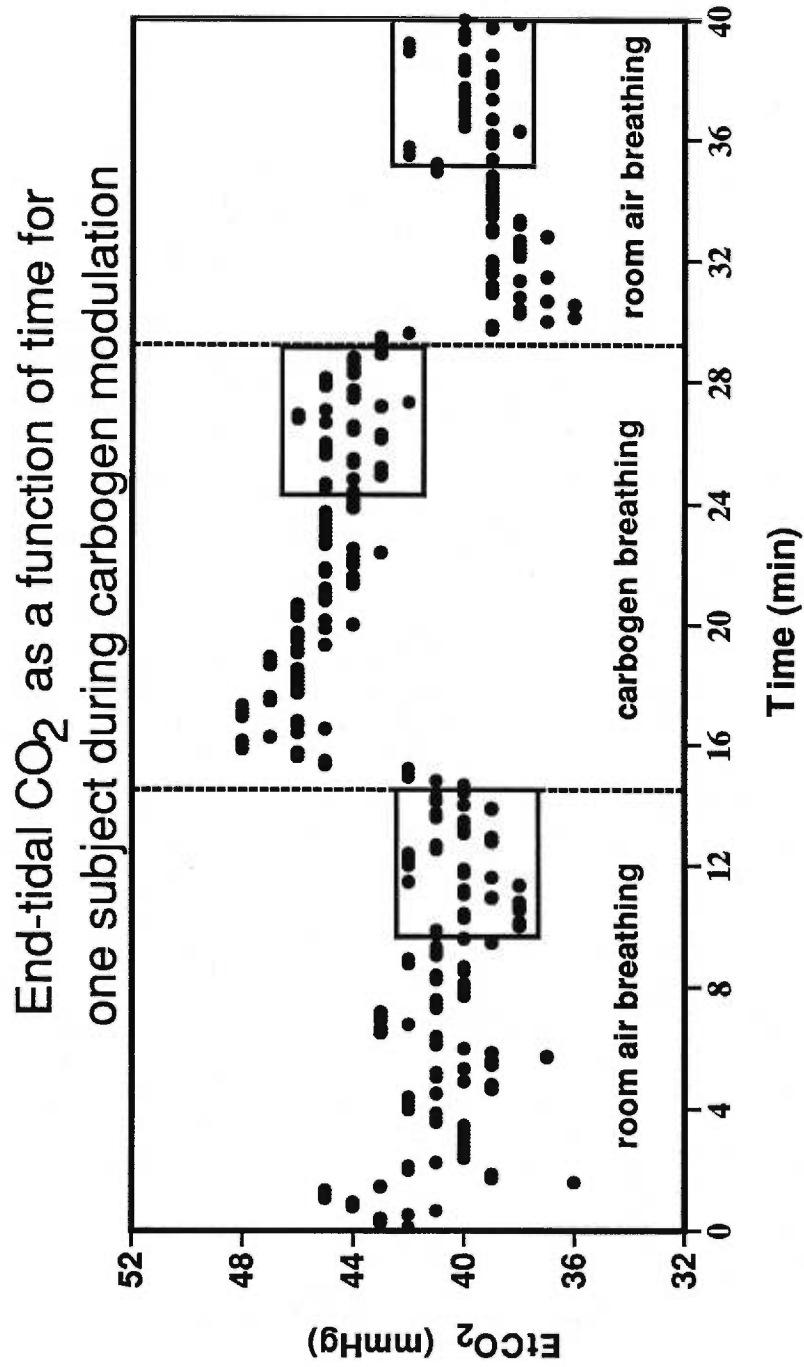


Figure 2. Figure illustrating the EtCO₂ variation as a function of time for one subject during the carbogen experiment. The large squares surrounding data points indicate the time frame when the BP, IOP and POBF data were acquired, and also represent the periods of time considered for statistical analyses of the EtCO₂, SaO₂, HR and RR variables.

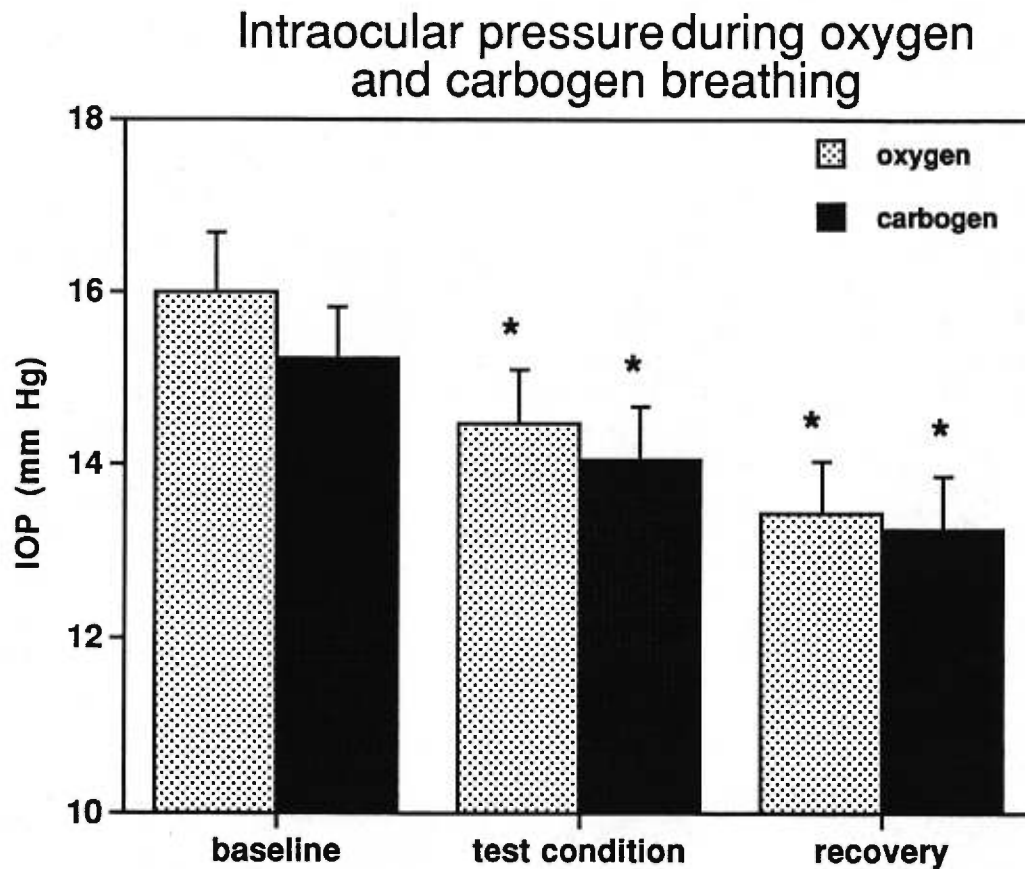


Figure 3. Figure illustrating the IOP for each condition during both pure oxygen and carbogen breathing experiments. The item "baseline" indicates the first recording in room air, "test condition" indicates either the oxygen or carbogen breathing period, and "recovery" indicates results obtained in room air 10 minutes later. The error bars illustrate the standard error of the mean; the asterisks represent data differing from baseline ($p=0.0001$).

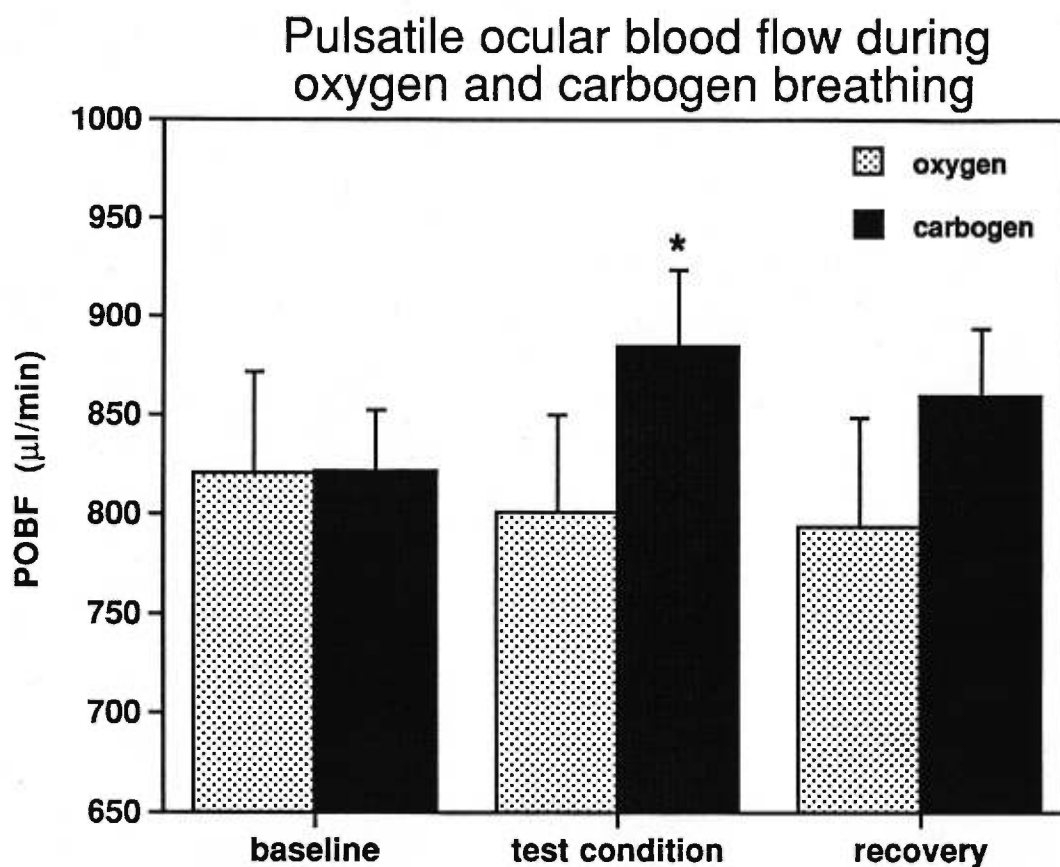


Figure 4. Figure illustrating the POBF for each condition during both pure oxygen and carbogen breathing experiments. The item "baseline" indicates the first recording in room air, "test condition" indicates either the oxygen or carbogen breathing period, and "recovery" indicates results obtained in room air 10 minutes later. The error bars illustrate the standard error of the mean; the asterisk represents data differing from baseline ($p=0.0222$).

DISCUSSION

Physiological variables

The SaO₂ increased with both O₂ and carbogen breathing, which indicates that systemic hyperoxia was achieved in both experiments.

The EtCO₂ increased on average by 10.1% during carbogen breathing, but this level of change differed among subjects, likely due to intersubject variations in response to the gas (26). Typically, the EtCO₂ raised quickly with inhalation of carbogen, to decrease slightly after during the 10 minute period of breathing this gas. This could likely be accounted for by the Haldane effect whereby an increase in blood PO₂ decreases the affinity of hemoglobin for CO₂ (27).

We did not monitor the RR in the first experiment involving pure O₂ breathing, but the RR was found to be reduced during carbogen breathing. This finding is probably related to the high O₂ content in the inspired gas. Hyperoxia is known to reduce the RR and the tidal volume, whereas CO₂ normally increases the RR and the tidal volume in order to increase the minute ventilation and better eliminate the excess of CO₂ (27). In the present study, even though carbogen was seen to decrease the RR, eight subjects reported that their breaths seemed to be amplified during inhalation of carbogen. The minute ventilation was not monitored, but it might be that the decrease in RR was compensated by an increase in the volume of inhaled and exhaled carbogen with each breath.

A decrease in heart rate during O₂ breathing has been reported by others before, (24) but is not a universal finding (28, 29). Similarly, some studies have indicated that increased CO₂ concentration in the inspired

air increases the HR (9, 29, 30), whereas other reports show that there is no change in HR (10). Those experiments were however not conducted with carbogen, so that no systemic hyperoxia was induced. In the present study, the increased SaO₂ likely inhibited the stimulating effect of CO₂ on HR.

The arterial BP did not vary with O₂ breathing, like has been reported elsewhere (28, 29). BP monitoring during hypercapnia not accompanied by hyperoxia shows that the BP remains unchanged (10, 29), or increases slightly (9, 23). Data on BP variations with carbogen breathing are limited; Schmetterer et al. (24) found an increase in the mean arterial blood pressure, and in a previous experiment (31), we found that 10 minutes of carbogen breathing increased the diastolic blood pressure only.

Intraocular pressure

The decrease in IOP can probably be accounted for by both O₂ breathing and repeated tonometry measurements. A reduction in IOP with O₂ breathing has in fact been reported in humans (32, 33) and rabbits (33). Other investigators, however, have not found similar results (23, 28). Since 10 to 20 seconds of corneal contact are required for each IOP recording with the ocular blood flow pneumatic tonometer, a control study was performed to see if the IOP measured with a precise and rapid method, therefore minimizing the ocular massaging effect of repeated tonometry, would also be reduced during O₂ breathing. Using a single Perkins measurement, we found a 1 mmHg reduction in IOP after a 5 minute period of 100% O₂ breathing ($p = 0.007$). These results suggest that part of the IOP changes are in fact related to O₂.

Pulsatile ocular blood flow

The mean POBF values for our baseline conditions (experiment 1: 821 $\mu\text{L}/\text{minute}$; experiment 2: 822 $\mu\text{L}/\text{minute}$) are in agreement with published normative data using the same system (34). Our data indicate that systemic hyperoxia did not alter the POBF. This parallels previous results in cats (35), but contrasts with other data showing that hyperoxia decreases choroidal blood flow (18, 19). Studies in man, investigating the effect of systemic hyperoxia on a more focal aspect of the choroidal circulation have demonstrated either no change (22), or a slight reduction (23, 24) in choroidal blood flow within the macular area. In the monkey, hyperoxygenation was found to alter the choriocapillary blood circulation, but only at the posterior pole (20). The POBF technique we used evaluates the global response of the ocular blood flow, and would likely not detect such perturbations restricted to a small area of the fundus.

The response of the POBF to an increased CO_2 concentration in the inspired air parallels studies investigating choroidal blood flow within the macula in humans (22-24), as well as most studies investigating choroidal circulation in animals (8, 18-21), with the exception of the one by Goldstick and Ernest (35) who found that CO_2 had little effect on the choroidal circulation.

Our POBF results represent new data confirming that the choroid reacts like the retinal (7-10, 13), optic nerve head (29), cerebral blood vessels (36, 37), as well as the vasculature of other organs (8) to an increase in blood CO_2 content. The exact mechanism underlying this vasodilation and consequent increase in blood flow remains unknown, but likely involves a reduction in arterial pH (8, 24, 38, 39).

The carbogen-induced vasodilation and increased blood flow in the choroidal vascular bed may increase O₂ diffusion from the choroid through the outer retina, providing a better oxygenation to the inner retinal layers compared to pure O₂ (11, 12), which is not efficient in supplying adequate oxygenation to the whole retina when the retinal circulation is absent or compromised (12, 40, 41).

Animal models investigating retinal PO₂, arterial and local pH, electrical activity of the retina and ocular circulation during inhalation of different CO₂/O₂ concentrations may be helpful to determine the relationship between those factors, and improve our knowledge of the influence of oxygen and carbogen on the ocular circulation and oxygenation to the retina. This could eventually lead to improved therapeutic modalities for various vascular/ischemic ocular disorders. One should however be careful when comparing results obtained in animals with human studies. Typically, animal studies are performed under systemic anesthesia, which may introduce a bias in experimental designs, especially when the vascular system is being investigated. It has been shown that some anesthetic agents impair blood flow (42, 43) and oxygen delivery to tissues (43), even when mechanical ventilation is provided. Lee et al. (44) have also demonstrated that anesthesia alters the cerebrovascular response to CO₂ inhalation. Therefore, the constant evolution of emerging noninvasive techniques such as the POBF, the laser interferometer and the laser Doppler flowmeter are instrumental in investigating choroidal blood flow in humans. Carefully controlled laboratory and clinical studies using such techniques might provide a better understanding of the effects of various drug therapies, ocular pathologies and physiological stress on the ocular hemodynamics.

Parallel objective and noninvasive investigations of visual function and ocular structure such as those provided through electrophysiological recordings or scanning laser tomography are also important to correlate visual function with altered ocular dynamics and structure.

ACKNOWLEDGEMENTS

We thank all our subjects for their participation. This work was supported by a Fonds de la recherche en santé du Québec post-graduate fellowship to CF; by the Canadian Optometric Education Trust Fund to CF and HK; and by the Natural Sciences and Engineering Research Council operating and equipment grants to HK.

REFERENCES

1. Bill A, Sperber GO. Control of retinal and choroidal blood flow. *Eye* 1990; 4:319-25.
2. Bill A. Blood circulation and fluid dynamics in the eye. *Physiol Rev* 1975; 55:383-417.
3. Deutsch TA, Read JS, Ernest JT, Goldstick TK. Effects of oxygen and carbon dioxide on retinal vasculature in humans. *Arch Ophthalmol* 1983; 101:1278-80.
4. Fallon TJ, Maxwell DL, Kohner EM. Retinal vascular autoregulation in conditions of hyperoxia and hypoxia using the blue field entoptic phenomenon. *Ophthalmology* 1985; 92:701-5.
5. Pakola SJ, Grunwald JE. Effects of oxygen and carbon dioxide on human retinal circulation. *Invest Ophthalmol Vis Sci* 1993; 34:2866-70.
6. Kagokawa H, Sakomoto T, Takakusaki K, Ogasawara H, Yoshida A. The effect of pure oxygen breathing on retinal blood flow in the cat using a new laser Doppler velocimetry system. *Invest Ophthalmol Vis Sci* 1997; 38:s781.
7. Sponsel WE, DePaul KL, Zetlan SR. Retinal hemodynamic effects of carbon dioxide, hyperoxia, and mild hypoxia. *Invest Ophthalmol Vis Sci* 1992; 33:1864-9.
8. Alm A, Bill A. The oxygen supply to the retina, II. Effects of high intra-ocular pressure and of increased arterial carbon dioxide tension on uveal and retinal blood flow in cats. *Acta Physiol Scand* 1972; 84:306-19.
9. Harino S, Grunwald JE, Petrig BJ, Riva CE. Rebreathing into a bag increases human retinal macular blood velocity. *Br J Ophthalmol* 1995; 79:380-3.
10. Harris A, Arend O, Wolf S, Cantor LB, Martin BJ. CO₂ dependence of retinal arterial and capillary blood velocity. *Acta Ophthalmol Scand* 1995; 73:421-4.

11. Berkowitz BA. Adult and newborn rat inner retinal oxygenation during carbogen and 100% oxygen breathing. Comparison using magnetic resonance imaging PO₂ mapping. *Invest Ophthalmol Vis Sci* 1996; 37:2089-98.
12. Yu DY, Cringle SJ, Alder VA, Su EN, Yu PK. Intraretinal oxygen distribution and choroidal regulation in the avascular retina of guinea pigs. *Am J Physiol* 1996; 270:H965-H973.
13. Arend O, Harris A, Martin BJ, Holin M, Wolf S. Retinal blood velocities during carbogen breathing using scanning laser ophthalmoscopy. *Acta Ophthalmol* 1994; 72:332-6.
14. Bill A, Nilsson SFE. Control of ocular blood flow. *J Cardiovascular Pharm* 1985; 7(suppl. 3):s96-102.
15. Kiel JW, Shepherd AP. Autoregulation of choroidal blood flow in the rabbit. *Invest Ophthalmol Vis Sci* 1992; 33:2399-2410.
16. Kiel JW. Choroidal myogenic autoregulation and intraocular pressure. *Exp Eye Res* 1994; 58:529-44.
17. Kiel JW, van Heuven WAJ. Ocular perfusion pressure and choroidal blood flow in the rabbit. *Invest Ophthalmol Vis Sci* 1995; 36:579-85.
18. Trokel S. Effect of respiratory gases upon choroidal hemodynamics. *Arch Ophthalmol* 1965; 73:838-42.
19. Friedman E, Chandra SR. Choroidal blood flow III. Effects of oxygen and carbon dioxide. *Arch Ophthalmol* 1972; 87:70-1.
20. Flower RW, Fryczkowski AW, McLeod DS. Variability in choriocapillaris blood flow distribution. *Invest Ophthalmol Vis Sci* 1995;36:1247-58.
21. Flower RW, Klein GJ. Pulsatile flow in the choroidal circulation: a preliminary investigation. *Eye* 1990; 4:310-8.
22. Riva CE, Cranstoun SD, Grunwald JE, Petrig BL. Choroidal blood flow in the foveal region of the human ocular fundus. *Invest Ophthalmol Vis Sci* 1994;35:4273-81.
23. Schmetterer L, Wolzt M, Lexer F, Alschinger C, Gouya G, Zanaschka G, Fassolt A, Eichler HG, Fercher AF. The effect of hyperoxia and hypercapnia on fundus pulsations in the macular and optic disc region in healthy young men. *Exp Eye Res* 1995; 61:685-90.

24. Schmetterer L, Lexer F, Findl O, Graselli U, Eichler HG, Wolzt M. The effect of inhalation of different mixtures of O₂ and CO₂ on ocular fundus pulsations. *Exp Eye Res* 1996; 63:351-5.
25. Silver DM, Farrell RA. Validity of pulsatile ocular blood flow measurements. *Survey Ophthalmol* 1994; 38 (suppl):s72-80.
26. Harris A, Martin BJ, Shoemaker JA. Regulation of retinal blood flow during blood gas perturbation. *J Glaucoma* 1994; 3(suppl. 1):s82-90.
27. Nunn JF. *Nunn's applied respiratory physiology*, 4th ed. Oxford: Butterworth-Heinemann, 1993.
28. Riva CE, Grunwald JE, Sinclair SH. Laser Doppler velocimetry study of the effect of pure oxygen breathing on retinal blood flow. *Invest Ophthalmol Vis Sci* 1983; 24:47-51.
29. Harris, A, Anderson DR, Pillunat L, Joos K, Knighton RW, Kagemann L, Martin BJ. Laser Doppler flowmetry measurement of changes in human optic nerve head blood flow in response to blood gas perturbations. *J Glaucoma* 1996; 5:258-65.
30. Cullen DJ, Eger EI. Cardiovascular effects of carbon dioxide in man. *Anesthesiology* 1974; 41:345-9
31. Faucher C, Kergoat H. The effect of carbogen breathing on neuro-retinal function in man. *Optom Vis Sci* 1997;74. Abstract accepted for publication.
32. Gallin-Cohen PF, Podos SM, Yablonski ME. Oxygen lowers intraocular pressure. *Invest Ophthalmol Vis Sci* 1980; 19:43-8.
33. Yablonski ME, Gallin P, Shapiro D. Effect of oxygen on aqueous humor dynamics in rabbits. *Invest Ophthalmol Vis Sci* 1985; 26:1781-4.
34. Massey AD, O'Brien C. Pulsatile ocular blood flow: a population study of normals. *Invest Ophthalmol Vis Sci* 1996; 37:s31.
35. Goldstick TK, Ernest JT. The effect of glucose, oxygen and carbon dioxide on choroidal blood flow. *Invest Ophthalmol Vis Sci* 1982; 22(suppl):194.

36. Kety SS, Schmidt CF. The effects of altered arterial tensions of carbon dioxide and oxygen on cerebral blood flow and cerebral oxygen consumption of normal young men. *J Clin Invest* 1948; 484-92.
37. Bereczki D, Wei L, Otsuka T, Hans FJ, Acuff V, Patlak C, Fenstermacher J. Hypercapnia slightly raises blood volume and sizably elevates flow velocity in brain microvessels. *Am J Physiol* 1993; 264:H1360-H1369.
38. Lassen NA. Brain extracellular pH: the main factor controlling cerebral blood flow. *Scand J Clin Lab Invest* 1968; 22:247-51.
39. Thorburn W. Recordings of applanating force at constant intraocular pressure. IV. Intraocular volume changes due to changes in blood content. *Acta Ophthalmol* 1972; 50:270-85.
40. Pournaras CJ, Riva CE, Tsacopoulos M, Strommer K. Diffusion of O₂ in the retina of anesthetized miniature pigs in normoxia and hyperoxia. *Exp Eye Res* 1989; 49:347-60.
41. Braun RD, Linsenmeier RA. Retinal oxygen tension and the electroretinogram during arterial occlusion in the cat. *Invest Ophthalmol Vis Sci* 1995; 36:523-41.
42. Lee JG, Hudetz AG, Smith JJ, Hillard CJ, Bosnjak ZJ, Kampine JP. The effects of halothane and isoflurane on cerebrocortical microcirculation and autoregulation as assessed by laser-Doppler flowmetry. *Anesthesia & Analgesia* 1994; 79:58-65.
43. Kerger H, Saltzman DJ, Gonzales A, Tsai AG, van Ackern K, Winslow RM, Intaglietta M. Microvascular oxygen delivery and interstitial oxygenation during sodium pentobarbital anesthesia. *Anesthesiology* 1997; 86:372-86.
44. Lee JG, Smith JJ, Hudetz AG, Hillard CJ, Bosnjak ZJ, Kampine JP. Laser-Doppler measurement of the effects of halothane and isoflurane on the cerebrovascular CO₂ response in the rat. *Anesthesia & Analgesia* 1995; 80:696-702

CHAPITRE 2

THE AFTER-EFFECT OF SYSTEMIC HYPEROXIA ON SCOTOPIC ERG IN MAN

ABSTRACT

Purpose. Systemic hyperoxia reduces retinal vessel calibre and blood flow to the retina. The purpose of this study was to determine the impact these vascular disturbances may have on the neuroretinal function in man.

Methods. Seventeen healthy young subjects, with 20/20 or better corrected visual acuity and no ocular disease volunteered for this study. The pupil of the right eye was dilated and the eye dark adapted for 30 minutes. Flash electroretinograms (ERG) and oscillatory potentials (OPs) were recorded with a Nicolet CA 1000 clinical averager, using a Jet type electrode. The retinal evoked responses to dim white flashes presented in a darkened Ganzfeld bowl were recorded 1) during room air breathing, 2) after 5 minutes of breathing 100% oxygen (O₂) within a high concentration oxygen mask, 3) immediately after the mask withdrawal and 4) 10 minutes later. The heart rate (HR) and hemoglobin oxygen saturation level (SaO₂) were monitored throughout the experiment.

Results. The SaO₂ increased during O₂ breathing and recovered its baseline value within 10 minutes of room air breathing ($p=0.0001$). The HR did not vary throughout the experiment. The amplitude of OP3 increased during O₂ breathing compared to its baseline value. The OP index and the amplitudes of OP1, OP2, OP4 and OP5 did not vary with systemic hyperoxia. The implicit time of all OPs remained stable throughout the experiment. The amplitudes and implicit times of both the a and b-waves were not altered during the O₂ breathing session. However, ten minutes after the end of O₂ breathing, the amplitudes of both the a and b-waves were reduced compared to their values measured at the time of the mask withdrawal, and their implicit times were delayed compared to their values measured at baseline and as soon as 100% O₂ breathing was stopped.

Conclusions. Our results indicate that systemic hyperoxia does not impair the neural function of generators located within the inner and outer layers of the retina. The increased response of OP3 identifies a component-specific sensitivity to altered oxygenation levels. The reduction in the electrical signal from the rods and cones once systemic normoxia was re-established points toward a relative hypoxic-like condition within the retina.

Key words: hyperoxia, electroretinogram, oscillatory potentials, vascular regulation, oxygen tension.

INTRODUCTION

Many factors are known to influence the perfusion of blood to the tissues. Mechanisms involved in the control of blood circulation include innervation from the central nervous system, various circulating substances, as well as local factors such as myogenic responses, local pH, carbon dioxide tension (PCO_2) and O_2 tension (PO_2) (1). The degree to which each of these factors is implicated in the control of blood flow varies between tissues.

Various provocative tests can be used to stress the vascular system and assess the regulatory capacity of a vascular bed. Modifications in the O_2 and/or CO_2 concentrations of the inspired air has been widely used to study the regulation of blood to the eye. Systemic hyperoxia induces vasoconstriction of the retinal vessels (2-4) and reduces retinal blood flow (3-5). Similar responses are found in the choroidal hemodynamics of albino rabbits (6) and cats (7). In contrast, hypercapnia increases retinal blood flow in cats (8), and also increases retinal blood velocity, and presumably blood flow in man (5, 9, 10). Hypercapnia increases choroidal blood flow and volume in rabbits (6) and cats (8, 7). Mild hypoxia (breathing 16% O_2) does not alter perimacular blood flow, (5) whereas moderate hypoxia (hemoglobin oxygen saturation level (SaO_2): 80% to 85%) increases both retinal blood flow and vessel diameter (3).

Carbogen, a gas mixture containing 4-7% CO_2 and 93-96% O_2 is used clinically for the management of central retinal artery occlusion. The expected effect of this mixture is that its O_2 content will increase oxygenation to the tissue, whereas its CO_2 content will counteract the O_2 induced vasoconstriction of retinal vessels and decrease in blood flow.

However, even if its utility is recognized clinically, the effect of carbogen on the ocular circulation has not been very well documented and published results remain controversial. Trokel (6) has shown that carbogen increases choroidal blood volume and flow, and reduces choroidal peripheral resistance in albino rabbits. More recently, carbogen was found to increase the velocity and density of perimacular leukocytes (5) as well as the retinal blood velocity in man without altering vessel diameter (11). However, other studies have shown that carbogen induces vasoconstriction of retinal vessels (2, 4) and reduces retinal blood flow and red blood cell velocity (4). It is only recently that studies have demonstrated that carbogen breathing is superior to O₂ alone in improving retinal oxygenation (12, 13).

In view of the effect a modulation of the inspired gas has on ocular circulation and retinal oxygenation, it is important to know if it also has an impact on the underlying perfused retinal neurons. Many authors have investigated the electrical activity of the retina in animals in response to systemic hyperoxia (14), hypoxia (14-17), and hypercapnia (14, 15, 18). In man, the light rise of the electrooculogram has been studied during hypoxia (19). To our knowledge, however, no study has been published on the effect of pure oxygen breathing on the electroretinogram (ERG) and oscillatory potentials (OPs) in man. In the present study, we used 100% O₂ breathing as a provocative test to determine the effect of systemic hyperoxia on the electrical activity of the dark-adapted retina in man. A scotopic level of retinal adaptation was chosen since it maximises the response of the retina to light stimulation, and it has been shown to be more sensitive to variables altering normal physiology.

MATERIALS AND METHODS

Subjects

Seventeen healthy subjects (5 males, 12 females) between 20 and 26 years of age volunteered for this study. All subjects had 20/20 or better monocular visual acuity and were free of any ocular or systemic disease. Written informed consent was obtained from each subject after the nature and procedures of the test session had been explained. All aspects of the experiment were approved by the Office for Human Research of our institution.

Recording the retinal potentials

The pupil of the right eye was dilated with 1 drop of cyclopentolate HCl 1%. A pre-gelled Ag/AgCl electrode applied to the skin near the temporal canthus of the right eye served as the reference electrode. Another pre-gelled Ag/AgCl electrode placed on the inner wrist served as the electrical ground. The right eye of the subject was covered with a light-tight patch and dark adapted for 30 minutes in dim room illumination prior to the measurements. The subject was comfortably seated on an adjustable ophthalmic chair. Just prior to any recording, and after all illumination in the room had been turned off, the eye-patch was transferred from the right eye to the left eye. A dim yellow light was then turned on to facilitate subsequent manipulations by the experimenter without changing the state of adaptation of the eye to be tested. The cornea of the right eye was anesthetised with one or two drops of proparacaine HCl 0.5%, and a Jet type electrode filled with methylcellulose was placed on the cornea. The light was turned off again and the subject was asked to fixate a low intensity red LED in the center of a darkened Ganzfeld bowl. An air circulation system was turned on in the Ganzfeld bowl throughout the experiment to improve the subject's comfort and ensure that rebreathing of expired CO₂ by the subject, if any, was minimal. To verify the quality of

recordings and repeatability of the waveform amplitude and timing characteristics, two consecutive series of 15, 100 ms epoch white flashes were presented to the right eye. The flashes were delivered by a Grass PS22 stroboscope (Grass Instruments, Quincy, MA) at a frequency of 0.3 Hz. The impedance of the electrodes was kept below 5 k Ω . The simultaneously recorded ERG and OP electrical signals were amplified by a Nicolet Biomedical CA 1000 clinical averager. The signals were then fed through an external analog filter with low and high band-pass filters adjusted to 1 Hz and 250 Hz for the ERG signals, and to 75 Hz and 250 Hz to highlight the OP components. Scotopic ERGs and OPs were recorded for 4 conditions: 1) during normal room air breathing (baseline), 2) at the end of a 5 minute period of 100% O₂ breathing, 3) immediately after removing the oxygen mask, and 4) 10 minutes later (recovery). The timing of the experimental protocol is illustrated in Figure 1. All electrical potentials were analysed in their amplitude and time domains. The amplitude of each electrical wave was taken as the difference in voltage between its peak and the preceding trough. The implicit time was measured from the time of presentation of the stimulus to the peak of the wave considered.

Oxygen breathing

Pure O₂ from a cylinder tank was administered to the subject through a high concentration oxygen mask with a one way valve and a reservoir bag (Inspiron, Intertech Resources Inc.). Our pilot experimentations revealed that the SaO₂ reaches a maximal and stable value within the first minute of O₂ breathing. A five minute period of O₂ breathing is therefore adequate to induce systemic hyperoxia and ensure the stability of blood oxygenation before and during recordings. The HR and SaO₂ were monitored with a Nellcor Symphony N-3000 pulse oximeter throughout the experiment. To that effect, a sensor placed on a finger enabled the estimation of the SaO₂ by passing red and

TIMING OF EXPERIMENTAL PROTOCOL

TEST CONDITIONS:

- Step #1) breathing room air
- Step #2) 5 min. 100% O₂
- Step #3) mask removal, 100% O₂ stopped
- Step #4) 10 min. after 100% O₂ stopped

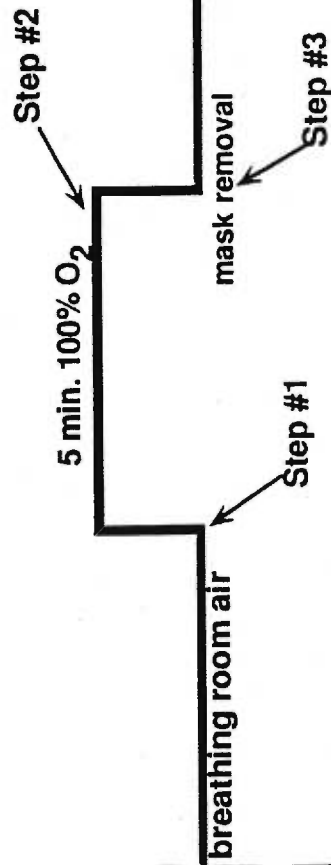


Figure 1. Figure illustrating the timing of experimental protocol after a 30 minute period of dark adaptation. Steps #1 to 4 indicate the start of ERG recordings for each test condition.

infrared light into the finger's arteriolar bed and by measuring the changes in light absorption during the pulsatile cycle. The experiment was done at sea level atmospheric pressure.

Statistical analyses

Analyses of variance (ANOVAs) procedures were used for comparison of data between conditions and across subjects. The differences were considered to be significant at an alpha level of 0.05.

RESULTS

Mean SaO₂ and HR results for 12 subjects are shown in Table I. Data for the other subjects were monitored "on line", but not specifically recorded. The SaO₂ increased from 98.1% to 99.4% during O₂ breathing ($p=0.0001$) and returned to its baseline level thereafter when the mask was removed. The baseline HR varied from 55 to 88 beats per minute (bpm) across subjects. No difference in heart rate was found across test conditions ($p=0.1761$).

Table 1 : Hemoglobin oxygen saturation level and heart rate

	Baseline	Oxygen	Mask removal	Recovery
SaO ₂ (%)	98.1	99.4 *	98.8	98.0
HR (bpm)	70.2	67.3	69.5	70.3

* $p=0.0001$

For each subject, five individual OPs were identified within the OP complex. An analysis of the OP index was also performed, and was derived from the sum of the amplitudes of the five individual OP wavelets.

An ANOVA ($p=0.0001$) performed across all OPs indicated that the amplitudes of all OPs, except for OP3, were not affected by the hyperoxic condition (Figure 2a). The amplitude of OP3 increased by 25.7% during 100% O₂ breathing (28.25 vs 35.50 μ V; Figure 2b) and recovered towards its baseline value thereafter. OP traces registered for one subject during the baseline and O₂ breathing conditions are illustrated in Figure 3. The OP index did not vary significantly with pure O₂ breathing ($p=0.1855$).

An ANOVA ($p=0.0001$) performed over the amplitudes of the a and b-waves revealed that they were not altered with pure O₂ breathing. However, the amplitudes of both the a and b-waves were reduced at the end of the recovery period, compared to their respective values measured immediately after the mask was removed. The a-wave showed a 9.1% reduction in amplitude (147.88 vs 134.44 μ V) between these two conditions, while the amplitude of the b-wave was reduced by 6.5% (456.06 vs 426.29 μ V; Figure 4). Traces for the a and b-waves registered for one subject at the moment the mask was removed, and 10 minutes later are presented in Figure 5 to illustrate the changes in amplitude and implicit time between these two test conditions.

There was no difference in the OP implicit times across test conditions (Figure 6). An ANOVA ($p=0.0001$) performed over the implicit times of the a and b-waves indicated that they did not vary with systemic hyperoxia, whereas they were slightly prolonged at recovery (24.76 and 45.83 msec) compared to their respective values at baseline (24.64 and 45.14 msec) and at the time immediately after the mask was removed (24.58 and 45.08 msec; Figure 7).

Oscillatory potential amplitudes during oxygen modulation

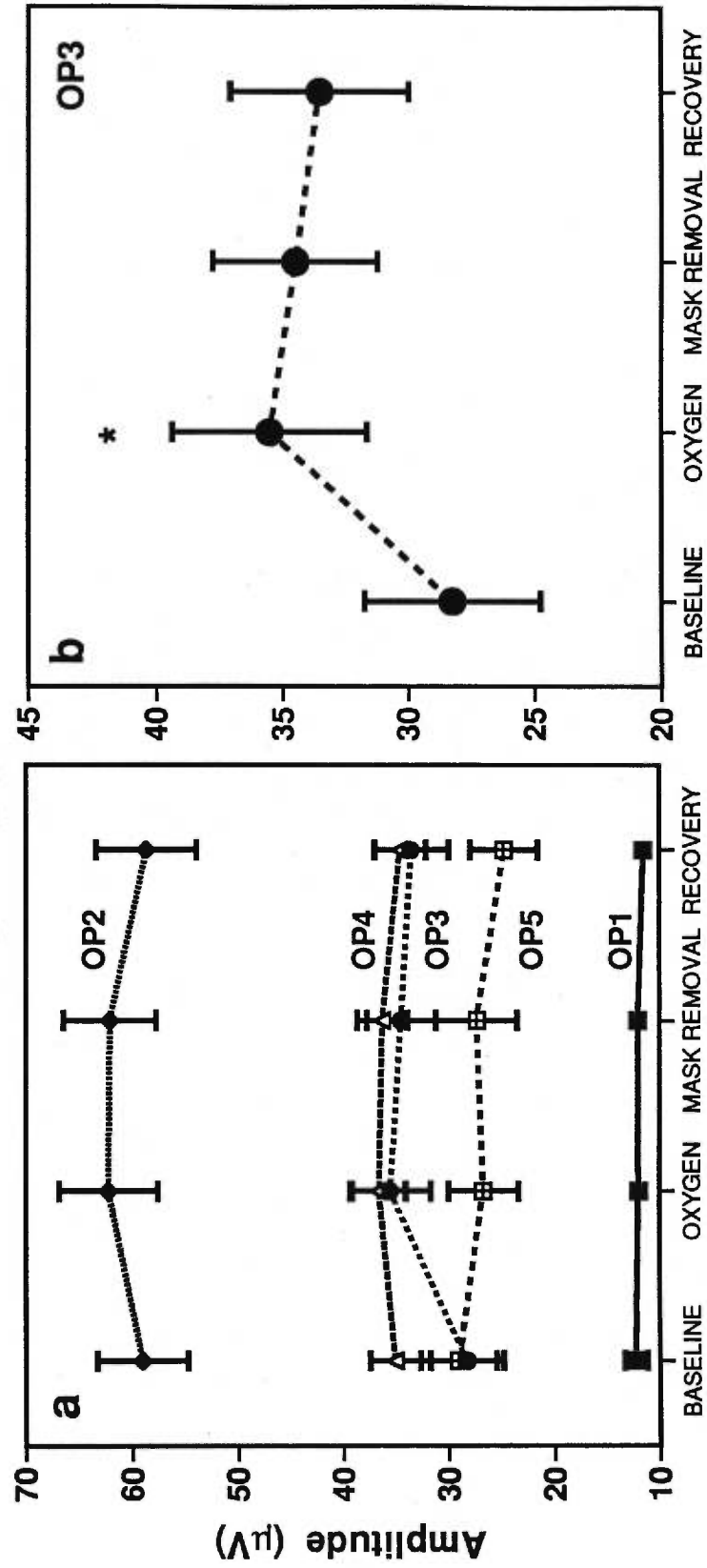


Figure 2. a) Amplitude of the OPs during test conditions. b) Variations of OP3 during the experiment. The asterisk indicates data significantly different from baseline. The error bars illustrate the standard error of the mean.

Variation of OP3 amplitude during oxygen breathing

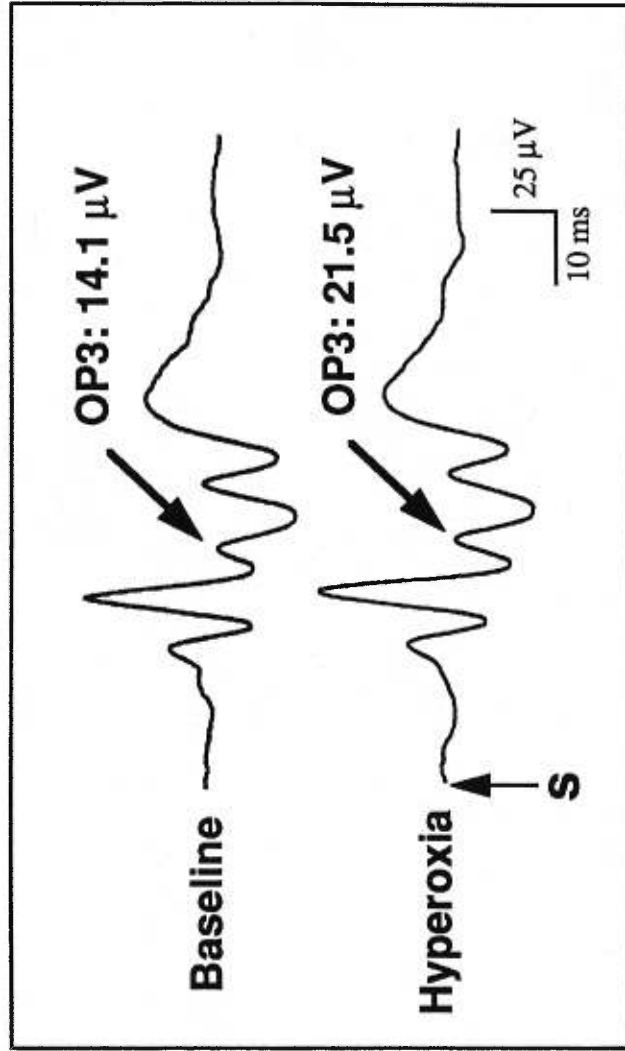


Figure 3. Figure showing the increase in OP3 amplitude during pure oxygen breathing for one subject. S: stimulus.

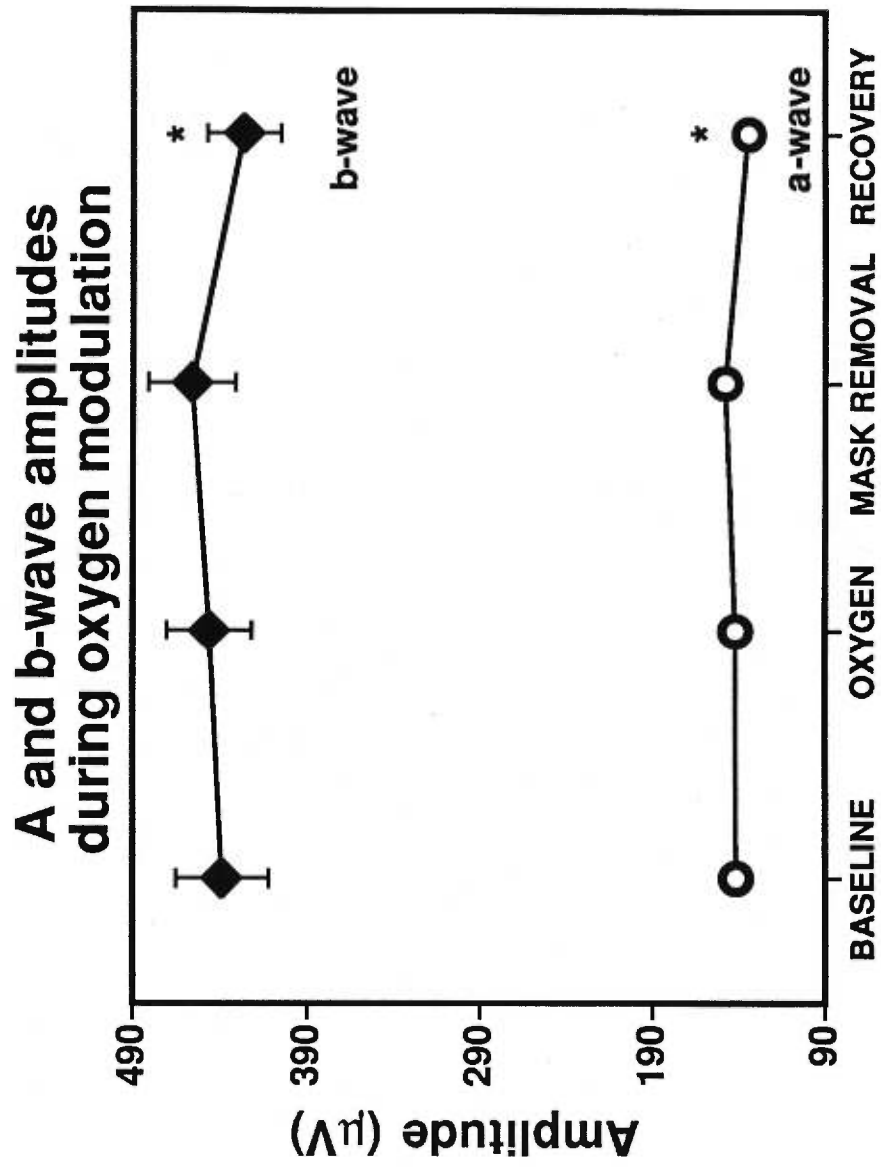


Figure 4. Amplitude of the ERG a and b-waves during O₂ modulation. The asterisks indicate data points significantly different from the mask removal condition; the error bars illustrate the standard error of the mean.

A and b wave amplitudes and implicit times after systemic hyperoxia

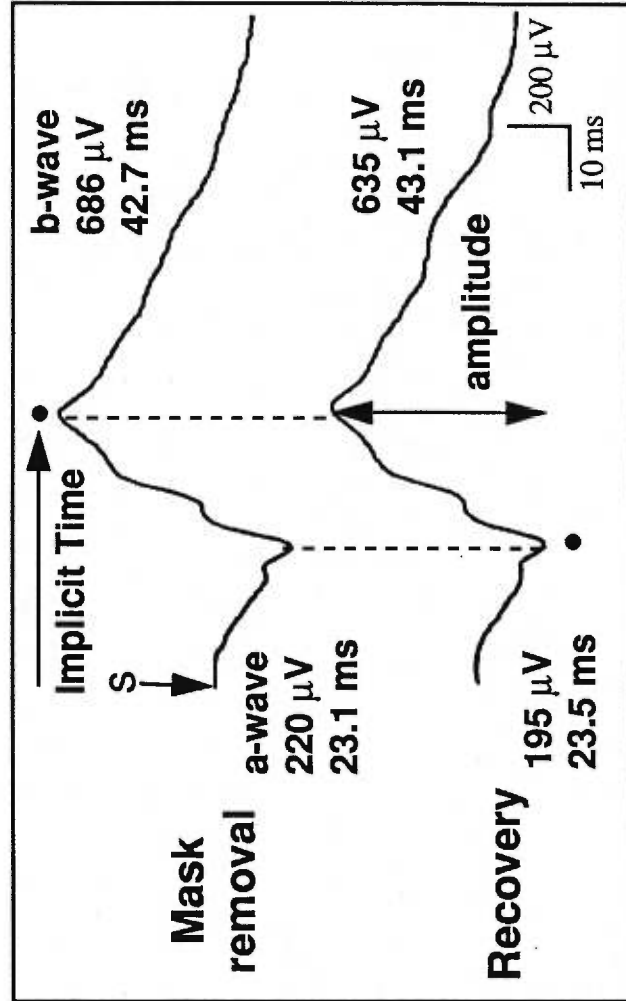


Figure 5. Figure illustrating the reduction in amplitude and the prolonged implicit times of the ERG a and b waves for one subject 10 minutes after the end of hyperoxia. S: stimulus.

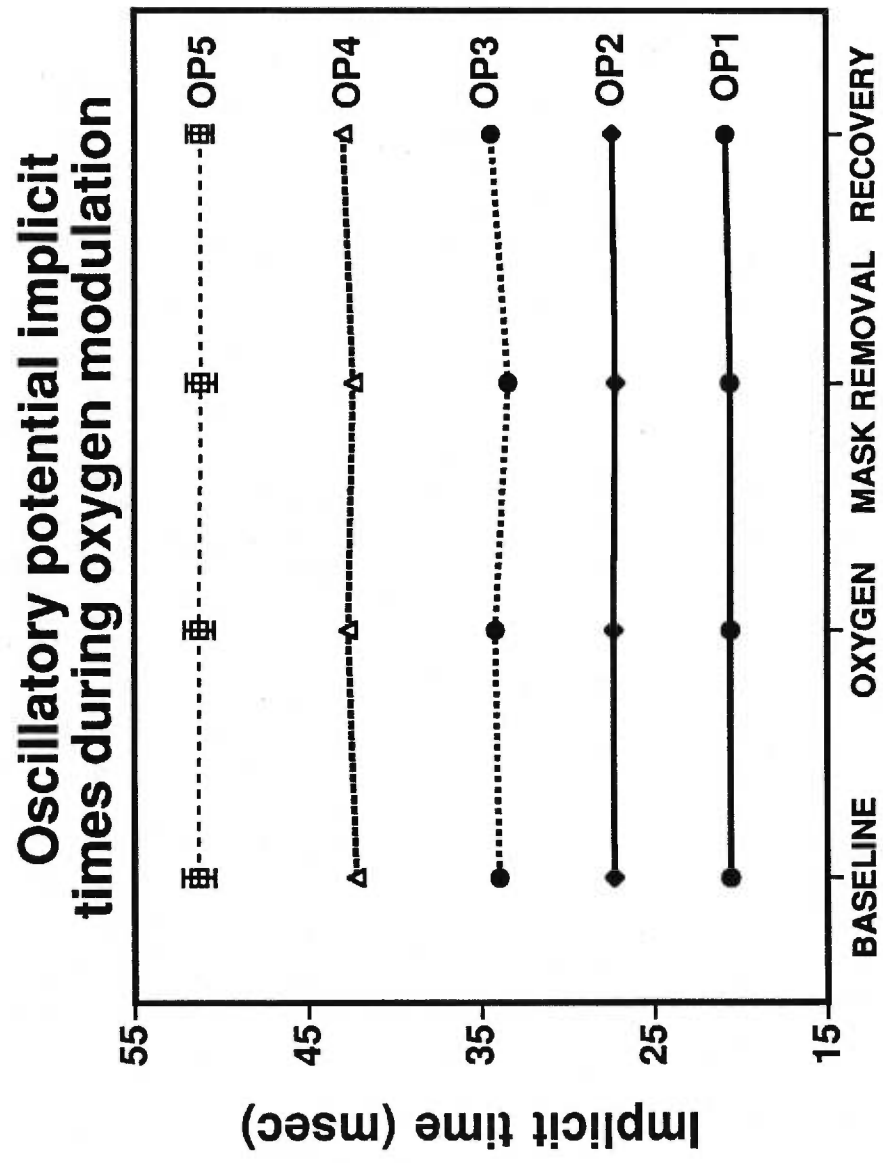


Figure 6. Figure illustrating the stability of the oscillatory potential implicit times throughout the experiment. The error bars indicate the standard error of the mean.

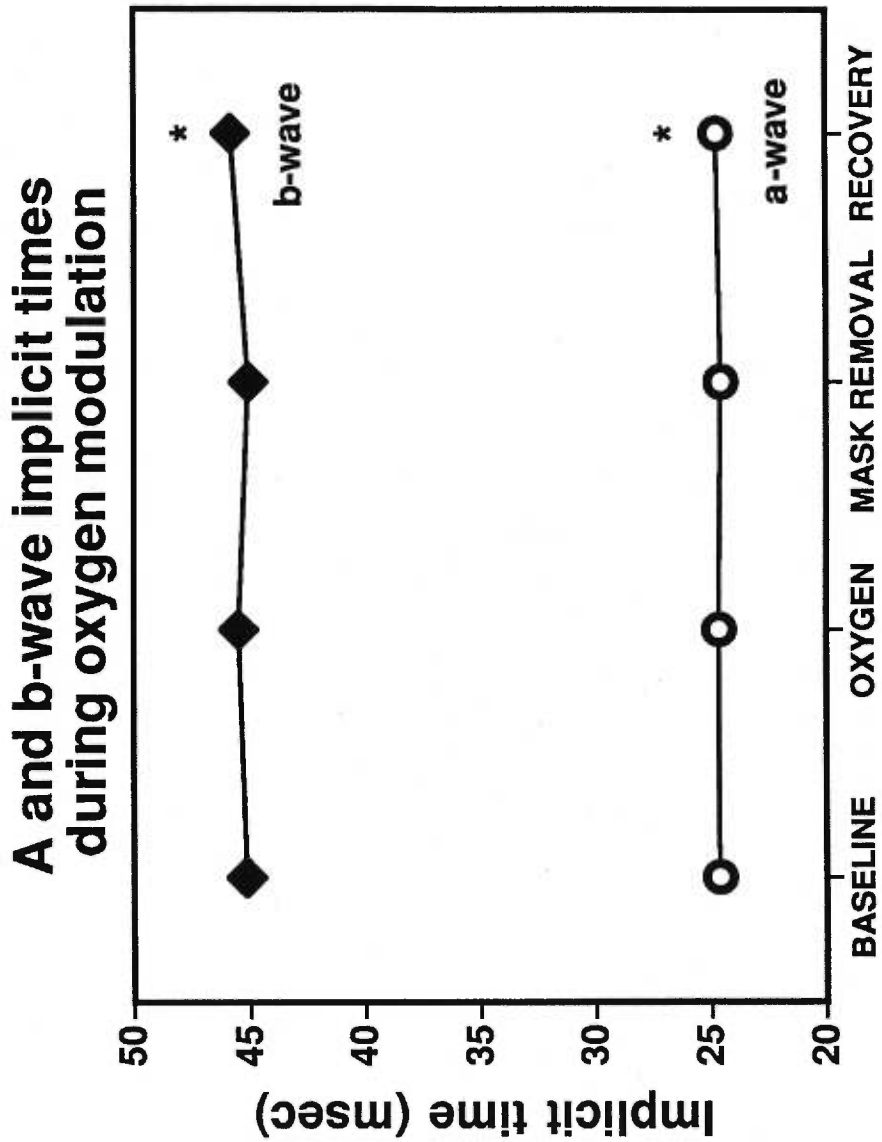


Figure 7. Implicit time of the ERG a and b-waves during O₂ modulation. The asterisks indicate the condition that achieved statistical significance compared to the baseline and mask removal conditions; the standard error of the mean were too small to be shown on the graph.

DISCUSSION

During hyperoxia

The SaO₂ increased during O₂ breathing, which indicates that additional O₂ in the inspired air was distributed throughout the body during the experiment, increasing blood oxygenation. The HR did not vary during O₂ breathing, a finding that parallels results reported in previous studies (4, 5).

Oscillatory potentials

An increase in blood O₂ did not reduce the amplitude, nor prolong the implicit time of the OPs. These wavelets are thought to originate from the area of the inner plexiform layer of the retina (20, 21), which is nourished by the central retinal artery circulation. They are vulnerable to vascular disturbances within the retina (21-25) and are therefore altered in the presence of diseases leading to retinal ischemia and hypoxia, such as diabetes (26-32). Since the OPs were not altered during pure O₂ breathing, our results indicate that the vasoconstriction of retinal vessels and decreased retinal blood flow that occur during systemic hyperoxia (2-4) did not place the inner retina at risk for inadequate O₂ delivery.

Only OP3 amplitude increased during O₂ breathing. This increase in OP3 amplitude was obtained in almost 90% of our subjects. This finding supports the notion that there are some "component-specific" elements within the OP complex, whereas individual OPs behave in different fashion to a common stimulus. This suggests that the individual OPs may be generated from cells distributed in different locations within the retina. Studies in the mudpuppy retina indicate that the earlier OPs arise more proximally than the later ones within the retina (33). It has also been suggested that OP5 in man is generated from more distal retinal

neurons (22). Results reported more recently confirm that the OPs have different topographic distribution on the surface of the eyeball (34, 35). Since OP3 behaved differently compared to the other OPs, our results bring further support to the notion that individual OPs are activated by several retinal generators, or by similar generators located in different areas within the retina.

Lovasik and Kergoat (24) have demonstrated that the earlier OPs in man are predominantly cone driven responses, while the later ones are driven primarily by the rod system. Other results indicate that OP3 is the only OP to be preserved during a 40% reduction in ocular perfusion pressure (22, 24). Combined with the results of the present study, this indicates that OP3 might result from an interaction between cones and rods, explaining its enhanced amplitude during pure O₂ breathing.

ERG b-wave

The amplitude and implicit time of the b-wave, which is generated by cells located within the inner retina, were not altered during pure O₂ breathing. This finding agrees with earlier results by Niemeyer et al. (14) who have shown that the b-wave of the cat retina was not modified by hyperoxia. They suggested that the integrity of the b-wave was maintained through autoregulation of the retinal arterial network. Pournaras et al. (36) have indicated that the retinal vasoconstriction and subsequent reduction in retinal blood flow induced by systemic hyperoxia contributed to the stability of the retinal PO₂ in the miniature pig. Regulation of the retinal PO₂ during pure O₂ breathing has also been demonstrated in cats (37). The existence of a similar regulatory mechanism in the human inner retina, maintaining constant the retinal PO₂ and possibly the nutrition to tissues, could explain the preservation of neural retinal function during hyperoxia, as assessed by the b-wave and OPs.

ERG a-wave

Our results have also shown that the a-wave, representing the activity of the photoreceptors, remains stable during pure O₂ breathing. The influence of systemic hyperoxia on the ERG a-wave has not been studied previously. Some insight into possible mechanisms explaining the preservation of this electrical activity can be gained through studies having examined the c-wave, a potential reflecting RPE function, during hyperoxia. The integrity of the c-wave depends on the depletion of potassium ions in the extracellular space between the photoreceptors and the RPE distal to the external limiting membrane (38). A reduction in the ERG c-wave has been reported in the cat during hyperoxia (14). This attenuation in the RPE activity was attributed to a reduction in the cornea-positive component generated by the apical membrane of the RPE. Because of the proximity of the choroid to the RPE, the authors suggested that a perturbation of the choroidal circulation likely contributed to the attenuation of the c-wave. The c-wave results from interactions between the photoreceptors and the RPE, whereas the a-wave is more specific to the activity of the photoreceptors themselves. While we did not study the ERG c-wave, the absence of any alteration in the a-wave in the present experiment suggests that the choroidal blood flow has been maintained or adjusted to optimize the O₂ supply to the photoreceptors. In a parallel study, we have shown that the pulsatile ocular blood flow (POBF), which reflects global choroidal flow, was not altered during pure O₂ breathing (39).

After hyperoxia

Pure O₂ breathing created an "after-effect" on the human ERG. The amplitudes of the a and b-waves decreased by 9.1% and 6.5%, respectively. This trend was observed in more than 70% of our subjects.

The implicit times of the a and b-waves increased slightly 10 minutes after the withdrawal of the oxygen mask, even though the SaO₂ had already returned to its baseline level by that time. This increased a and b-waves latency found in room air at the end of the experiment was present in almost 90% of our subjects. Oscillations of the standing potential were found in the cat following the end of systemic hypoxia (40), but similar behavior in the ERG signals has never been reported following systemic hyperoxia. An earlier report (14) has shown that the c-wave of the cat ERG recovered to its baseline value within 10 minutes after the end of pure O₂ breathing, and the b-wave remained stable during and after hyperoxia, findings that differ from our results. These differences may be related either to species-dependant particularities, or to the experimental protocols. The pharmacological agents used to paralyze and anesthetize animals, and possibly the intubation used for mechanical ventilation, may interfere with the ocular circulation and alter the retinal response to light stimulation.

Linsenmeier and Yancey (37) have studied the PO₂ in the dark adapted cat retina during systemic hyperoxia. Even though they did not study in detail the transition from hyperoxia to air, they have noticed that the PO₂ appeared to have a small undershoot in some animals, i.e. the intraretinal PO₂ measured after the discontinuation in O₂ administration seemed to be lower than before hyperoxia. Since the retinal PO₂ is already relatively low in normoxic conditions compared to other tissues (13, 16, 17, 41, 42), and is even lower during dark adaptation (17, 41), a reduction in the local PO₂ to a lower level than its initial value following hyperoxia could result in a transient "hypoxia-like" condition that may affect the response of the retinal cells to light stimulation. It has been shown in earlier reports that hypoxia alters the ERG components (14-16). The present experiment was conducted in dark adaptation. Assuming that

the retinal PO₂, a variable that could not be evaluated here, was lower after systemic hyperoxia than before the administration of O₂, the alteration in the ERG a and b waves could be explained by a sudden decrease in retinal oxygenation. If this was the case, the same experiment conducted in photopic conditions would probably result in a smaller reduction, or in no change in the ERG a and b waves; hypothesis that will be tested in our laboratory.

In the present study, the relative reduction in the b-wave amplitude was smaller than the one of the a-wave. The alteration of the b-wave following the end of pure O₂ breathing has to be explained, at least partially, by the alteration of the a-wave. An alteration of the a-wave entrains an alteration of the b-wave for two major reasons: 1) the b-wave is measured from the negative peak of the a-wave to its positive peak, (Figure 5) and 2) a decreased a-wave indicates a deficit in the activity of the first order neurons, the photoreceptors, which will likely be reflected onto the second order neurons, represented by the b-wave. Hypoxia exerts its major effects on the RPE-photoreceptor complex (40, 41), and affects the outer retina more than the inner retina (16). If the assumption is made that the interruption of hyperoxia did create an "hypoxia-like" effect, these studies imply that the a-wave would have been more affected than the b-wave. Finally, the OPs, which are known to be more sensitive than the b-wave to hypoxia or ischemia, were not depressed during the experiment, indicating that the O₂ supply to the inner retina was adequate.

Other findings in cats suggest a shrinkage of the subretinal space during hypoxia and its swelling in hyperoxia (42), which would alter the O₂-dependent processes and could influence the interactions between the RPE and the neural retina. It is not known, however, if similar mechanisms are present in the human retina, and our experimental

protocol can not address this issue. If present, and depending on its induction time, such a swelling of the subretinal space could likely influence the ERG signal.

Other factors potentially involved in the after-effect reported here have been considered but not retained. 1) A perturbation in the choroidal blood flow, which nourishes the photoreceptors, could have affected the a-wave. Even though the response of choroidal blood flow to systemic hyperoxia remains controversial in cats and rabbits (6, 7, 43), studies have shown that it is reduced at the posterior pole in monkeys (44) and at the macula in man (45, 46). As mentioned earlier, we have shown that the POBF was not altered during or after pure O₂ breathing (39) The ERG representing the global electrical activity of the retina would likely not be altered by localized changes of blood flow at the posterior pole or at the macula. Furthermore, since the POBF, which is a global index of blood flow within the choroid, was not altered, nutrition to the photoreceptors was likely adequate. 2) Variations in the local pH during systemic hyperoxia are unlikely to have affected the ERG, since the pH is little affected by hyperoxia (12-14) or mild hypoxia (14). 3) Finally, variables linked with our experimental protocol such as changes in retinal adaptation, apposition of electrodes or the pressure of a face mask are unlikely to have affected the results. A control study performed under the same protocol, but while breathing room air only, showed that the amplitude and implicit time of the retinal potentials were not altered.

In summary, systemic hyperoxia did not have detrimental effects on the neural activity of the inner retina in man during dark adaptation. However, the alteration of the a and b waves after the interruption of pure O₂ breathing may indicate a reduction of the local PO₂ to a lower value than before systemic hyperoxia, or a perturbation in the interaction between the RPE, the photoreceptors and the other neurons of the retina

due to an imbalance in the various O₂-dependent processes. Further investigations are needed to determine the timing characteristics of this after-effect, and to better define the processes leading to the ERG alteration after systemic hyperoxia.

ACKNOWLEDGEMENTS

We thank all our subjects for their participation. This work was supported by a Fonds de la recherche en santé du Québec post-graduate fellowship to CF; by the Canadian Optometric Education Trust Fund to CF and HK; and by the Natural Sciences and Engineering Research Council operating and equipment grants to HK.

REFERENCES

1. Bill A, Sperber GO. Control of retinal and choroidal blood flow. *Eye* 1990; 4:319-25.
2. Deutsch TA, Read JS, Ernest JT, Goldstick TK. Effects of oxygen and carbon dioxide on retinal vasculature in humans. *Arch Ophthalmol* 1983; 101:1278-80.
3. Fallon TJ, Maxwell DL, Kohner EM. Retinal vascular autoregulation in conditions of hyperoxia and hypoxia using the blue field entoptic phenomenon. *Ophthalmology* 1985; 92:701-5.
4. Pakola SJ, Grunwald JE. Effects of oxygen and carbon dioxide on human retinal circulation. *Invest Ophthalmol Vis Sci* 1993; 34:2866-70.
5. Sponsel WE, DePaul KL, Zetlan SR. Retinal hemodynamic effects of carbon dioxide, hyperoxia, and mild hypoxia. *Invest Ophthalmol Vis Sci* 1992; 33:1864-9.
6. Trokel S. Effect of respiratory gases upon choroidal hemodynamics. *Arch Ophthalmol* 1965; 73:838-42.
7. Friedman E, Chandra SR. Choroidal blood flow III. Effects of oxygen and carbon dioxide. *Arch Ophthalmol* 1972; 87:70-1.
8. Alm A, Bill A. The oxygen supply to the retina, II. Effects of high intraocular pressure and of increased arterial carbon dioxide tension on uveal and retinal blood flow in cats. *Acta Physiol Scand* 1972; 84:306-19.
9. Harino S, Grunwald JE, Petrig BJ, Riva CE. Rebreathing into a bag increases human retinal macular blood velocity. *Br J Ophthalmol* 1995; 79:380-3.
10. Harris A, Arend O, Wolf S, Cantor LB, Martin BJ. CO₂ dependence of retinal arterial and capillary blood velocity. *Acta Ophthalmol Scand* 1995; 73:421-4.
11. Arend O, Harris A, Martin BJ, Holin M, Wolf S. Retinal blood velocities during carbogen breathing using scanning laser ophthalmoscopy. *Acta Ophthalmol* 1994; 72:332-6.

12. Berkowitz BA. Adult and newborn rat inner retinal oxygenation during carbogen and 100% oxygen breathing. Comparison using magnetic resonance imaging PO₂ mapping. *Invest Ophthalmol Vis Sci* 1996; 37:2089-98.
13. Yu DY, Cringle SJ, Alder VA, Su EN, Yu PK. Intraretinal oxygen distribution and choroidal regulation in the avascular retina of guinea pigs. *Am J Physiol* 1996; 270:H965-H973.
14. Niemeyer F, Nagahara K, Demant E. Effects of change in arterial PO₂ and PCO₂ on the electroretinogram in the cat. *Invest Ophthalmol Vis Sci* 1982; 23:678-83.
15. Linsenmeier RA, Mines AH, Steinberg RH. Effects of hypoxia on the light peak and electroretinogram of the cat. *Invest Ophthalmol Vis Sci* 1983; 24:37-46.
16. Linsenmeier RA. Electrophysiological consequences of retinal hypoxia. *Graefe's Arch Clin Exp Ophthalmol* 1990; 228:143-50.
17. Linsenmeier RA, Braun RD. Oxygen distribution and consumption in the cat retina during normoxia and hypoxemia. *J Gen Physiol* 1992; 99:177-97.
18. Hiroi K, Yamamoto F, Honda Y. Analysis of electroretinogram during systemic hypercapnia with intraretinal K⁺-microelectrodes in cats. *Invest Ophthalmol Vis Sci* 1994; 35:3957-61.
19. Linsenmeier RA, Smith VC, Pokorny J. The light rise of the electrooculogram during hypoxia. *Clin Vis Sci* 1987; 2:111-6.
20. Ogden TE. The oscillatory waves of the primate electroretinogram. *Vis Res* 1973; 13:1059-74.
21. Speros P, Price J. Oscillatory potentials. History, techniques and potential use in the evaluation of disturbances of retinal circulation. *Surv Ophthalmol* 1981; 25:237-52.
22. Kergoat H, Lovasik JV. The effects of altered retinal vascular perfusion pressure on the white flash scotopic ERG and oscillatory potentials in man. *Electroencephalogr Clin Neurophysiol* 1990; 75:306-22.

23. Lovasik JV, Kothe AC, Kergoat H. Improving the diagnostic power of electroretinography by transient alteration of the ocular perfusion pressure. *Optom Vis Sci* 1992; 69: 85-94.
24. Lovasik JV, Kergoat H. Influence of transiently altered retinal vascular perfusion pressure on rod/cone contribution to scotopic oscillatory potentials. *Ophthalmol Physiol Opt* 1991; 11:370-80.
25. Kergoat H, Forcier P. Correlation of an exercise-induced increase in systemic circulation with the neural retinal function in humans. *Doc Ophthalmol* 1996; 92:145-57.
26. Simonsen SE. The value of the oscillatory potential in selecting juvenile diabetics at risk of developing proliferative retinopathy. *Acta Ophthalmol* 1980; 58:865-78.
27. Bresnick GH, Korth K, Groo A, Palta M. Electroretinographic oscillatory potentials predict progression of diabetic retinopathy Preliminary report. *Arch Ophthalmol* 1984; 102:1307-11.
28. Bresnick GH, Palta M. Predicting progression to severe proliferative diabetic retinopathy. *Arch Ophthalmol* 1987; 105:810-4.
29. Holopigian K, Seiple W, Lorenzo M, Carr R. A comparison of photopic and scotopic electroretinographic changes in early diabetic retinopathy. *Invest Ophthalmol Vis Sci* 1992; 33:2773-80.
30. Li X, Sun X, Hu Y, Huang J, Zhang H. Electroretinographic oscillatory potentials in diabetic retinopathy. An analysis in the domains of time and frequency. *Doc Ophthalmol* 1992; 81:173-9.
31. Lovasik JV, Kergoat H. Electroretinographic results and ocular vascular perfusion in type I diabetes. *Invest Ophthalmol Vis Sci* 1993; 34:1731-43.
32. Van Der Torren K, Mulder P. Comparison of the second and third oscillatory potentials with oscillatory potential power in diabetic retinopathy. *Doc Ophthalmol* 1993; 83:111-8.
33. Wachtmeister L, Dowling JE. The oscillatory potentials of the mudpuppy retina. *Invest Ophthalmol Vis Sci* 1978; 17:1176-88.
34. Tremblay F, Lam SR. Distinct electroretinographic oscillatory potential generators as revealed by field distribution. *Doc Ophthalmol* 1993; 84:279-89.

35. Lachapelle P, Benoit J, Guité P. The effect of in vivo retinal cooling on the electroretinogram of the rabbit. *Vis Res* 1996; 36:339-44.
36. Pournaras CJ, Riva CE, Tsacopoulos M, Strommer K. Diffusion of O₂ in the retina of anesthetized miniature pigs in normoxia and hyperoxia. *Exp Eye Res* 1989; 49:347-60.
37. Linsenmeier RA, Yancey CM. Effects of hyperoxia on the oxygen distribution in the intact cat retina. *Invest Ophthalmol Vis Sci* 1989; 30:612-8.
38. Berson EL. Electrical phenomena in the retina. In: Hart WM, ed. *Adler's physiology of the eye, clinical application*. St.Louis: Mosby Year Book, 1992:641-707.
39. Kergoat H, Faucher C. The effect of systemic hyperoxia on the pulsatile choroidal blood flow. *Invest Ophthalmol Vis Sci* 1997; 38:s781.
40. Linsenmeier RA, Steinberg RH. Mechanisms of hypoxic effects on the cat DC electroretinogram. *Invest Ophthalmol Vis Sci* 1986; 27:1385-94.
41. Steinberg RH. Monitoring communications between photoreceptors and pigment epithelial cells: effects of « mild » systemic hypoxia. *Invest Ophthalmol Vis Sci* 1987; 28:1888-1904.
42. Cao W, Govardovskii V, Li JD, Steinberg RH. Systemic hypoxia dehydrates the space surrounding photoreceptors in the cat retina. *Invest Ophthalmol Vis Sci* 1996; 37:586-96.
43. Goldstick TK, Ernest JT. The effect of glucose, oxygen and carbon dioxide on choroidal blood flow. *Invest Ophthalmol Vis Sci* 1982; 22(suppl):194.
44. Flower RW, Fryczkowski AW, McLeod DS. Variability in choriocapillaris blood flow distribution. *Invest Ophthalmol Vis Sci* 1995;36:1247-58.
45. Schmetterer L, Wolzt M, Lexer F, Alschinger C, Gouya G, Zanaschka G, Fassolt A, Eichler HG, Fercher AF. The effect of hyperoxia and hypercapnia on fundus pulsations in the macular and optic disc region in healthy young men. *Exp Eye Res* 1995; 61:685-90.

46. Schmetterer L, Lexer F, Findl O, Graselli U, Eichler HG, Wolzt M. The effect of inhalation of different mixtures of O₂ and CO₂ on ocular fundus pulsations. *Exp Eye Res* 1996; 63:351-5.

CHAPITRE 3

EFFECT OF CARBOGEN BREATHING ON THE SCOTOPIC ERG AND OSCILLATORY POTENTIALS IN MAN

ABSTRACT

Introduction. Carbogen is used in the management of central retinal artery occlusion (CRAO) to optimize retinal oxygenation. However, its effect on neuroretinal function has not been documented yet. The purpose of this study was to evaluate the effect of carbogen breathing on scotopic ERGs in man.

Methods. 18 healthy young adults volunteered for the study. After pupillary dilation and retinal dark adaptation, 2 consecutive series of 15 dim white flashes were presented in a Ganzfeld bowl. A Jet electrode was used to record ERG: 1) during roomair breathing, 2) 10 minutes after the beginning of carbogen breathing through a high concentration oxygen mask, 3) immediately after removing the mask, and 4) 10 minutes later. The ERG signals were amplified, filtered and averaged with a Nicolet CA-1000 clinical averager. The end-tidal CO₂ (EtCO₂), hemoglobin oxygen saturation (SaO₂), respiratory rate (RR), heart rate (HR), and arterial blood pressure (BP) were monitored throughout the experiment.

Results. The EtCO₂, SaO₂ and diastolic BP increased with carbogen, ($p=0.0001$) while both RR and HR were reduced ($p\leq 0.0005$). The implicit times of all ERG components remained stable throughout the experiment. The amplitude of OP1 to OP4 did not vary, whereas OP5 decreased by 23.66% with carbogen and by 21.85% at the end of the experiment. No change was found in the amplitude of the a-wave, whereas the b-wave was reduced by 9.19% ten minutes after the end of carbogen breathing ($p=0.0001$).

Conclusions. OP5 may be more sensitive than the other ERG components to an hypercapnia-induced reduction in arteriolar / retinal pH. The alteration of the OP5 and b-wave amplitudes 10 minutes after the end of carbogen breathing may be due to a slower recovery of pH after hypercapnia, in spite of a low EtCO₂.

Key words: electroretinogram, oscillatory potentials, carbogen, hypercapnia, hyperoxia.

INTRODUCTION

Carbogen, a gas mixture containing 4-7% carbon dioxide (CO_2) and 93-96% oxygen (O_2) is used clinically as an emergency procedure for the management of central retinal artery occlusion (CRAO). The rationale is that the stimulating effect of CO_2 on the ocular hemodynamics (1-12) should counteract the inhibitory effects of O_2 on blood vessel diameter (13-16) and blood flow (4, 14, 15), and improve oxygenation to the retina.

In animals, carbogen breathing was found to alter the b-wave (17, 18) and increase the c-wave amplitude (17) of the ERG. To our knowledge, however, no study has investigated the effects of carbogen breathing on retinal function in man.

In a parallel study (19), we have shown that the a and b-waves of the scotopic ERG in healthy young adults were not affected during pure O_2 breathing, but were depressed shortly after 100% O_2 breathing was stopped. We proposed that this « after-effect » may have reflected a « pseudo-hypoxic » condition within the retina, subsequent to a sudden decrease of O_2 concentration in the inspired air after a short period of hyperoxia.

The purpose of this study was to investigate the impact carbogen breathing has on the human ERG and OPs, and to evaluate whether the addition of CO_2 to O_2 may prevent the after-effect of pure O_2 on the ERG a and b-waves reported previously.

MATERIAL & METHODS

Subjects

Eighteen healthy young adults (9 males, 9 females) between 18 and 26 years of age volunteered for this study. All subjects had 20/20 or better corrected monocular visual acuity and were free of any ocular or systemic disease. Written informed consent was obtained from each subject after all experimental procedures had been explained. All aspects of the experiment had been approved by the Office for Human Research of our institution.

Recording the retinal potentials

The subject was comfortably seated on an adjustable ophthalmic chair. The pupil of the right eye was dilated with 1 drop of cyclopentolate HCl 1%, and the eye was then covered with a light-tight patch and dark adapted for 30 minutes in dim room illumination. Pregelled Ag/AgCl electrodes were applied on the skin near the temporal canthus of the right eye and on the inner wrist to serve as the reference electrode and electrical ground, respectively. Just prior to any recording, all illumination in the room was turned off and the eye-patch was transferred to the left eye. A dim yellow light was then turned on to facilitate subsequent manipulations by the experimenter without changing the state of adaptation of the eye to be tested. A Jet type electrode filled with methylcellulose was placed on the anesthetized cornea (1-2 gtt proparacaine HCl 0.5%). The impedance of all electrodes was kept below 5 k Ω . The yellow light was turned off again and the subject was asked to fixate a low intensity red LED in the center of a darkened Ganzfeld bowl. An air circulation system was turned on in the Ganzfeld bowl throughout the experiment to improve the subject's comfort and ensure that rebreathing of expired CO₂ by the subject, if any, was minimal during recordings effected without the face mask. To verify the quality and

repeatability of the ERG and OP recordings, two consecutive series of 15 white flashes (100 ms epochs) delivered by a Grass PS22 stroboscope (Grass Instruments, Quincy, MA) were presented to the right eye at a frequency of 0.3 Hz. The simultaneously recorded ERG and OP electrical signals were amplified by a Nicolet Biomedical CA-1000 clinical averager. The signals were then fed through an external analog filter with low and high band-pass filters adjusted to 1 and 250 Hz for the ERG signals, and to 75 and 250Hz for the OP components. Scotopic ERGs and OPs were recorded: 1) during normal room air breathing (baseline), 2) at the end of a 10 minute period of carbogen breathing, 3) immediately after removing the mask, and 4) 10 minutes later (recovery).

The amplitude of each retinal waveform was taken as the difference in voltage between its peak and the preceding trough. The implicit time was considered as the time difference between the presentation of the stimulus and the peak of the wave.

Carbogen breathing

Carbogen from a cylinder tank containing 5% CO₂ and 95% O₂ was administered through high concentration disposable oxygen masks with a one-way valve and a 1L reservoir bag (Inspiron, Intertech Resources Inc.) modified beforehand to optimize airtightness. To that effect, tape was applied on the holes of one side of the mask, to reduce the amount of room air penetration during the inspiration. For similar purposes, the rubber valve covering the holes on the other side of the mask was enlarged with a bigger soft plastic disc. Care was taken to ensure that these holes were not blocked, thus allowing easy evacuation of the expired gas through the valve and avoiding a build-up of pressure inside the mask. The flow rate of carbogen was started at 8.5 L/minute, and adjusted for each subject according to the speed at which the reservoir bag was deflated and inflated during the respiratory cycle. Our

pilot studies have shown that a 10 minute period of carbogen breathing was adequate to ensure the stabilization of the end-tidal CO_2 (EtCO_2). The experiment was conducted at sea level atmospheric pressure.

Physiological variables

The heart rate (HR), hemoglobin oxygen saturation level (SaO_2), EtCO_2 and respiratory rate (RR) were monitored throughout testing, and recorded every 8 seconds with a $\text{EtCO}_2/\text{SaO}_2$ monitor (model 7100, CO_2SMO , Novametrix, Medical Systems Inc.). A sensor was placed on one finger to estimate the SaO_2 and HR by pulse oximetry.

A disposable nasal cannula (no 1606, Salter Labs, Arvin, California) was connected to the monitor for EtCO_2 and RR monitoring. The tips of the two tubes of the cannula inserted in the nostrils were cut whenever required to fit a subject's nose. The subject was asked to breathe as normally as possible by the nose only, to enable a portion of the expired gas to be evacuated by the cannula, and collected and analysed by the capnograph. The remaining of the expired gas was evacuated through the one-way valve on the side of the face mask.

The arterial BP was monitored with a 90601 SpaceLabs monitor (SpaceLabs, Inc., Redmond, WA). Two consecutive measurements of systolic, diastolic and mean arterial BP were started 2 to 3 minutes before the ERG recording for all experimental conditions, except the removal of the mask. For this latter condition, arterial BP measurements were not performed in view of the tight time constraints of the experimental protocol.

Statistical analyses

Analyses of variance (ANOVAs) procedures were used for comparison of data between test conditions and across subjects. The differences were considered to be significant at an alpha level of 0.05.

RESULTS

Physiological variables

Carbogen breathing was well tolerated by all subjects. The EtCO₂ was increased by a mean of 7.05% during carbogen breathing ($p=0.0001$). As soon as the mask was removed, the mean EtCO₂ among subjects was 4.4% lower than its initial value in room air, and had not recovered fully yet 10 minutes after the end of carbogen breathing. A typical curve of EtCO₂ as a function of time within the experiment is illustrated in Figure1 for one subject.

The mean SaO₂ increased from 97.2% to 98.5% during carbogen breathing, decreased to 97.9% as soon as the mask was removed, to finally recover baseline values (97.2%) within 10 minutes of normal room air breathing ($p=0.0001$).

The RR decreased from 17.7 to 16.3 breaths/minute during carbogen breathing, increased to 18.9 breaths/minute when the mask was removed and returned to 17.6 breaths/minute after 10 minutes in room air ($p=0.0001$).

The HR was reduced from 75.5 to 73.5 bpm during carbogen breathing, and was restored and maintained to its baseline value thereafter as soon as the mask was removed ($p=0.0005$).

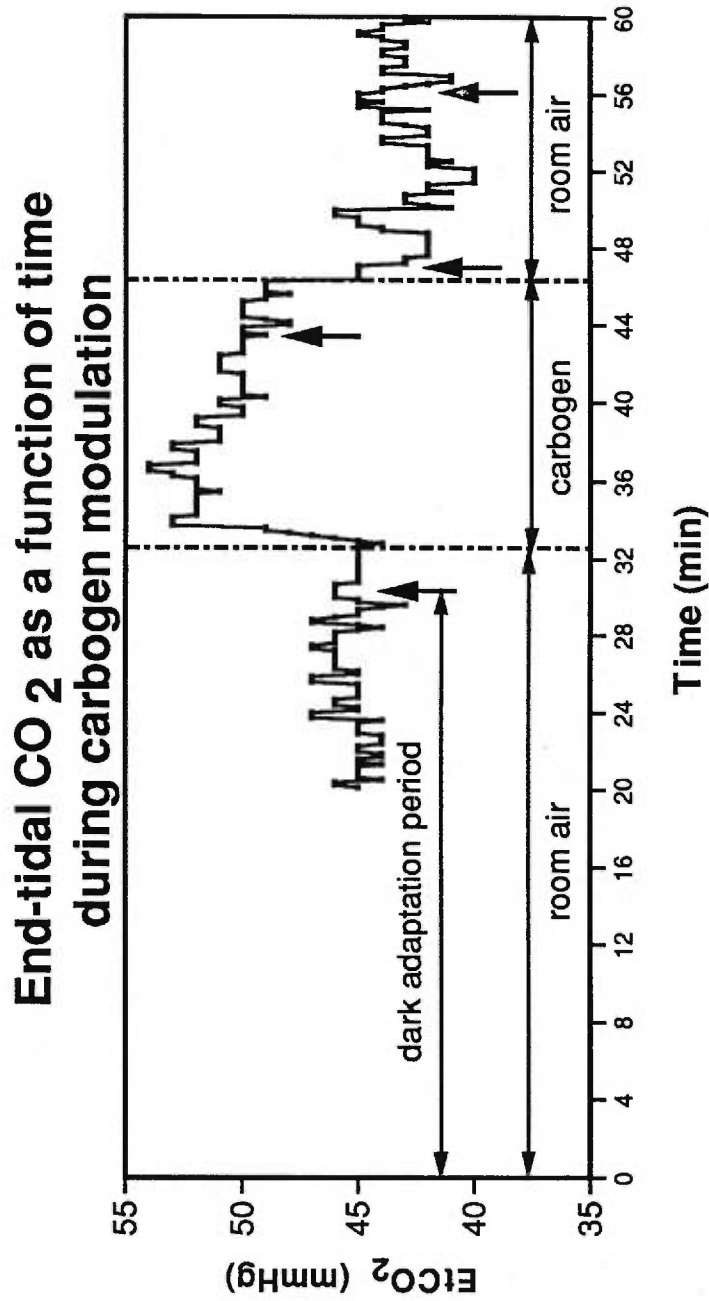


Figure 1. The end-tidal CO₂ monitoring was started ten minutes before the end of the 30 minute dark adaptation period. The vertical arrows indicate when the ERG recordings were started for each test condition.

All subjects had normal arterial blood pressures. The systolic and mean arterial BP remained stable throughout the experiment, whereas the diastolic BP increased from 72.3 to 74.9 mm Hg during carbogen breathing ($p=0.0001$).

Electrophysiological findings

All electrical potentials were analysed in their amplitude and time domains. The amplitude and implicit time of the a-wave were not altered throughout testing. Figure 2a illustrates the ERG waveform recorded for one subject at baseline and 10 minutes after the end of carbogen breathing. The implicit time of the b-wave remained unchanged throughout the experiment. The b-wave amplitude was not affected during carbogen breathing, neither immediately after the removal of the mask. However, an ANOVA ($p=0.0001$) performed over the a and b-wave amplitudes indicated that 10 minutes after the end of carbogen breathing, the b-wave amplitude was 9.2% lower than it was at the beginning of the experiment (Figure 3).

In all subjects, 5 OP wavelets were extracted from the ascending portion of the b-wave for all 4 conditions. The implicit times of all OPs, as well as the amplitudes of OP1 to OP4 remained stable throughout the experiment. The ANOVA ($p=0.0001$) performed across all OP amplitudes showed that the amplitude of OP5, however, was reduced from 34.5 to 26.3 μV (-23.7%) during carbogen breathing, was back to its baseline value when the mask was removed (30.6 μV), and was lowered again to 26.9 μV (-21.9% compared to baseline) 10 minutes later. This is illustrated in Figure 4, and in Figure 2b for one subject.

The impact of carbogen breathing on the scotopic ERG b-wave and OP5

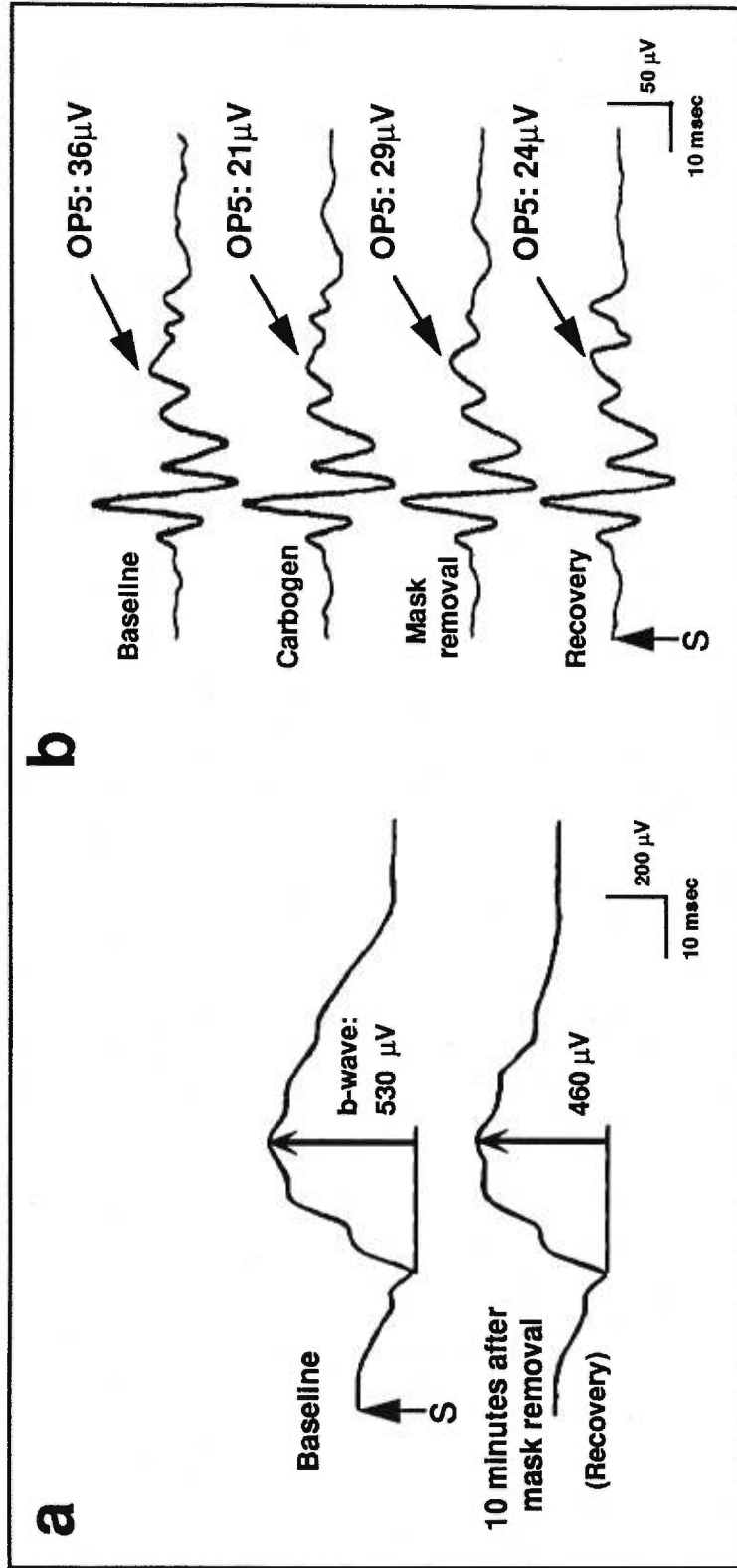


Figure 2. a) ERG waveform recorded for one subject at baseline and 10 minutes after the end of carbogen breathing. b) Variation of OP5 amplitude through the experiment for the same subject as in a. S: stimulus.

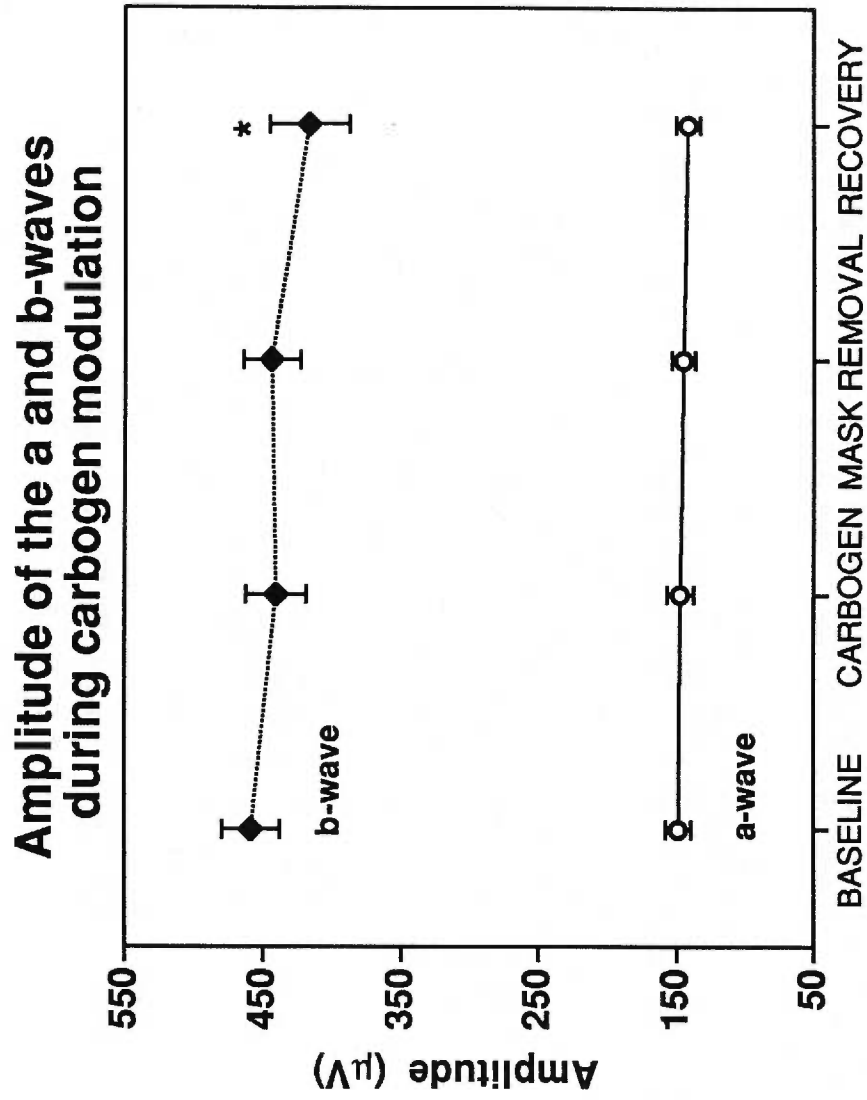


Figure 3. Amplitude of the ERG a and b-waves throughout the experiment. The asterisk indicates data differing from baseline; the error bars illustrate the standard error of the mean.

Amplitude of the oscillatory potentials during carbogen modulation

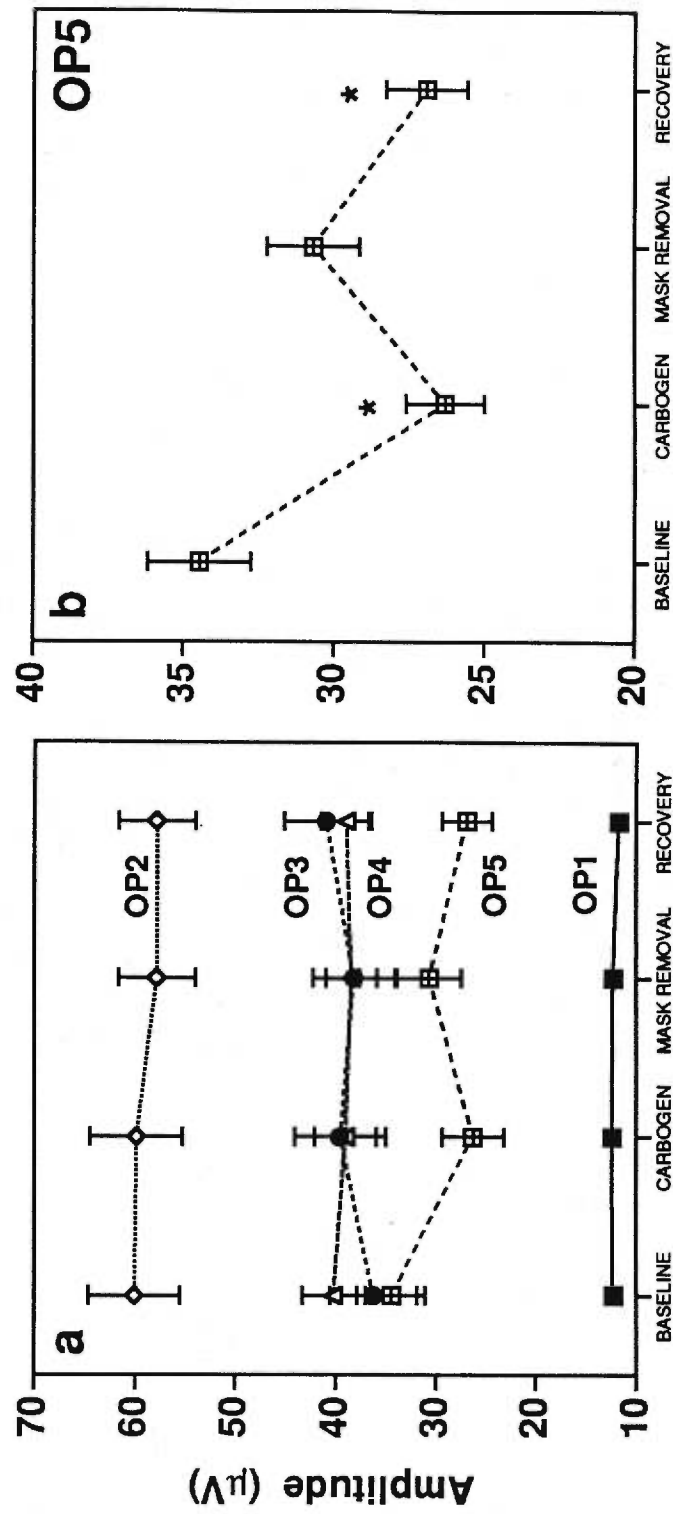


Figure 4. a) Amplitude of the OPs for the various test conditions. b) Variation of OP5 amplitude throughout the experiment. The asterisks indicate data differing from baseline.

DISCUSSION

Physiological variables

The increase in both SaO_2 and EtCO_2 indicates that systemic hyperoxia and hypercapnia were achieved during carbogen breathing. In the normal, healthy, conscious subject, the EtCO_2 is a good index of alveolar PCO_2 (20), and there is a strong relationship between EtCO_2 and arterial pH. Systemic hypercapnia decreases both the arterial (21, 22, 23) and tissue (21, 22, 24) pH. CO_2 is the main factor influencing intracellular pH, which in turn strongly affects cellular metabolism. While the pH was not monitored in the present experiment, previous studies have shown that it decreases during carbogen breathing (17, 25).

The HR and RR were both reduced during carbogen breathing, replicating data previously obtained in our laboratory (12). O_2 and CO_2 usually have opposite effects on the respiratory function and cardiovascular system. O_2 normally reduces the ventilation (24) and heart rate (11, 26). The ventilatory response to CO_2 varies greatly among normal subjects (24), but moderate hypercapnia usually stimulates both the ventilation (24) and HR (20). Data on the systemic response of the cardiovascular and respiratory systems to carbogen are limited. Our results of a reduced HR and RR therefore suggest that the high O_2 content of carbogen probably had a greater influence than CO_2 on these physiological variables.

Only the diastolic BP was significantly increased during carbogen breathing. Arterial BP is usually stable during systemic hyperoxia (11, 27, 28). The response of the arterial blood pressure to hypercapnia varies among subjects (20). It generally increases (8, 10, 11,20) or remains

unchanged (9, 28). Our increase in diastolic BP may therefore have been linked to the CO₂ content of carbogen.

Electrophysiological findings

1) During carbogen breathing

The ERG a and b-waves

Neither the a-wave, reflecting photoreceptor activity, nor the b-wave, originating from the inner layers of the retina, were affected during carbogen breathing and its associated increase in SaO₂ and EtCO₂. Animal studies have shown that hypercapnia with or without hyperoxia is accompanied by a reduction in the ERG b-wave amplitude (17, 18, 22, 29, 30) and in the light peak (22, 29), and by an increase in the c-wave amplitude (17, 22, 29, 30). To our knowledge, no data exist in man for comparison. The results of the present study however parallel our recent findings showing that systemic hyperoxia does not alter the ERG a and b-waves (19), but contrasts with previous results reported in animals during systemic hypercapnia. Animal studies however, are generally conducted under anesthesia, neuromuscular block and mechanical ventilation. Furthermore, some anesthetic agents impair blood flow (31,32), cerebrovascular responses to CO₂ (33) and microvascular O₂ delivery (32). Most anesthetics, as well as spinal analgesia also impair the cardiovascular response to increased PCO₂ (20). Moreover, other pharmacological agents used in animal studies, as well as mechanical ventilation, may perturb the pulmonary function, cardiovascular system and central nervous system, and therefore influence the basal electrical activity of the retina in response to light stimulation. All manipulations performed in the present study were noninvasive, and the results obtained are certainly closer to the clinical situation where carbogen is administered to a patient for the management of a pathological condition.

If increased arterial levels of CO₂ have in fact a detrimental effect on retinal activity by a direct action on cell metabolism, it might be that the hypercapnia-induced increase in both retinal (2, 4, 5, 8, 9) and choroidal (1-3, 6, 7, 10-12) blood flow helps to eliminate the excess of CO₂ and to improve retinal oxygenation (25, 34), and therefore counterbalances that depressing effect.

Oscillatory potentials

OP1 through OP4, as was the case for the a and b-waves, remained stable during the carbogen breathing period, whereas OP5 was reduced in amplitude in all subjects, except one. It would appear therefore that the inner retinal function was not totally preserved during systemic hypercapnia. OP5 was more susceptible than the other OPs and the b-wave to the physiologic stress brought about by carbogen. OP5 is not affected by pure O₂ breathing (19). Therefore, it is unlikely that the O₂ content of carbogen was responsible for its attenuation in the present study. CO₂, on the other hand, is known to decrease the intracellular pH (22, 24) and may have influenced the electrical activity of the generators of OP5.

Other studies have shown that OP5 was particularly sensitive to changes in the ocular perfusion pressure, while the other OPs were little or not modified (35-37). A reduction in OP5 amplitude was also reported during physical exercise (38), which can lead to both metabolic acidosis and changes in the ocular perfusion pressure. The unique behavior of OP5 to carbogen breathing once again points to its enhanced sensitivity to conditions altering normal physiology. The component-specific alteration of one wavelet of the OP-complex supports the more widely accepted notion that individual OPs are separated entities that may react differently to similar stress or stimuli (35, 38-44).

2) After carbogen breathing

The ERG a-wave

The a-wave remained unchanged throughout the experiment. In a parallel study (19), we have shown that the a-wave was not affected during 100% O₂ breathing, but was reduced and delayed 10 minutes after the end of hyperoxia. It was suggested that a « pseudo-hypoxic » condition was induced by a sudden decrease in the O₂ supply to the retina. In the present study, the a-wave was not affected 10 minutes after the end of carbogen breathing, even though the O₂ administration was suddenly reduced from 95% (carbogen) to 21% (air). Likely, the addition of CO₂ to the hyperoxic gas preserved photoreceptor function and prevented the attenuation of the a-wave after systemic hyperoxia. An increase in choroidal blood flow may have contributed to the preservation of the a-wave. Elevated arterial CO₂ increases choroidal blood flow in animals (1-3, 7, 45). In humans, CO₂ alone (6, 10) or as a carbogen mixture (11) increases choroidal blood flow within the macula. Carbogen also increases the pulsatile ocular blood flow in man (12). The increase in blood flow with carbogen breathing is accompanied by a better oxygenation of the outer retina (25, 34) and likely reduces or prevents the installation of the « pseudo-hypoxic » condition previously reported after pure O₂ breathing. This could explain the preservation of the a-wave integrity throughout the experiment.

The ERG b-wave

The b-wave was reduced in amplitude 10 minutes after the end of carbogen breathing, even though by then the EtCO₂ was reduced slightly below its normal value. This reduction in the b-wave amplitude, observed in two thirds of our subjects, is qualitatively similar, but quantitatively larger than the one reported earlier with pure O₂ breathing (9% vs 6%).

This might be attributed to CO₂/pH perturbations. Hypercapnia reduces the arterial and tissue pH (22-24). Tsacopoulos and Levy (46) have shown that the pH within the inner retinal layers takes 10 to 13 minutes after the end of CO₂ administration to recover its baseline value. The outer retinal pH was not evaluated by Tsacopoulos and Levy (46), but Hiroi et al. (30) hypothesized that it would recover more rapidly than within the inner retina because of the higher blood flow in the choroid compared to the retinal blood flow. Similarly, this time differential in pH normalization could explain the preservation of the a-wave integrity after carbogen breathing in the presence of an altered b-wave.

Alternatively, if one assumes a similar recovery pattern of pH within the outer and inner retinal layers, the reduction in the b-wave amplitude while the response of the photoreceptors is preserved may simply indicate a higher sensitivity of the inner retina to acidosis, as suggested in earlier reports (29, 30).

Oscillatory potentials

OP1 to OP4 remained stable after carbogen breathing was stopped, maintaining their baseline values. The amplitude of OP5 was restored to baseline as soon as carbogen breathing was stopped, but was lowered again 10 minutes later for most of the subjects. As soon as the mask was removed, the EtCO₂ dropped rapidly, while the SaO₂ remained higher than its baseline value in room air. Also, it is likely that retinal blood flow, which increases with CO₂ breathing (2, 4, 5, 8, 9) was still higher than baseline value, in view of the very short period of time elapsed between the removal of the mask and the beginning of the ERG recording (<15 seconds). The combined effect of a low EtCO₂, high SaO₂ and high retinal blood flow may have contributed to adequate

oxygenation and perfusion of the retina, therefore normalizing the electrical signal derived from the neural generators of OP5.

The subsequent reduction in OP5 amplitude 10 minutes after it just recovered to baseline value was unexpected. Since no change in OP5 was observed during or after pure O₂ breathing (19), an hyperoxia-induced after-effect can not explain this finding. The SaO₂ had recovered to baseline values, and it is likely that any change in retinal blood flow would also have normalized by then. The reduction in both SaO₂ and retinal blood flow after the end of carbogen breathing, possibly combined with a lower retinal pH than before hypercapnia (46) may be involved in the attenuation of OP5 10 minutes after the end of carbogen breathing.

Furthermore, it has been suggested that a sudden decrease in PCO₂ after a period of systemic hypercapnia results in a further elevation of the plasma catecholamine level than the one already present during the CO₂ breathing period (20). It was also suggested that variations in plasma catecholamines might have been involved in the attenuation of OP5 found after physical exercise (38). It might be that catecholamines may also play a role in the electrophysiological changes reported here, subsequent to systemic hypercapnia.

CONCLUSIONS

In summary, our results have shown that the addition of CO₂ to O₂ can prevent the O₂-induced impairment in the dark adapted photoreceptor electrical activity (the a-wave) reported earlier. Carbogen breathing however decreases the amplitude of OP5, and is also

accompanied by a decrease in the b-wave and OP5 amplitudes 10 minutes after its administration is stopped.

Since there are numerous clinical applications of carbogen therapy (20, 47, 48), further investigations are required to better detail the impact of carbogen breathing on retinal function, as well as the timing characteristics of such alterations to insure that prolonged therapy is not detrimental to neural function.

ACKNOWLEDGEMENTS

We thank all our subjects for their participation. This work was supported by a Fonds de la recherche en santé du Québec post-graduate fellowship to CF; by the Canadian Optometric Education Trust Fund to CF and HK; and by the Natural Sciences and Engineering Research Council operating and equipment grants to HK.

REFERENCES

1. Trokel S. Effect of respiratory gases upon choroidal hemodynamics. *Arch Ophthalmol* 1965; 73:838-42.
2. Alm A, Bill A. The oxygen supply to the retina, II. Effects of high intraocular pressure and of increased arterial carbon dioxide tension on uveal and retinal blood flow in cats. *Acta Physiol Scand* 1972; 84:306-19.
3. Friedman E, Chandra SR. Choroidal blood flow III. Effects of oxygen and carbon dioxide. *Arch Ophthalmol* 1972; 87:70-1.
4. Sponsel WE, DePaul KL, Zetlan SR. Retinal hemodynamic effects of carbon dioxide, hyperoxia, and mild hypoxia. *Invest Ophthalmol Vis Sci* 1992; 33:1864-9.
5. Arend O, Harris A, Martin BJ, Holin M, Wolf S. Retinal blood velocities during carbogen breathing using scanning laser ophthalmoscopy. *Acta Ophthalmol* 1994; 72:332-6.
6. Riva CE, Cranstoun SD, Grunwald JE, Petrig BL. Choroidal blood flow in the foveal region of the human ocular fundus. *Invest Ophthalmol Vis Sci* 1994; 35:4273-81.
7. Flower RW, Fryczkowski AW, McLeod DS. Variability in choriocapillaris blood flow distribution. *Invest Ophthalmol Vis Sci* 1995; 36:1247-58.
8. Harino S, Grunwald JE, Petrig BJ, Riva CE. Rebreathing into a bag increases human retinal macular blood velocity. *Br J Ophthalmol* 1995; 79:380-3.
9. Harris A, Arend O, Wolf S, Cantor LB, Martin BJ. CO₂ dependence of retinal arterial and capillary blood velocity. *Acta Ophthalmol Scand* 1995; 73:421-4.
10. Schmetterer L, Wolzt M, Lexer F, Alschinger C, Gouya G, Zanaschka G, Fassolt A, Eichler HG, Fercher AF. The effect of hyperoxia and hypercapnia on fundus pulsations in the macular and optic disc region in healthy young men. *Exp Eye Res* 1995; 61:685-90.
11. Schmetterer L, Lexer F, Findl O, Graselli U, Eichler HG, Wolzt M. The effect of inhalation of different mixtures of O₂ and CO₂ on ocular fundus pulsations. *Exp Eye Res* 1996; 63:351-5.

12. Kergoat H, Faucher C. Carbogen breathing increases the pulsatile ocular blood flow. *Optom Vis Sci* 1997; 74. Abstract accepted for publication.
13. Deutsch TA, Read JS, Ernest JT, Goldstick TK. Effects of oxygen and carbon dioxide on retinal vasculature in humans. *Arch Ophthalmol* 1983; 101:1278-80.
14. Fallon TJ, Maxwell DL, Kohner EM. Retinal vascular autoregulation in conditions of hyperoxia and hypoxia using the blue field entoptic phenomenon. *Ophthalmology* 1985; 92:701-5.
15. Pakola SJ, Grunwald JE. Effects of oxygen and carbon dioxide on human retinal circulation. *Invest Ophthalmol Vis Sci* 1993; 34:2866-70.
16. Bachmann K, Vilser W, Riemer TH, Strobel J, Lang GE. The effect of oxygen-inhalation on retinal vessels. *Invest Ophthalmol Vis Sci* 1997; 38:s779.
17. Niemeyer F, Nagahara K, Demant E. Effects of change in arterial PO_2 and PCO_2 on the electroretinogram in the cat. *Invest Ophthalmol Vis Sci* 1982; 23:678-83.
18. Dawson WW, Parmer R, Hope GM. Division of the pattern-evoked retinal response by respiratory acidosis. *Vis Res* 1988; 28:363-9.
19. Faucher C., Kergoat H. Component-specific changes in the oscillatory potentials during transient systemic hyperoxia. *Invest Ophthalmol Vis Sci* 1997; 38: s888.
20. Nunn JF. *Nunn's applied respiratory physiology*, 4th ed. Oxford: Butterworth-Heinemann, 1993.
21. Lassen NA. Brain extracellular pH: the main factor controlling cerebral blood flow. *Scand J Clin Lab Invest* 1968; 22:247-51.
22. Linsenmeier RA, Mines AH, Steinberg RH. Effects of hypoxia on the light peak and electroretinogram of the cat. *Invest Ophthalmol Vis Sci* 1983; 24:37-46.
23. Tortora GJ, Grabowski SR. *Principes d'anatomie et de physiologie*, nouvelle édition. Anjou: CEC collégial et universitaire, 1994.

24. Dempsey JA, Pack AI, eds. Regulation of breathing, 2nd edition. New York: Marcel Decker Inc., 1995 (Lenfant C, ed. Lung biology in health and disease, vol 79).
25. Berkowitz BA. Adult and newborn rat inner retinal oxygenation during carbogen and 100% oxygen breathing. Comparison using magnetic resonance imaging PO₂ mapping. Invest Ophthalmol Vis Sci 1996; 37: 2089-98.
26. Dripps RD, Comroe JH Jr. The effect of the inhalation of high and low oxygen concentrations on respiration, pulse rate, ballisto-cardiogram and arterial oxygen saturation (oximeter) of normal individuals. Am J Physiol 1947; 149:277-91.
27. Riva CE, Grunwald JE, Sinclair SH. Laser Doppler velocimetry study of the effect of pure oxygen breathing on retinal blood flow. Invest Ophthalmol Vis Sci 1983; 24:47-51.
28. Harris, A, Anderson DR, Pillunat L, Joos K, Knighton RW, Kagemann L, Martin BJ. Laser Doppler flowmetry measurement of changes in human optic nerve head blood flow in response to blood gas perturbations. J Glaucoma 1996; 5:258-65.
29. Niemeyer G, Steinberg RH. Differential effects of pCO₂ and pH on the ERG and light peak of the perfused cat eye. Vis Res 1984; 24:275-80.
30. Hiroi K, Yamamoto F, Honda Y. Analysis of electroretinogram during systemic hypercapnia with intraretinal K⁺-microelectrodes in cats. Invest Ophthalmol Vis Sci 1994; 35:3957-61.
31. Lee JG, Hudetz AG, Smith JJ, Hillard CJ, Bosnjak ZJ, Kampine JP. The effects of halothane and isoflurane on cerebrocortical microcirculation and autoregulation as assessed by laser-Doppler flowmetry. Anesthesia & Analgesia 1994; 79:58-65.
32. Kerger H, Saltzman DJ, Gonzales A, Tsai AG, van Ackern K, Winslow RM, Intaglietta M. Microvascular oxygen delivery and interstitial oxygenation during sodium pentobarbital anesthesia. Anesthesiology 1997; 86:372-86.
33. Lee JG, Smith JJ, Hudetz AG, Hillard CJ, Bosnjak ZJ, Kampine JP. Laser-Doppler measurement of the effects of halothane and isoflurane on the cerebrovascular CO₂ response in the rat. Anesthesia & Analgesia 1995; 80:696-702.

34. Yu DY, Cringle SJ, Alder VA, Su EN, Yu PK. Intraretinal oxygen distribution and choroidal regulation in the avascular retina of guinea pigs. *Am J Physiol* 1996; 270:H965-H973.
35. Kergoat H, Lovasik JV. The effects of altered retinal vascular perfusion pressure on the white flash scotopic ERG and oscillatory potentials in man. *Electroencephalogr Clin Neurophysiol* 1990; 75:306-22.
36. Lovasik JV, Kergoat H. Influence of transiently altered retinal vascular perfusion pressure on rod/cone contribution to scotopic oscillatory potentials. *Ophthalmol Physiol Opt* 1991; 11:370-80.
37. Lovasik JV, Kothe AC, Kergoat H. Improving the diagnostic power of electroretinography by transient alteration of the ocular perfusion pressure. *Optom Vis Sci* 1992; 69: 85-94.
38. Kergoat H, Forcier P. Correlation of an exercise-induced increase in systemic circulation with the neural retinal function in humans. *Doc Ophthalmol* 1996; 92:145-57.
39. Wachtmeister L. Further studies of the chemical sensitivity of the oscillatory potentials of the electroretinogram (ERG). I. GABA and glycine antagonists. *Acta Ophthalmol* 1980; 58:712-25.
40. Wachtmeister L. Further studies of the chemical sensitivity of the oscillatory potentials of the electroretinogram (ERG). II. Glutamate, aspartate and dopamine antagonists. *Acta Ophthalmol* 1980; 59:247-58.
41. Wachtmeister L. Further studies of the chemical sensitivity of the oscillatory potentials of the electroretinogram (ERG). III. Some Ω amino acids and ethanol. *Acta Ophthalmol* 1980; 59:609-19.
42. Coupland SG. Oscillatory potential changes related to stimulus intensity and light adaptation. *Doc Ophthalmol* 1987; 66:195-205.
43. Tremblay F, Lam SR. Distinct electroretinographic oscillatory potential generators as revealed by field distribution. *Doc Ophthalmol* 1993; 84:279-89.
44. Lachapelle P, Benoit J, Guité P. The effect of in vivo retinal cooling on the electroretinogram of the rabbit. *Vis Res* 1996; 36:339-44.
45. Flower RW, Klein GJ. Pulsatile flow in the choroidal circulation: a preliminary investigation. *Eye* 1990; 4:310-8.

46. Tsacopoulos M, Levy S. Intraretinal acid-base studies using pH glass microelectrodes: effect of respiratory and metabolic acicosis and alkalosis on inner-retinal pH. *Exp Eye Res* 1976; 23:495-504.
47. Laurence VM, Ward R, Dennis IF, Bleehen NM. Carbogen breathing with nicotinamide improves the oxygen status of tumours in patients. *Br J Cancer* 1995; 72:198-205.
48. Cerniglia GJ, Wilson DF, Pawlowski M, Vinogradov S, Biaglow J. Intravascular oxygen distribution in subcutaneous 9L tumors and radiation sensitivity. *J Appl Physiol* 1997; 82:1939-1945.

CONCLUSIONS

FLOT SANGUIN OCULAIRE PULSATILE ET RÉTINE EXTERNE

Le FSOP, qui est un indice global représentant principalement la circulation choroïdienne, n'a pas été affecté par la respiration d'oxygène pur. Cependant, l'ajout de 5% de CO₂ à l'oxygène a eu pour effet d'augmenter le FSOP de près de 8%.

La choroïde irrigue les couches externes de la rétine, soit l'ÉPR et les photorécepteurs, la réponse de ces derniers ayant été évaluée par l'onde a de l'ERG scotopique. Les conditions d'adaptation de la rétine lors des expériences sur le FSOP et l'électrophysiologie rétinienne étant différentes (photopique vs scotopique), on ne peut relier directement les résultats obtenus pour chacune des expériences. Nous pouvons à tout le moins tenter d'établir certaines relations.

La stabilité du FSOP lors de l'inspiration d'oxygène pur a probablement contribué à la préservation de l'onde a, tandis que l'augmentation du FSOP en présence de CO₂ aurait servi à optimiser l'oxygénation des couches externes de la rétine, tout en favorisant l'élimination du CO₂ en excès et donc la ré-équilibration du pH rétinien.

L'altération du signal électrique provenant des photorécepteurs, l'onde a de l'ERG, 10 minutes après la fin de l'hyperoxie systémique était inattendue. Nous avons suggéré la possibilité de l'installation d'une condition de « pseudo-hypoxie » rétinienne occasionnée par la réduction subite de la concentration de l'oxygène administré de 100 à 21% (air ambiant). L'addition de 5% de CO₂ à l'oxygène (carbogène) a permis une augmentation du FSOP, qui a possiblement empêché la création de cet effet de « pseudo-hypoxie » rétinienne, tel que démontré

par la préservation de l'onde a après la période de respiration de carbogène.

La comparaison de nos résultats avec des courbes obtenues lors d'enregistrements d'ERG à différents niveaux d'O₂ inférieurs à 21% afin de créer un état d'hypoxie permettrait de vérifier en partie notre hypothèse de « pseudo-hypoxie » rétinienne. De plus, étant donné que la rétine consomme une plus grande quantité d'O₂ en conditions scotopiques que photopiques, l'enregistrement d'ERG à la lumière pourrait apporter des informations supplémentaires concernant cet « après-effet » rapporté pour la première fois.

RÉTINE INTERNE

Les couches internes de la rétine sont nourries par la circulation rétinienne en provenance de l'artère centrale de la rétine, que nous n'avons pas investiguée dans le cadre de ce travail, mais dont les réactions aux variations des concentrations sanguines en O₂ et CO₂ sont bien documentées. L'évaluation des POs et de l'onde b de l'ERG nous a permis d'évaluer la fonction neuronale des cellules situées dans les couches plus internes de la rétine.

Les POs ont été les seules composantes de l'ERG à être affectées pendant la respiration d'oxygène et de carbogène, démontrant leur sensibilité accrue aux variations métaboliques et vasculaires à l'intérieur de la rétine. Une augmentation de l'amplitude d'OP3 a en effet été constatée lors de l'inspiration d'oxygène pur, tandis que la respiration de carbogène a entraîné une réduction de l'amplitude d'OP5. La réaction différente des POs individuels selon les gaz utilisés appuie une notion de

plus en plus acceptée, selon laquelle les POs seraient des entités de différentes origines.

L'onde b de l'ERG est générée en rétine interne par les neurones de deuxième ordre et/ou les cellules de Müller. Nous avons suggéré que son altération après l'inspiration d'oxygène pur était probablement liée à l'altération de l'onde a générée par les photorécepteurs, neurones de premier ordre. Par contre, la réduction de l'amplitude d'OP5 et de l'onde b après la fin de la période de respiration de carbogène sans que l'onde a ne soit affectée indique que les effets du carbogène sur l'électrophysiologie rétinienne ont été limités à la rétine interne. Ces résultats peuvent démontrer soit que la circulation sanguine rétinienne est moins efficace que la choroïde pour éliminer le CO_2 et rétablir le pH rétinien, ou que la rétine interne est plus sensible aux perturbations de pH causées par l'augmentation de la concentration de CO_2 dans le sang.

L'ensemble de ces résultats nous amène à conclure que l' O_2 a peu d'effet sur la circulation choroïdienne, mais que le CO_2 agit sur la choroïde de la même façon que sur les vaisseaux sanguins rétiniens et cérébraux. De plus, bien que l'oxygène pur et le carbogène aient peu d'influence sur l'activité électrique de la rétine durant leur utilisation, certaines composantes de l'ERG sont affectées quelques minutes après la fin de leur administration. Il importe donc de poursuivre les études à ce sujet afin de déterminer objectivement la fonction rétinienne à différents intervalles de temps suivant l'arrêt de la respiration de ces gaz, dont les utilités cliniques sont variées.

BIBLIOGRAPHIE

- Alm A, Bill A. The oxygen supply to the retina, II. Effects of high intra-ocular pressure and of increased arterial carbon dioxide tension on uveal and retinal blood flow in cats. *Acta Physiol Scand* 1972; 84:306-19.
- Arend O, Harris A, Martin BJ, Holin M, Wolf S. Retinal blood velocities during carbogen breathing using scanning laser ophthalmoscopy. *Acta Ophthalmol* 1994; 72:332-6.
- Bachmann K, Vilser W, Riemer TH, Strobel J, Lang GE. The effect of oxygen-inhalation on retinal vessels. *Invest Ophthalmol Vis Sci* 1997; 38:s779.
- Bereczki D, Wei L, Otsuka T, Hans FJ, Acuff V, Patlak C, Fenstermacher J. Hypercapnia slightly raises blood volume and sizably elevates flow velocity in brain microvessels. *Am J Physiol* 1993; 264:H1360-H1369.
- Berkowitz BA. Adult and newborn rat inner retinal oxygenation during carbogen and 100% oxygen breathing. Comparison using magnetic resonance imaging PO₂ mapping. *Invest Ophthalmol Vis Sci* 1996; 37:2089-98.
- Berson EL. Electrical phenomena in the retina. In: Hart WM, ed. *Adler's physiology of the eye, clinical application*. St.Louis: Mosby Year Book, 1992:641-707.
- Bill A. Blood circulation and fluid dynamics in the eye. *Physiol Rev* 1975; 55:383-417.
- Bill A, Nilsson SFE. Control of ocular blood flow. *J Cardiovascular Pharm* 1985; 7(suppl. 3):s96-102.
- Bill A, Sperber GO. Control of retinal and choroidal blood flow. *Eye* 1990; 4:319-25.
- Braun RD, Linsenmeier RA. Retinal oxygen tension and the electroretinogram during arterial occlusion in the cat. *Invest Ophthalmol Vis Sci* 1995; 36:523-41.
- Bresnick GH, Korth K, Groo A, Palta M. Electroretinographic oscillatory potentials predict progression of diabetic retinopathy Preliminary report. *Arch Ophthalmol* 1984; 102:1307-11.
- Bresnick GH, Palta M. Predicting progression to severe proliferative diabetic retinopathy. *Arch Ophthalmol* 1987; 105:810-4.

- Brown JL, Hill JH, Burke RE. The effect of hypoxia on the human electroretinogram. *Am J Ophthalmol* 1957; 44:57-67.
- Cao W, Govardovskii V, Li JD, Steinberg RH. Systemic hypoxia dehydrates the space surrounding photoreceptors in the cat retina. *Invest Ophthalmol Vis Sci* 1996; 37:586-96.
- Carr RE, Siegel IM. The electrodiagnostic testing of the visual system: a clinical guide. Philadelphia: F.A. Davis Company, 1990.
- Cerniglia GJ, Wilson DF, Pawlowski M, Vinogradov S, Biaglow J. Intravascular oxygen distribution in subcutaneous 9L tumors and radiation sensitivity. *J Appl Physiol* 1997; 82:1939-1945.
- Coupland SG. Oscillatory potential changes related to stimulus intensity and light adaptation. *Doc Ophthalmol* 1987; 66:195-205.
- Cullen DJ, Eger EI. Cardiovascular effects of carbon dioxide in man. *Anesthesiology* 1974; 41:345-9
- Dawson WW, Parmer R, Hope GM. Division of the pattern-evoked retinal response by respiratory acidosis. *Vis Res* 1988; 28:363-9.
- Dempsey JA, Pack AI, eds. Regulation of breathing, 2nd edition. New York: Marcel Decker Inc., 1995 (Lenfant C, ed. Lung biology in health and disease, vol 79).
- Deutsch TA, Read JS, Ernest JT, Goldstick TK. Effects of oxygen and carbon dioxide on retinal vasculature in humans. *Arch Ophthalmol* 1983; 101:1278-80.
- Dripps RD, Comroe JH Jr. The effect of the inhalation of high and low oxygen concentrations on respiration, pulse rate, ballistocardiogram and arterial oxygen saturation (oximeter) of normal individuals. *Am J Physiol* 1947; 149:277-91.
- Fallon TJ, Maxwell DL, Kohner EM. Retinal vascular autoregulation in conditions of hyperoxia and hypoxia using the blue field entoptic phenomenon. *Ophthalmology* 1985; 92:701-5.
- Faucher C., Kergoat H. Component-specific changes in the oscillatory potentials during transient systemic hyperoxia. *Invest Ophthalmol Vis Sci* 1997; 38: s888.

- Faucher C, Kergoat H. The effect of carbogen breathing on neuro-retinal function in man. *Optom Vis Sci* 1997;74. Résumé accepté pour publication
- Flower RW, Fryczkowski AW, McLeod DS. Variability in choriocapillaris blood flow distribution. *Invest Ophthalmol Vis Sci* 1995;36:1247-58.
- Flower RW, Klein GJ. Pulsatile flow in the choroidal circulation: a preliminary investigation. *Eye* 1990; 4:310-8.
- Friedman E, Chandra SR. Choroidal blood flow III. Effects of oxygen and carbon dioxide. *Arch Ophthalmol* 1972; 87:70-1.
- Gallin-Cohen PF, Podos SM, Yablonski ME. Oxygen lowers intraocular pressure. *Invest Ophthalmol Vis Sci* 1980; 19:43-8.
- Goldstick TK, Ernest JT. The effect of glucose, oxygen and carbon dioxide on choroidal blood flow. *Invest Ophthalmol Vis Sci* 1982; 22(suppl):194.
- Harino S, Grunwald JE, Petrig BJ, Riva CE. Rebreathing into a bag increases human retinal macular blood velocity. *Br J Ophthalmol* 1995; 79:380-3.
- Harris A, Anderson DR, Pillunat L, Joos K, Knighton RW, Kagemann L, Martin BJ. Laser Doppler flowmetry measurement of changes in human optic nerve head blood flow in response to blood gas perturbations. *J Glaucoma* 1996; 5:258-65.
- Harris A, Arend O, Wolf S, Cantor LB, Martin BJ. CO₂ dependence of retinal arterial and capillary blood velocity. *Acta Ophthalmol Scand* 1995; 73:421-4.
- Harris A, Martin BJ, Shoemaker JA. Regulation of retinal blood flow during blood gas perturbation. *J Glaucoma* 1994; 3(suppl. 1):s82-90.
- Hiroi K, Yamamoto F, Honda Y. Analysis of electroretinogram during systemic hypercapnia with intraretinal K⁺-microelectrodes in cats. *Invest Ophthalmol Vis Sci* 1994; 35:3957-61.
- Holopigian K, Seiple W, Lorenzo M, Carr R. A comparison of photopic and scotopic electroretinographic changes in early diabetic retinopathy. *Invest Ophthalmol Vis Sci* 1992;33:2773-80.

- Kagokawa H, Sakomoto T, Takakusaki K, Ogasawara H, Yoshida A. The effect of pure oxygen breathing on retinal blood flow in the cat using a new laser Doppler velocimetry system. *Invest Ophthalmol Vis Sci* 1997; 38:s781.
- Kerger H, Saltzman DJ, Gonzales A, Tsai AG, van Ackern K, Winslow RM, Intaglietta M. Microvascular oxygen delivery and interstitial oxygenation during sodium pentobarbital anesthesia. *Anesthesiology* 1997; 86:372-86.
- Kergoat H, Faucher C. Carbogen breathing increases the pulsatile ocular blood flow. *Optom Vis Sci* 1997; 74. Résumé accepté pour publication.
- Kergoat H, Faucher C. The effect of systemic hyperoxia on the pulsatile choroidal blood flow. *Invest Ophthalmol Vis Sci* 1997; 38:s781.
- Kergoat H, Forcier P. Correlation of an exercise-induced increase in systemic circulation with the neural retinal function in humans. *Doc Ophthalmol* 1996; 92:145-57.
- Kergoat H, Lovasik JV. The effects of altered retinal vascular perfusion pressure on the white flash scotopic ERG and oscillatory potentials in man. *Electroencephalogr Clin Neurophysiol* 1990; 75:306-22.
- Kety SS, Schmidt CF. The effects of altered arterial tensions of carbon dioxide and oxygen on cerebral blood flow and cerebral oxygen consumption of normal young men. *J Clin Invest* 1948; 484-92.
- Kiel JW. Choroidal myogenic autoregulation and intraocular pressure. *Exp Eye Res* 1994; 58:529-44.
- Kiel JW, Shepherd P. Autoregulation of choroidal blood flow in the rabbit. *Invest Ophthalmol Vis Sci* 1992; 33:2399-2410.
- Kiel JW, van Heuven WAJ. Ocular perfusion pressure and choroidal blood flow in the rabbit. *Invest Ophthalmol Vis Sci* 1995;36:579-85.
- Kothe AC. Human ocular haemodynamics I. Choroidal blood flow. *Can J Optom* 1993; 55:160-5.
- Krakau CET. A model for pulsatile and steady ocular blood flow. *Graefes Arch Clin Exp Ophthalmol* 1995; 233:112-8.
- Krakau CET, Wilke K. On repeated tonometry. *Acta Ophthalmol* 1971; 49:611-4.

- Lachapelle P, Benoit J, Guité P. The effect of in vivo retinal cooling on the electroretinogram of the rabbit. *Vis Res* 1996; 36:339-44.
- Langham ME, Farrell RA, O'Brien V, Silver DM, Schilder P. Blood flow in the human eye. *Acta Ophthalmol (Supp)* 1989; 191:9-13.
- Langham ME, Grebe R, Hopkins S, Marcus S, Sebag M. Choroidal blood flow in diabetic retinopathy. *Exp Eye Res* 1991; 53:167-73.
- Laurence VM, Ward R, Dennis IF, Bleehen NM. Carbogen breathing with nicotinamide improves the oxygen status of tumours in patients. *Br J Cancer* 1995; 72:198-205.
- Lassen NA. Brain extracellular pH: the main factor controlling cerebral blood flow. *Scand J Clin Lab Invest* 1968; 22:247-51.
- Lee JG, Hudetz AG, Smith JJ, Hillard CJ, Bosnjak ZJ, Kampine JP. The effects of halothane and isoflurane on cerebrocortical microcirculation and autoregulation as assessed by laser-Doppler flowmetry. *Anesthesia & Analgesia* 1994; 79:58-65.
- Lee JG, Smith JJ, Hudetz AG, Hillard CJ, Bosnjak ZJ, Kampine JP. Laser-Doppler measurement of the effects of halothane and isoflurane on the cerebrovascular CO₂ response in the rat. *Anesthesia & Analgesia* 1995; 80:696-702.
- Li X, Sun X, Hu Y, Huang J, Zhang H. Electroretinographic oscillatory potentials in diabetic retinopathy. An analysis in the domains of time and frequency. *Doc Ophthalmol* 1992; 81:173-9.
- Linsenmeier RA. Electrophysiological consequences of retinal hypoxia. *Graefe's Arch Clin Exp Ophthalmol* 1990; 228:143-50.
- Linsenmeier RA, Braun RD. Oxygen distribution and consumption in the cat retina during normoxia and hypoxemia. *J Gen Physiol* 1992; 99:177-97.
- Linsenmeier RA, Mines AH, Steinberg RH. Effects of hypoxia on the light peak and electroretinogram of the cat. *Invest Ophthalmol Vis Sci* 1983; 24:37-46.
- Linsenmeier RA, Smith VC, Pokorny J. The light rise of the electrooculogram during hypoxia. *Clin Vis Sci* 1987; 2:111-6.

- Linsenmeier RA, Steinberg RH. Mechanisms of hypoxic effects on the cat DC electroretinogram. *Invest Ophthalmol Vis Sci* 1986; 27:1385-94.
- Linsenmeier RA, Yancey CM. Effects of hyperoxia on the oxygen distribution in the intact cat retina. *Invest Ophthalmol Vis Sci* 1989; 30:612-8.
- Lovasik JV, Kergoat H. Electroretinographic results and ocular vascular perfusion in type I diabetes. *Invest Ophthalmol Vis Sci* 1993;34:1731-43.
- Lovasik JV, Kergoat H. Influence of transiently altered retinal vascular perfusion pressure on rod/cone contribution to scotopic oscillatory potentials. *Ophthalmol Physiol Opt* 1991; 11:370-80.
- Lovasik JV, Kothe AC, Kergoat H. Improving the diagnostic power of electroretinography by transient alteration of the ocular perfusion pressure. *Optom Vis Sci* 1992; 69: 85-94.
- Massey AD, O'Brien C. Pulsatile ocular blood flow: a population study of normals. *Invest Ophthalmol Vis Sci* 1996; 37:s31.
- Moses RA. Repeated applanation tonometry. *Ophthalmologica* 1961; 142:663-8.
- Niemeyer F, Nagahara K, Demant E. Effects of change in arterial PO_2 and PCO_2 on the electroretinogram in the cat. *Invest Ophthalmol Vis Sci* 1982; 23:678-83.
- Niemeyer G, Steinberg RH. Differential effects of pCO_2 and pH on the ERG and light peak of the perfused cat eye. *Vis Res* 1984; 24:275-80.
- Nunn JF. *Nunn's applied respiratory physiology*, 4th ed. Oxford: Butterworth-Heinemann, 1993.
- Ogden TE. The oscillatory waves of the primate electroretinogram. *Vis Res* 1973; 13:1059-74.
- Pakola SJ, Grunwald JE. Effects of oxygen and carbon dioxide on human retinal circulation. *Invest Ophthalmol Vis Sci* 1993; 34:2866-70.

- Pournaras CJ, Riva CE, Tsacopoulos M, Strommer K. Diffusion of O₂ in the retina of anesthetized miniature pigs in normoxia and hyperoxia. *Exp Eye Res* 1989; 49:347-60.
- Riva CE, Cranstoun SD, Grunwald JE, Petrig BL. Choroidal blood flow in the foveal region of the human ocular fundus. *Invest Ophthalmol Vis Sci* 1994; 35:4273-81.
- Riva CE, Grunwald JE, Sinclair SH. Laser Doppler velocimetry study of the effect of pure oxygen breathing on retinal blood flow. *Invest Ophthalmol Vis Sci* 1983; 24:47-51.
- Schilder P. Ocular blood flow changes with increased vascular resistance external and internal to the eye. *Acta Ophthalmol (Supp)* 1989; 191:19-23.
- Schmetterer L, Lexer F, Findl O, Graselli U, Eichler HG, Wolzt M. The effect of inhalation of different mixtures of O₂ and CO₂ on ocular fundus pulsations. *Exp Eye Res* 1996; 63:351-5.
- Schmetterer L, Wolzt M, Lexer F, Alschinger C, Gouya G, Zanaschka G, Fassolt A, Eichler HG, Fercher AF. The effect of hyperoxia and hypercapnia on fundus pulsations in the macular and optic disc region in healthy young men. *Exp Eye Res* 1995; 61:685-90.
- Silver DM, Farrell RA. Validity of pulsatile ocular blood flow measurements. *Survey Ophthalmol* 1994; 38 (suppl):s72-80.
- Simonsen SE. The value of the oscillatory potential in selecting juvenile diabetics at risk of developing proliferative retinopathy. *Acta Ophthalmol* 1980; 58:865-78.
- Speros P, Price J. Oscillatory potentials. History, techniques and potential use in the evaluation of disturbances of retinal circulation. *Surv Ophthalmol* 1981; 25:237-52.
- Sponsel WE, DePaul KL, Zetlan SR. Retinal hemodynamic effects of carbon dioxide, hyperoxia, and mild hypoxia. *Invest Ophthalmol Vis Sci* 1992; 33:1864-9.
- Steinberg RH. Monitoring communications between photoreceptors and pigment epithelial cells: effects of « mild » systemic hypoxia. *Invest Ophthalmol Vis Sci* 1987; 28:1888-1904.

- Thorburn W. Recordings of appanating force at constant intraocular pressure. IV. Intraocular volume changes due to changes in blood content. *Acta Ophthalmol* 1972; 50:270-85.
- Tortora GJ, Grabowski SR. Principes d'anatomie et de physiologie, nouvelle édition. Anjou: CEC collégial et universitaire, 1994.
- Tremblay F, Lam SR. Distinct electroretinographic oscillatory potential generators as revealed by field distribution. *Doc Ophthalmol* 1993; 84:279-89.
- Trokel S. Effect of respiratory gases upon choroidal hemodynamics. *Arch Ophthalmol* 1965; 73:838-42.
- Tsacopoulos M, Levy S. Intraretinal acid-base studies using pH glass microelectrodes: effect of respiratory and metabolic acicosis and alkalosis on inner-retinal pH. *Exp Eye Res* 1976; 23:495-504.
- Van Der Torren K, Mulder P. Comparison of the second and third oscillatory potentials with oscillatory potential power in diabetic retinopathy. *Doc Ophthalmol* 1993; 83:111-8.
- Wachtmeister L. Further studies of the chemical sensitivity of the oscillatory potentials of the electroretinogram (ERG). I. GABA and glycine antagonists. *Acta Ophthalmol* 1980; 58:712-25.
- Wachtmeister L. Further studies of the chemical sensitivity of the oscillatory potentials of the electroretinogram (ERG). II. Glutamate, aspartate and dopamine antagonists. *Acta Ophthalmol* 1980; 59:247-58.
- Wachtmeister L. Further studies of the chemical sensitivity of the oscillatory potentials of the electroretinogram (ERG). III. Some Ω amino acids and ethanol. *Acta Ophthalmol* 1980; 59:609-19.
- Wachtmeister L, Dowling JE. The oscillatory potentials of the mudpuppy retina. *Invest Ophthalmol Vis Sci* 1978; 17:1176-88.
- Yablonski ME, Gallin P, Shapiro D. Effect of oxygen on aqueous humor dynamics in rabbits. *Invest Ophthalmol Vis Sci* 1985; 26:1781-4.
- Yu DY, Cringle SJ, Alder VA, Su EN, Yu PK. Intraretinal oxygen distribution and choroidal regulation in the avascular retina of guinea pigs. *Am J Physiol* 1996; 270:H965-H973.

ANNEXE I

INFLUENCE DE L'OXYGÈNE SUR LA TONOMÉTRIE À APPLANATION SANS CONTACT PROLONGÉ AVEC LA CORNÉE

INTRODUCTION

Dans l'expérience traitant de l'influence de l'oxygène (O₂) et du carbogène sur le flot sanguin oculaire pulsatile (FSOP), la pression intraoculaire (PIO) était diminuée pendant la respiration d'oxygène et la mesure de FSOP. Nous avons suggéré que la répétition de mesures de FSOP avec un tonographe pouvait contribuer à réduire la PIO par un effet de massage oculaire à cause du contact prolongé (de 10 à 20 secondes) de la sonde de l'appareil sur la cornée. Le but de cette expérience contrôle était de déterminer si l'hyperoxie systémique induisait une réduction de la PIO lorsque cette dernière est prise par tonométrie à applanation sans contact prolongé avec la cornée.

MATÉRIEL ET MÉTHODES

Sujets

20 sujets (11 femmes, 9 hommes) âgés entre 19 et 34 ans, ayant une bonne santé oculaire et systémique, se sont portés volontaires pour cette étude.

Pression intraoculaire

Après l'instillation d'une ou 2 gouttes de proparacaine HCl 0,5% et l'application de fluorescéine sodique à l'oeil droit, une seule mesure de PIO a été prise avec un tonomètre à applanation de type Perkins pour chacune des conditions suivantes :

- 1) à l'air ambiant, après au moins 10 minutes de repos en position assise;
- 2) à l'air ambiant, 15 minutes après la première mesure, pour s'assurer de la stabilité de la PIO à l'intérieur d'une courte période de temps pour chaque sujet;

3) pendant la respiration de 100% d'O₂ après une période d'attente de 10 minutes à l'air ambiant.

Respiration d'oxygène

Un masque à oxygène muni d'une valve à sens unique et d'un sac réservoir était placé sur le visage du sujet et ajusté avec le plus d'étanchéité possible. Le sujet devait respirer de l'O₂ à 100% provenant d'une bombonne pendant 5 minutes. Le débit d'oxygène était ajusté à 5 L/minute, et le sujet devait respirer le plus normalement possible.

La saturation en oxygène de l'hémoglobine étaient vérifiées par oxymétrie tout au long de l'expérience, sans toutefois être enregistrée.

RÉSULTATS

La PIO moyenne à l'air ambiant était de 14,73 mmHg pour la première mesure, et de 14,95 mmHg pour la seconde. Ces deux valeurs n'étaient pas différentes l'une de l'autre. La PIO a été significativement réduite à 13,93 mmHg ($p=0,0016$) pendant la respiration d'oxygène (figure 1). Le changement de PIO lors de la respiration d'O₂ variait entre +0,5 et -4,0 mmHg. La PIO a été diminuée chez 12 des 20 sujets par rapport à la moyenne des 2 mesures de base, est restée stable chez 3 sujets, alors qu'elle a été augmentée d'un maximum de 0,5 mmHg chez les 5 autres sujets.

DISCUSSION

La PIO est réduite d'environ 1 mmHg pendant l'inspiration d'O₂. Une réduction de PIO avec l'O₂ a également été rapportée chez le lapin (Gallin-Cohen et col. 1980, Yablonski et col. 1985) et l'humain. (Gallin-Cohen et col. 1980) Cette réduction a été attribuée à une diminution de la pression veineuse épisclérale plutôt qu'à une réduction de la production d'humeur aqueuse. (Yablonski et col. 1985) D'autres études démontrent par contre que l'O₂ n'influence pas la PIO. (Riva et col. 1983, Schmetterer et col. 1995)

Dans la présente étude, la réduction de la PIO est vraisemblablement due à l'hyperoxie. Il est peu probable que la technique utilisée ait influencé la valeur de la PIO obtenue. Il est vrai que la prise de mesures répétées de tonométrie à applanation à intervalles de 1 minute réduit la PIO, (Moses 1961, Krakau et Wilke 1971) mais cette dernière est pratiquement totalement rétablie à son niveau initial en 15 minutes. (Krakau et Wilke 1971) De plus, la prise de mesures uniques séparées de 5 minutes avec un tonomètre à applanation n'entraîne aucune diminution de PIO. (Krakau et Wilke 1971)

La PIO évaluée avec un tonomètre de type Perkins est réduite durant la respiration d'O₂. Cette diminution est toutefois inférieure à celle observée lors de notre expérience principale sur l'influence de l'O₂ et du carbogène sur le FSOP. Nous pouvons donc conclure que l'hyperoxie et la répétition de mesures successives de PIO accompagnée d'un contact prolongé entre la sonde du tonographe et la cornée ont tous deux contribué à réduire la PIO.

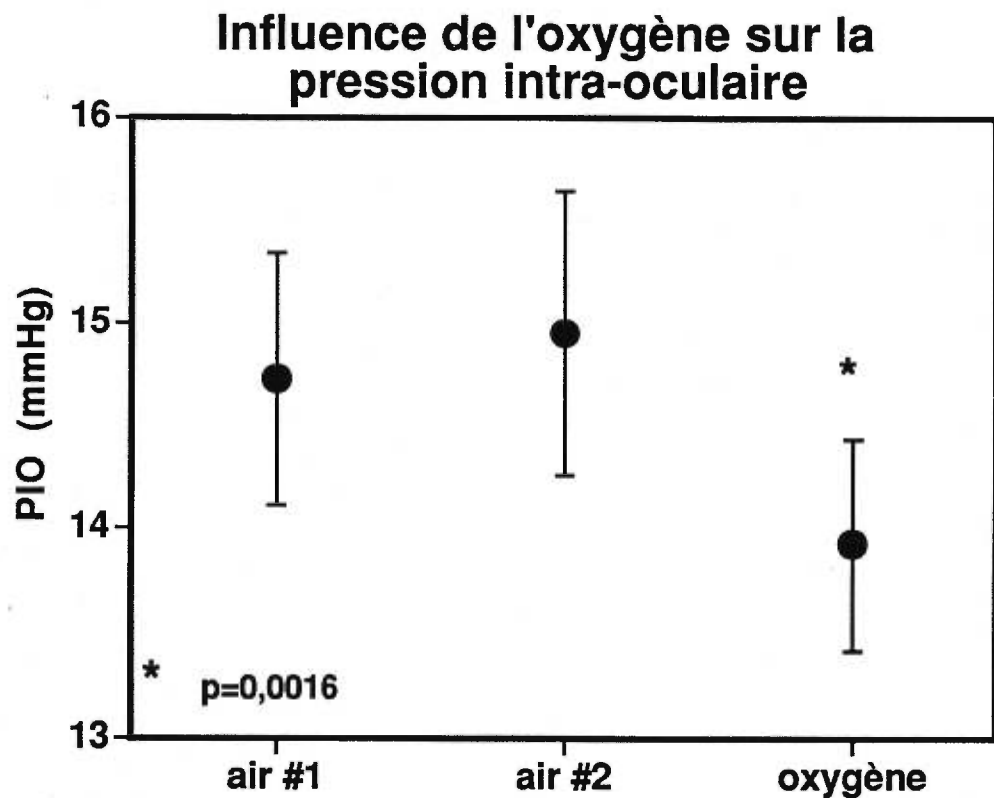


Figure 1. Figure illustrant la réduction de la PIO mesurée par tonométrie à aplplanation (Perkins) pendant la respiration d'oxygène pur. Air #1 : tonométrie mesurée à l'air ambiant après 10 minutes en position assise; air #2 : mesure de PIO à l'air ambiant, 15 minutes après la première mesure; oxygène : PIO à la fin d'une période de 5 minutes de respiration d'oxygène pur.

RÉFÉRENCES

Gallin-Cohen PF, Podos SM, Yablonski ME. Oxygen lowers intraocular pressure. *Invest Ophthalmol Vis Sci* 1980; 19:43-8.

Krakau CET, Wilke K. On repeated tonometry. *Acta Ophthalmol* 1971; 49:611-4.

Moses RA. Repeated applanation tonometry. *Ophthalmologica* 1961; 142:663-8.

Riva CE, Grunwald JE, Sinclair SH. Laser Doppler velocimetry study of the effect of pure oxygen breathing on retinal blood flow. *Invest Ophthalmol Vis Sci* 1983; 24:47-51.

Schmetterer L, Wolzt M, Lexer F, Alschinger C, Gouya G, Zanaschka G, Fassolt A, Eichler HG, Fercher AF. The effect of hyperoxia and hypercapnia on fundus pulsations in the macular and optic disc region in healthy young men. *Exp Eye Res* 1995; 61:685-90.

Yablonski ME, Gallin P, Shapiro D. Effect of oxygen on aqueous humor dynamics in rabbits. *Invest Ophthalmol Vis Sci* 1985; 26:1781-4.

ANNEXE II

STABILITÉ DE L'ÉLECTRORÉTINOGRAMME ET DES POTENTIELS OSCILLATOIRES DANS LE TEMPS

INTRODUCTION

Certaines composantes de l'électrorétinogramme (ERG) et des potentiels oscillatoires (POs) ont été modifiées lors des expériences traitant de l'effet de l'oxygène (O₂) pur et du carbogène sur la fonction neuro-rétinienne. Le but de cette étude était de s'assurer que les changements observés lors de ces expériences avec l'O₂ et le carbogène n'étaient pas entraînés par d'autres facteurs qui seraient liés au protocole expérimental, tels la pression du masque exercée sur le visage, ou encore le niveau d'adaptation des photorécepteurs après plusieurs enregistrements consécutifs.

MATÉRIEL ET MÉTHODES

Six adultes (5 femmes, 1 homme) ayant une bonne santé oculaire et systémique, âgés de 21 à 24 ans ont participé à cette étude contrôlée.

Les POs et les ERGs ont été enregistrés suite à la présentation d'éclairs (2 séries de 15 éclairs blancs; fenêtre d'enregistrement : 100 msec) générés par un stroboscope (PS22, Grass Instruments, Quincy, MA). Les éclairs ont été présentés à une fréquence de 0.3 Hz dans une coupole de Ganzfeld. Une électrode active de type « Jet » a été utilisée pour enregistrer les potentiels rétinien, en condition scotopique. Les signaux électriques ont été filtrés, puis amplifiés par un système d'enregistrement des potentiels évoqués (Nicolet Biomedical CA-1000). Tous les enregistrements ont été faits à l'air ambiant seulement, à la pression atmosphérique normale du niveau de la mer.

La pression artérielle, la fréquence cardiaque, la saturation en O₂ de l'hémoglobine (SaO₂), le CO₂ de fin d'expiration (EtCO₂) et la fréquence respiratoire ont été évalués tout au long des expériences.

Expérience 1

Pour s'assurer que la présentation d'éclairs successifs ne modifie pas la réponse rétinienne, les potentiels rétinien ont été enregistrés chez quatre des sujets pour chacune des conditions suivantes :

- 1) après 30 minutes d'adaptation à l'obscurité, au repos et en position assise;
- 2) 10 minutes plus tard;
- 3) de 30 secondes à 1 minute après;
- 4) après une autre période d'attente de 10 minutes.

Lors des enregistrements électrophysiologiques de cette expérience contrôle aucun masque n'était porté, mais pour chaque condition d'enregistrement, la tête du sujet était placée devant la coupole de Ganzfeld à une distance qui tenait compte de la position du masque dans les expériences originales.

Expérience 2

Afin de vérifier que la pression exercée par un masque sur le visage du sujet n'influence pas les signaux électriques en provenance de la rétine, les ERGs et les POs ont été enregistrés chez les deux autres sujets pour les quatre conditions suivantes :

- 1) après 30 minutes d'adaptation à l'obscurité, au repos et en position assise;
- 2) à la fin d'une période de 10 minutes pendant laquelle le sujet portait un masque à oxygène modifié de sorte que l'air inspiré et expiré ne

provenait que de l'air ambiant. Pour ce faire, la portion centrale du masque recouvrant normalement le nez et la bouche a été complètement enlevée, afin de conserver uniquement la portion périphérique du masque qui prend appui sur le visage.

3) immédiatement après le retrait du masque;

4) 10 minutes plus tard, sans masque.

La tête du sujet était placée devant la coupole de Ganzfeld dans la même position pour chacune des quatre conditions, que le masque soit porté ou non. Ce masque modifié était porté uniquement pour la condition 2, recréant ainsi les conditions d'enregistrement des expériences originales.

RÉSULTATS

La pression artérielle était normale pour tous les sujets des deux expériences. Il n'y a eu aucune variation de pression artérielle, de fréquence cardiaque, de SaO_2 , d' EtCO_2 ou de fréquence respiratoire tout au long des expériences ($p > 0,05$).

Pour les 6 sujets, les ondes a, b, ainsi que les 5 POs étaient présents pour les 4 enregistrements. Pour chacune des deux expériences, aucune différence significative d'amplitude ou de latence n'a été observée entre les différents enregistrements ($p > 0,05$).

La stabilité dans le temps des amplitudes et latences des ondes a et b, ainsi que des POs est illustrée aux figures 1 à 4 pour l'expérience 1, et aux figures 5 à 8 pour l'expérience 2. Les amplitudes des potentiels enregistrés pour les deux sujets ayant participé à l'expérience 2 sont indiquées au tableau 1.

CONCLUSIONS

Nous n'avons constaté aucun changement des amplitudes et temps de latence des ondes a et b de l'ERG ou des POs lors de mesures répétées à intervalles respectant le protocole expérimental suivi lors des expériences sur l'influence de l'O₂ et du carbogène sur la fonction neuro-rétinienne. Nous concluons donc que les modifications électrophysiologiques observées dans les expériences précédentes sont entraînées par les gaz respirés, et non pas par les autres conditions d'enregistrement liées au protocole expérimental. Ainsi, la pose et le retrait de l'électrode active entre les périodes d'enregistrement, la pression exercée par un masque sur le visage du sujet, ou encore la répétition d'éclairs de lumière aux intervalles de temps considérés n'affectent pas les réponses électriques de la rétine.

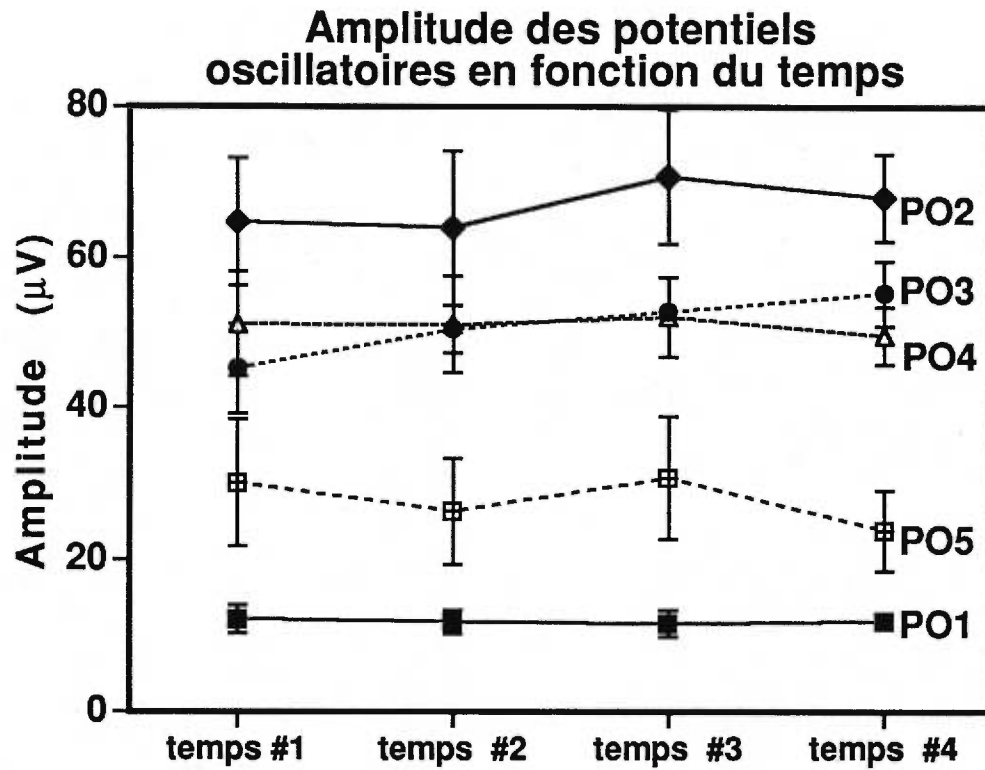


Figure 1. Figure illustrant la stabilité de l'amplitude des potentiels oscillatoires dans le temps durant l'expérience 1. Temps #1 : après 30 minutes d'adaptation à l'obscurité; temps #2 : 10 minutes plus tard; temps #3 : de 30 secondes à une minute après la dernière mesure; temps #4 : après une autre période d'attente de 10 minutes. Les barres d'erreur indiquent l'erreur standard moyenne.

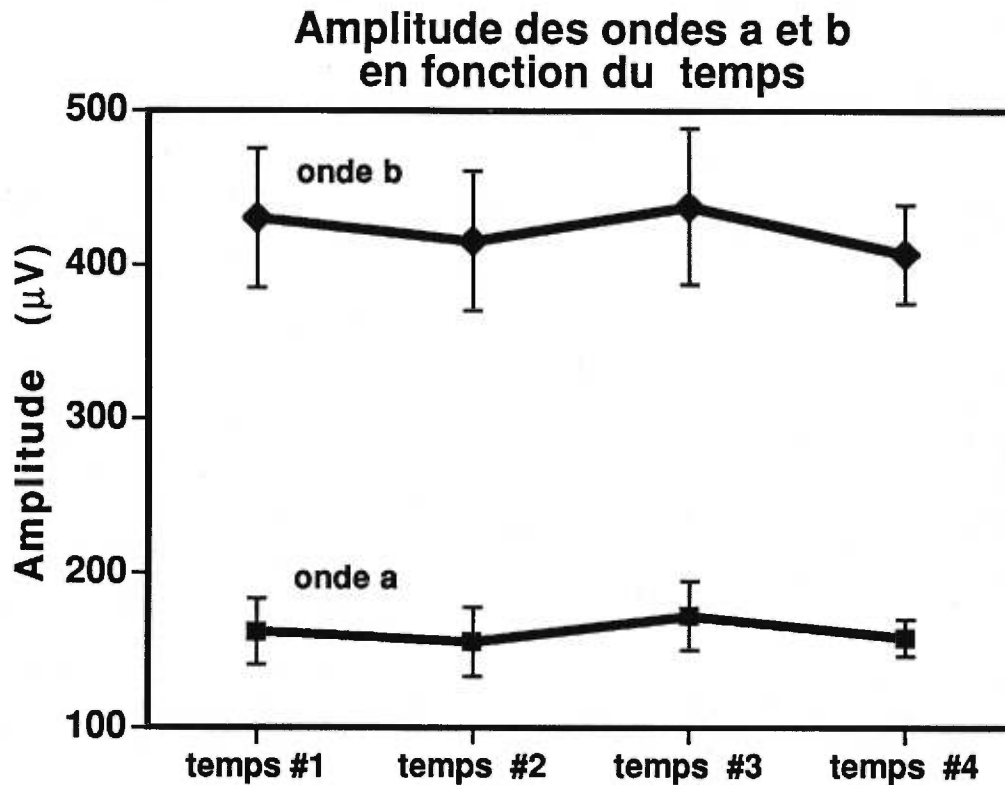


Figure 2. Figure illustrant la stabilité de l'amplitude des ondes a et b dans le temps durant l'expérience 1. Temps #1: après 30 minutes d'adaptation à l'obscurité; temps #2 : 10 minutes plus tard; temps #3 : de 30 secondes à une minute après la dernière mesure; temps #4 : après une autre période d'attente de 10 minutes. Les barres d'erreur indiquent l'erreur standard moyenne.

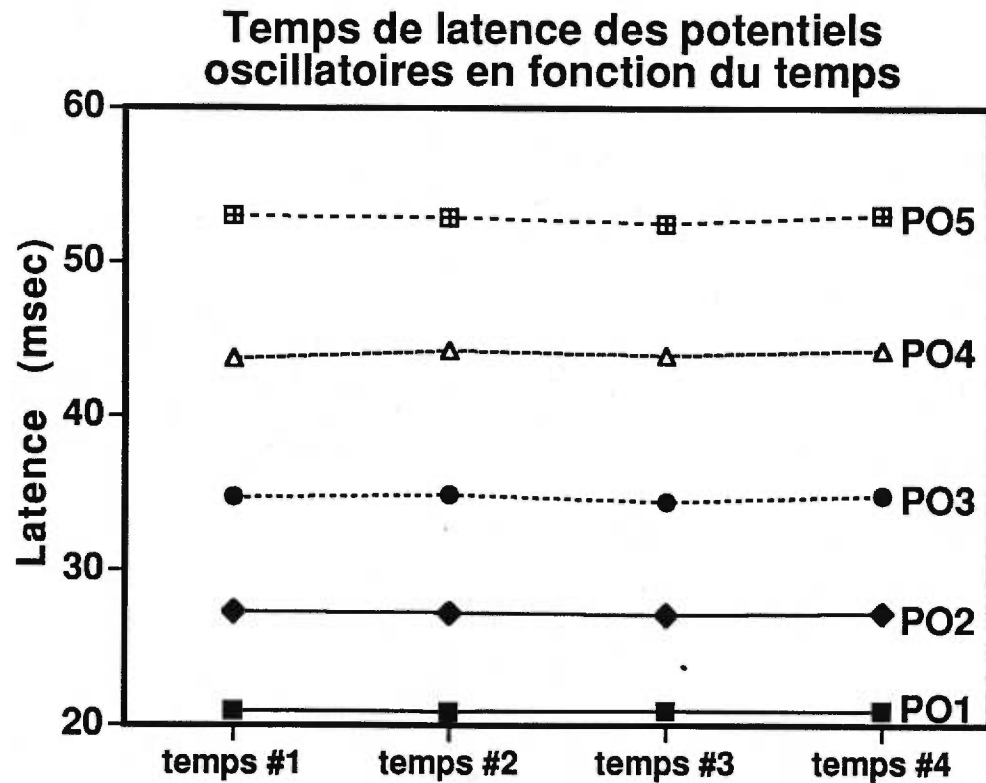


Figure 3. Figure illustrant la stabilité de la latence des potentiels oscillatoires dans le temps durant l'expérience 1. Temps #1 : après 30 minutes d'adaptation à l'obscurité; temps #2 : 10 minutes plus tard; temps #3 : de 30 secondes à une minute après la dernière mesure; temps #4 : après une autre période d'attente de 10 minutes. L'erreur standard moyenne est trop faible pour apparaître sur le graphique.

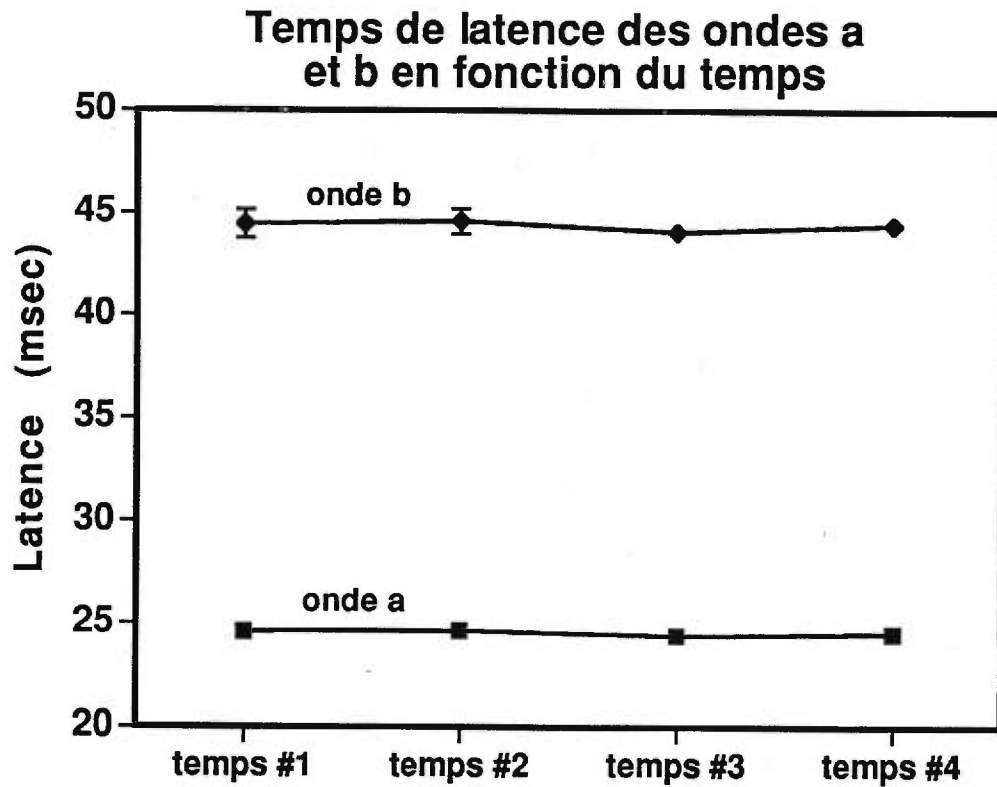


Figure 4. Figure illustrant la stabilité du temps de latence des ondes a et b dans le temps durant l'expérience 1. Temps #1 : après 30 minutes d'adaptation à l'obscurité; temps #2 : 10 minutes plus tard; temps #3 : de 30 secondes à une minute après la dernière mesure; temps #4 : 10 minutes plus tard. Les barres d'erreur illustrent l'erreur standard moyenne.

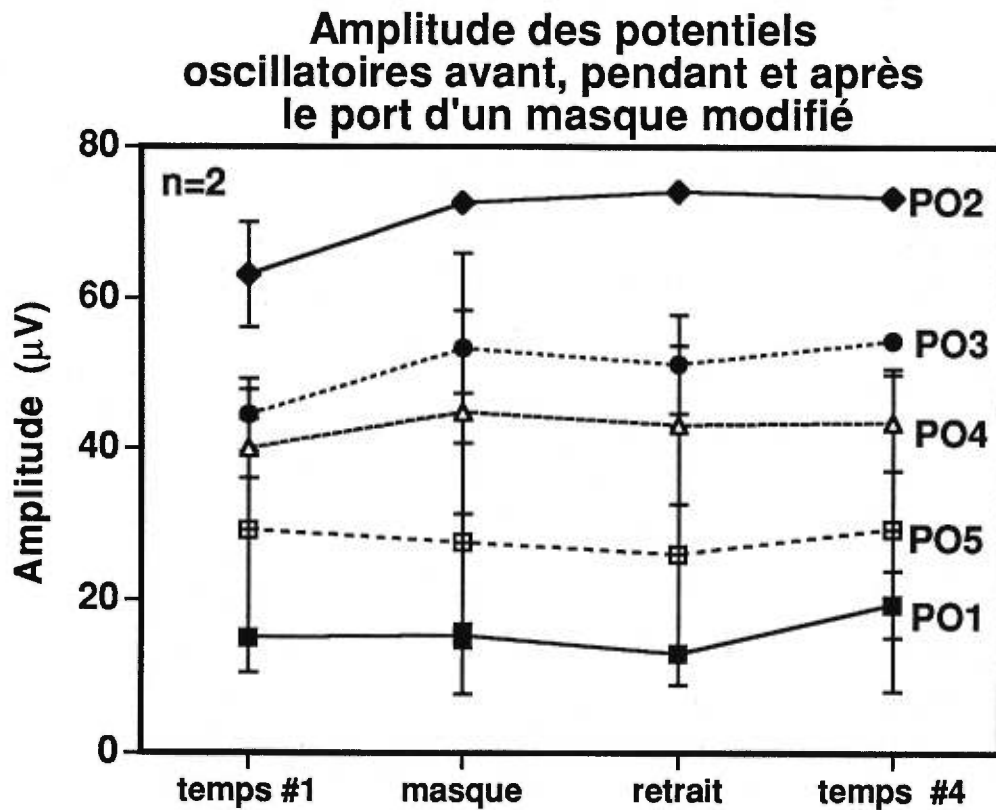


Figure 5. Figure illustrant la stabilité de l'amplitude des potentiels oscillatoires durant le port d'un masque modifié (expérience 2). Temps #1 : après 30 minutes d'adaptation à l'obscurité; masque : à la fin d'une période de 10 minutes pendant laquelle le masque était porté; retrait : immédiatement après avoir enlevé le masque; temps #4 : 10 minutes plus tard. Les barres d'erreur indiquent l'erreur standard moyenne.

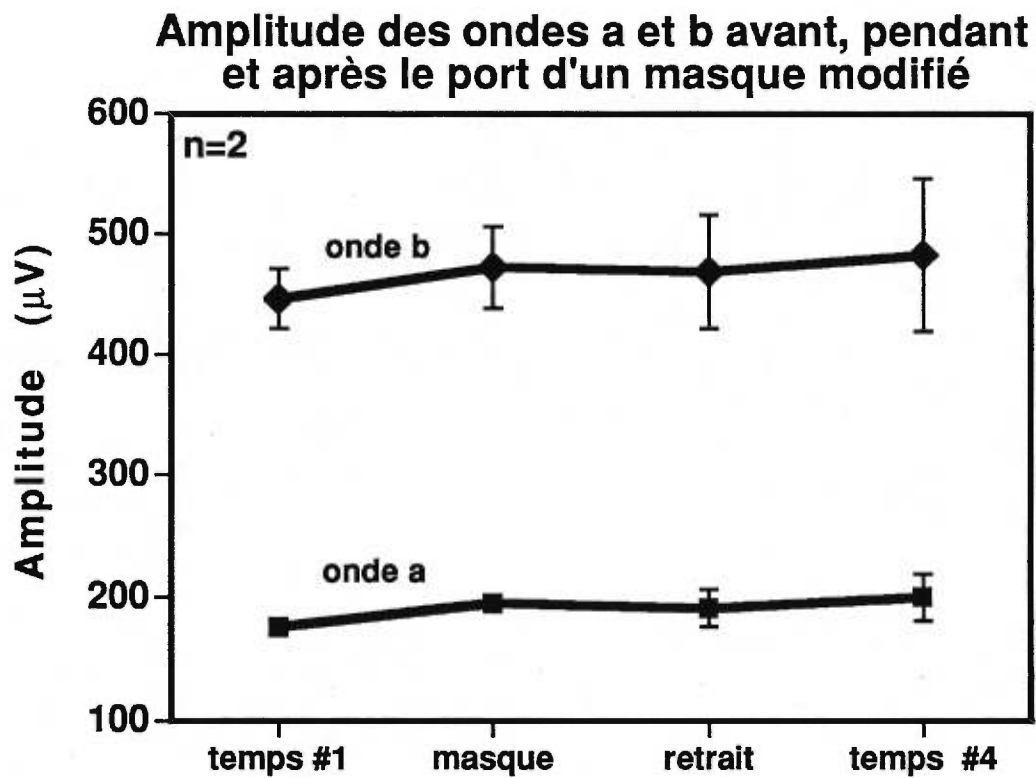


Figure 6. Figure illustrant la stabilité de l'amplitude des ondes a et b durant le port d'un masque modifié (expérience 2). Temps #1 : après 30 minutes d'adaptation à l'obscurité; masque : à la fin d'une période de 10 minutes pendant laquelle le masque était porté; retrait : immédiatement après avoir enlevé le masque; temps #4 : après une période d'attente de 10 minutes. Les barres d'erreur indiquent l'erreur standard moyenne.

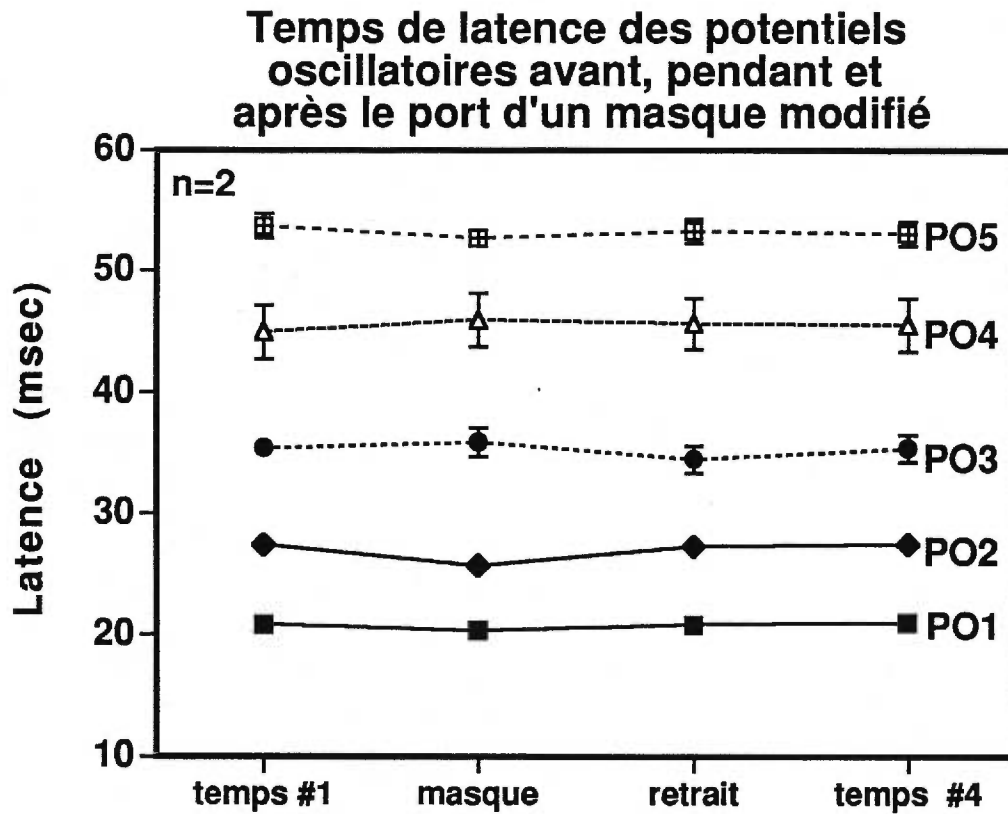


Figure 7. Figure illustrant la stabilité de la latence des potentiels oscillatoires durant le port d'un masque modifié (expérience 2). Temps #1 : après 30 minutes d'adaptation à l'obscurité; masque : à la fin d'une période de 10 minutes pendant laquelle le masque était porté; retrait : immédiatement après avoir enlevé le masque; temps #4 : 10 minutes plus tard. Les barres d'erreur illustrent l'erreur standard moyenne.

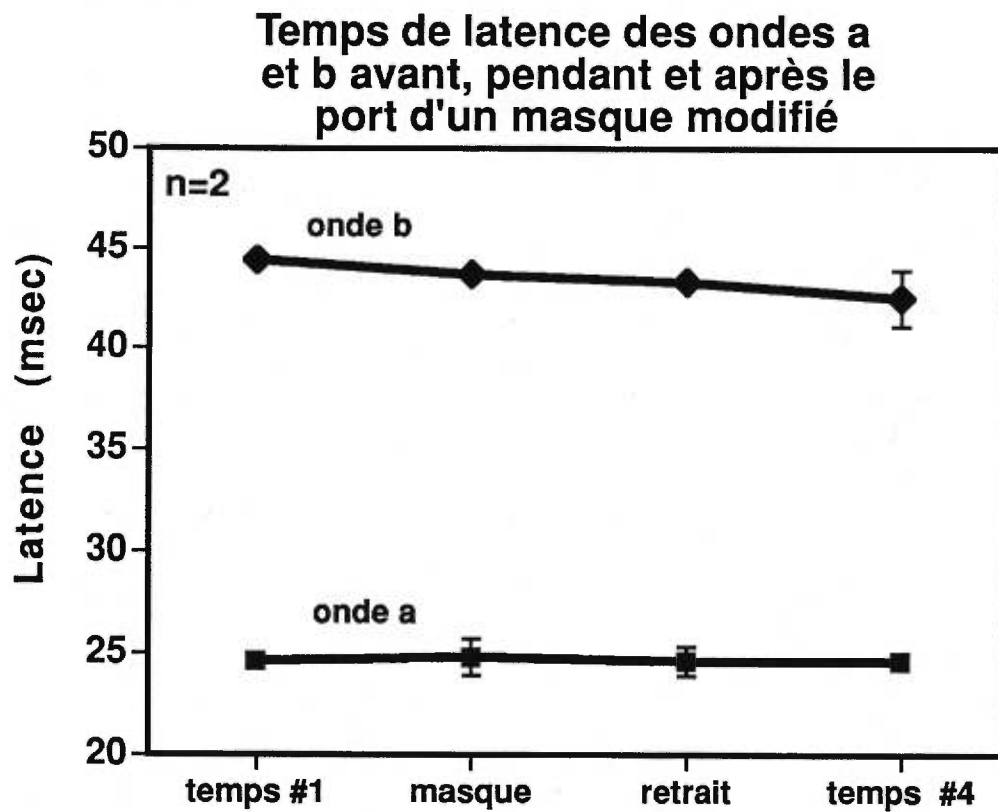


Figure 8. Figure illustrant la stabilité du temps de latence des ondes a et b durant le port d'un masque modifié (expérience 2). Temps #1 : après 30 minutes d'adaptation à l'obscurité; masque : à la fin d'une période de 10 minutes pendant laquelle le masque était porté; retrait : immédiatement après avoir enlevé le masque; temps #4 : 10 minutes plus tard. Les barres d'erreur illustrent l'erreur standard moyenne.

Amplitude des potentiels oscillatoires et des ondes a et b (expérience 2)

onde	condition	SUJET 1	SUJET 2	MOYENNE
		(μV)	(μV)	(μV)
OP1	niveau de base	14,6	15,5	15,1
	masque	13,7	16,8	15,3
	retrait	14,1	11,8	13,0
	10 minutes plus tard	15,0	23,8	19,4
OP2	niveau de base	70,0	56,1	63,1
	masque	73,1	72,1	72,6
	retrait	73,3	74,9	74,1
	10 minutes plus tard	74,3	72,3	73,3
OP3	niveau de base	39,7	49,3	44,5
	masque	40,8	65,9	53,4
	retrait	44,7	57,8	51,3
	10 minutes plus tard	53,6	55,1	54,4
OP4	niveau de base	36,1	43,9	40,0
	masque	31,3	58,4	44,9
	retrait	32,6	53,7	43,2
	10 minutes plus tard	37,1	49,9	43,5
OP5	niveau de base	10,5	47,9	29,2
	masque	7,7	47,4	27,6
	retrait	8,3	43,7	26,0
	10 minutes plus tard	8,0	50,7	29,4
onde a	niveau de base	183	169	176,0
	masque	189	201	195,0
	retrait	176	206	191,0
	10 minutes plus tard	181	219	200,0
onde b	niveau de base	421	471	446,0
	masque	438	506	472,0
	retrait	421	516	468,5
	10 minutes plus tard	419	546	482,5

Tableau 1.